Regulation of STAMP2 by Proinflammatory Cytokines in Prostate Cancer Cells

Nicklas Pihlstrøm

Thesis for the Master of Science degree
in Molecular Biosciences

Department of Biosciences
Faculty of Mathematics and Natural Sciences

UNIVERSITETET I OSLO

Januar 2016

2016

Regulation of STAMP2 by Proinflammatory Cytokines in Prostate Cancer Cells

Nicklas Pihlstrøm

http://www.duo.uio.no/

Trykk: Reprosentralen, Universitetet i Oslo

Acknowledgements

The work presented here was carried out in the laboratory of Professor Fahri Saatcioglu at the Department of Biosciences, University of Oslo, from January to Desember 2015.

I would like to express my gratitude to Fahri, for noticing me in one of his classes and offering me the opportunity to come and be part of his excellent group of researchers. I would further thank him for his open-door policy, his dedicated support and guidance, to me as well as all his group members.

I would especially like to thank Dr. Yang Jin. As my supervisor, Jin has gladly shared of his great experience, has shown me great patience and has always been utmost helpful. His guidance throughout this project has been invaluable.

Thanks to all my colleagues in the FS lab, both former and present members, for creating the wonderful working environment we share, both professionally and socially.

I also would last but not least like to thank my friends and family, whose continued care and support despite my absence or absentminded presence during this period has been crucial for me.

Nicklas Pihlstrøm

Oslo, January 2016

Contents

Abstract

Six-transmembrane protein of the prostate (STAMP2) is an iron reductase that is associated with the progression of prostate cancer (PCa). PCa is the most commonly diagnosed cancer type in Norway and ranks second among men worldwide. Localized PCa is curable. Metastatic PCa is treated with androgen deprivation therapy (ADT), but all patients develop resistance and disease invariably recur as the terminal castration resistant prostate cancer (CRPC) type. STAMP2 is regulated by androgens, and its expression falls after ADT, but also recurs in androgen-independent CRPC. STAMP2 is critical for PCa cell survival and growth, and is therefore seen as a potential therapeutic target. In other cellular contexts, STAMP2 is involved in modulating cellular responses to fluctuations in nutrients and to inflammatory stimuli. Proinflammatory cytokines induce STAMP2 expression in several cell types, but this has not been established in PCa cells before.

Results showing that the proinflammatory cytokines interleukin 6 (IL-6), interleukin 1beta (IL-1β) and tumor necrosis factor alpha (TNFα) induce STAMP2 mRNA expression in the PCa cell line LNCaP are presented in this study. Potential mechanisms of cytokine-mediated *STAMP2* induction were investigated. Signal transducer and activator of transcription (STAT) 3 was found to be critical for IL-6-mediated *STAMP2* induction, and the MAP kinases extracellular signal-regulated kinases (ERK) 1 and 2 were also implicated in the process. IL-1β is a less potent positive regulator of *STAMP2* than IL-6 in LNCaP. It was found to regulate *STAMP2* expression by a mechanism that further needs to be established, but one that involved both nuclear factor kappaB, STAT3 and ERK1/2. As chronic inflammation is believed to be promoting tumor growth and metastasis, and has established links with PCa, these preliminary results position STAMP2 as a prime suspect at the intersection of PCa progression and inflammation in future studies of the mechanisms driving development of CRPC.

Presented in this study is also the identification on mRNA level of a novel short isoform variant of STAMP2, called STAMP2_v1 (variant 1). Predictions of STAMP2_v1 structure suggest that is a severely altered protein, one that lacks the catalytic activity of STAMP2. STAMP2_v1 mRNA was detected at low levels in PCa cells and has a limited tissue distribution, but was detected at high levels in immune cells, indicating that it may play a novel role in immune biology.

Abbreviations

aa	Amino acid
ADT	Androgen-deprivation therapy
AKT	RAC-alpha serine/threonine-protein kinase
AMACR	α-methylacyl-CoA racemase
AP-1	Activating protein 1
AR	Androgen receptor
ATF	Cyclic AMP-dependent transcription factor
BCR	Biochemical recurrence
bp	Base pairs
BPH	Benign prostate hyperplasia
C/EBPα	CCAAT/enhancer-binding protein alpha
CRPC	Castration resistant prostate cancer
DD	Death domain
ECM	Extracellular matrix
ERK	Extracellular-signal regulated kinase
FAD	Flavin adenine dinucleotide
FAK	Focal adhesion kinase
FMN	Flavin mononucleotide
FNO	F420:NADP+ Oxidoreductase
FRE	Ferric reductase
GAB1	GRB2-associated-binding protein 1
GFP	Green fluorescent protein
gp130	Glycoprotein 80 (IL-6Rβ)
gp80	Glycoprotein 80 (IL-6Rα)
GRB2	Growth factor receptor bound protein 2
HEK	Human embryonal kidney cells
IKK	Inhibitor of nuclear factor kappa B kinase
IL-1R1	Type 1 IL-1 receptor
IL-1RAcP	IL-1 receptor accessory protein
IL-1β	Interleukin 1beta
IL-6	Interleukin 6
IL-6Rα	Interleukin 6 receptor alpha
IL-6Rβ	Interleukin 6 receptor beta
IL-8	Interleukin 8
IRAK	IL-1 receptor activated protein kinase
IκB	Inhibitor of kappa B
JAK	Janus kinase
JNK	c-Jun N-terminal kinase
KLK4	Kallikrein 4
LNCaP	Lymph node carcinoma of the prostate
LPS	Lipopolysaccharide
mAb	Monoclonal antibody
MAP3K	Mitogen activated protein kinase kinase kinase
MAPK	Mitogen activated protein kinase
MEK	Dual specificity mitogen-activated protein kinase kinase
MetS	Metabolic syndrome
mTORC1	Mammalian target of rapamycin complex 1
MYD88	Myeloid differentiation primary response gene 88
NADPH	Nicotinamide adenine dinucleotide phosphate
NF-κB	Nuclear factor kappaB
NOX	NADPH oxidases
ORF	Open reading frame
PCa	Prostate cancer
PDK1	3-phosphoinositide-dependent protein kinase 1
PH	Pleckstrin homology domain
PI3K	Phosphatidyl-inositol-3 kinase
PIN	Prostatic intra-epithelial neoplasia
PIP3	Phosphatidylinositol-3,4,5-triphosphate
PSA	Prostate specific antigen
PTM	Post-translational modification
R1881	Synthetic androgen
ROS	Reactive oxygen species
RT-qPCR	Real-time quantitative polymerase chain reaction

SH2	Src homology 2 domain
SHP2	SH2-domain containing phosphatase 2
shRNA	Short hairpin RNA
sIL-6Rα	Soluble IL-6Rα
siRNA	Short interfering RNA
SOS	Sons of sevenless
STAMP	Six-transmembrane proteins of the prostate
STAT	Signal transducers and activators of transcription
STEAP	Six-transmembrane epithelial antigen of prostate
TAB	TGFβ-activated kinase binding proteins
TAK	Transforming growth factorβ-activated kinase
TIARP	TNFα-induced adipose-related protein
TIR	Toll- and IL-1R-like domains

TM	Transmembrane
TMPRSS 2	Transmembrane protease serine 2
TNFα	Tumor necrosis factor alpha
TPL2	Tumor progression locus 2 (MAP3K8)
TRAF	Tumor necrosis factor-associated factor
Tsap6	Tumor suppressor activated pathway 6
UTR	Untranslated region
VAT	Visceral white adipose tissue
VCaP	Vertebral carcinoma of the prostate
VEGF	Vascular endothelial growth factor
wt	Wild-type

1 Introduction

1.1 Prostate cancer

According to the GLOBOCAN 2012 cancer statistics report by the World Health Organization, prostate cancer (PCa) was the fourth most commonly diagnosed type of cancer overall, and the second most commonly diagnosed cancer among men after lung cancer [1]. According to the Norwegian National Cancer Registry, PCa was the cancer type with the highest overall number of new cases in Norway in 2014, independently of gender (kreftregisteret.no), although more people suffered from lung- and colorectal cancer-specific deaths. National and global PCa statistics are summarized in table 1.

Table 1: PCa statistics on new cases, PCa-specific deaths and patients surviving diagnosis. National statistics are numbers of incidence, mortality and total prevalence in 2014. Global statistics are estimated numbers of incidence, mortality and 5-year prevalence in 2012.

Region	Incidence	Mortality	Prevalence
Norway, 2014	4889	1093	41,841
Global, 2012	1,095,000	307,000	3,858,000
Europe, 2012	420,000	101,000	1,513,000
United States, 2012	233,000	30,000	980,000
Developing countries, 2012	353,000	165,000	987,000

After the adoption of prostate-specific antigen (PSA) screening some 25 years ago, PCa incidence rates have risen dramatically in the Western world (North America, Western Europe, Australia and New Zealand) and these countries ranked highest in global incidence statistics in 2012 (globocan.iarc.fr). The PSA test is controversial; although it arguably has contributed to earlier diagnoses of PCa, it is not cancer-specific [2]. Elevated levels of PSA can just as likely be attributed to other factors such as trauma, prostatitis or the common condition of benign prostate hyperplasia (BPH). A major concern is that PSA screening leads to over-treatment of PCa; some patients with asymptomatic, indolent disease that is unlikely to become clinically relevant undergo invasive procedures as radiation therapy and/or radical

prostatectomy, with associated risks of side-effects. New biomarkers better able to stratify patient sub-groups are therefore in great demand [2]. Members of the six-transmembrane proteins of the prostate (STAMP)-family have been suggested as potential candidates, as is discussed below.

1.1.1 Prostate cancer treatment in Norway

PSA screening without other symptoms account for the majority of PCa diagnoses in Norway (60% of cases in 2013), while a minority of cases are detected after patients report various lower urinary tract symptoms (LUTS) [3]. Diagnosed patients are assigned to low, intermediate or high risk groups, and cancer treatment plans are initiated according to European Association of Urology guidelines [4]. Tumor-lymph node-metastasis (TNM) cancer staging [5] and histological analysis of needle biopsies by Gleason cell differentiation scoring [6], together with PSA level, age and general health are used to assign risk. Patients with localized disease at the time of diagnosis are generally cured. The use of radical prostatectomy with curative intent in Norway has increased over the last ten years to 45% of all cases in 2012. Use of radiation as sole curative therapy has correspondingly been reduced from 40 to 20 % of yearly cases over this period, but is increasingly used as post-operative adjuvant therapy as more high risk patients undergo surgery. Since the start of the practice in 2009, a smaller sub-group of patients categorized as low-risk have been put on active surveillance (AS) programs. These include frequent PSA testing, re-biopsies and use of diagnostic MR imaging, reflecting the increasing awareness of how AS pose a lower risk to patient quality of life than invasive treatment in some cases. PCa-specific mortality has been stable or in modest decline over this period while incidence rates have increased, leading to increased survival rates overall [3].

1.1.2 Prostate cancer tumorigenesis

Initiation and progression of PCa are linked to endogenous risk factors as oxidative stress, hormone levels, inflammation, race, family history and old age, and exogenous risk factors associated with lifestyle and occupation, such as smoking, diet, exercise and environmental carcinogens [7]. Formation of prostatic intra-epithelial neoplasia (PIN), a morphological state characterized by focal hyperplasia of prostate luminal epithelial cells, is considered as an initial event in PCa development [8]. PINs can develop further into adenocarcinomas of the

prostate, distinguishable by the loss of basal cells markers and increased expression of proliferative and luminal markers, e.g. α-methylacyl-CoA racemase (AMACR) [9]. Most prostate adenocarcinomas are of a hematological indistinguishable acinar type, although other, rare sub-types exist. More clinically relevant sub-types that remain to be fully classified might exist on the genetic level [10].

A majority of prostate adenocarcinomas remain indolent, but some 10% eventually break senescence and re-activates developmental signaling pathways leading to aggressive growth [9]. As discussed above, PCa is curable as long as such cases of clinically relevant disease are detected and treated while still restricted to the prostate gland. Patient outlooks are much worse when cancers acquire the potential to invade neighboring tissue outside the prostate and metastasize to other parts of the body. In the case of PCa, these are initially local lymph nodes, and then commonly distant metastases in bone, lung, liver and brain [9]. The progressional steps of PCa tumorigenesis is illustrated in figure 1.

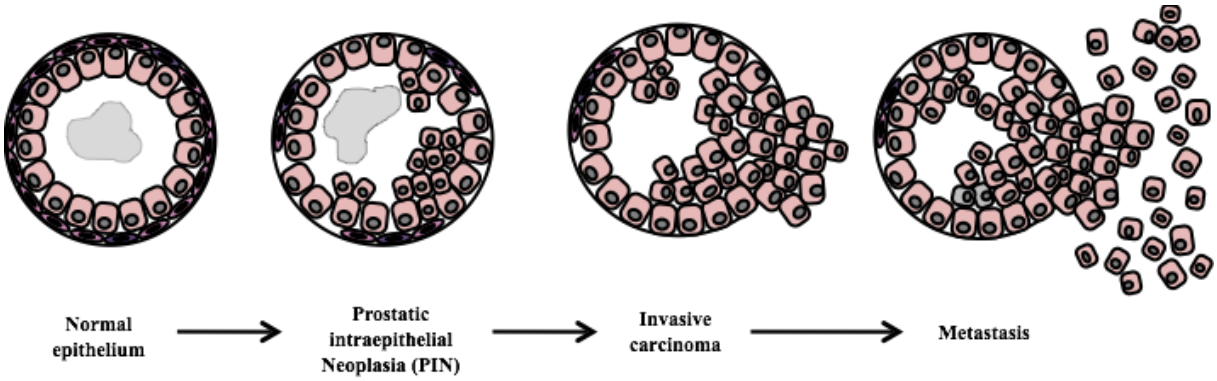

Figure 1: Morphological steps in the transformation of ductal prostate epithelial cells into metastatic PCa. The figure is adapted from [9] with permission from DR. Michael Shen.

Both normal prostate and PCa cells depend on circulating androgen hormones to activate androgen receptor (AR)-regulated gene expression [11, 12]. The AR regulates transcription of hundreds of genes involved in survival, development and proliferation of these cells. That forms the basis of chemical androgen-deprivation therapy (ADT), which at present is the only treatment option for advanced PCa along with cytotoxic drugs. Initial responses to ADT are good, with near complete remission, but disease invariably recur within months or a few years as a more aggressive, ADT resistant, androgen-independent form called castration resistant

prostate cancer (CRPC). CRPC is lethal, and only palliative treatment is available. Besides development of better diagnostic and prognostic biomarkers, identifying genetic and molecular mechanisms driving development of CRPC that could serve as therapeutic targets is now the major focus area of PCa research. Renewed expression of PSA, also called biochemical recurrence (BCR), is used as a biomarker of relapse of PCa as CRPC. Being an AR-regulated gene, recurrence of PSA indicates that AR-mediated expression is re-initiated in CRPC. Development of second-generation antagonists targeting the mutated or amplified hormone-independent AR variants shown to be involved in CRPC development therefore receives much attention [11, 12].

1.2 Cancer and inflammation

As noted above, inflammation is considered one of the endogenous risk factors which may play a role in the development of PCa [7]. It has long been accepted that human cancers are associated with cells of the immune system. In 1986, HF Dvorak published a paper where he used the phrase "wounds that do not heal" in his description of tumors. Dvorak described multiple similarities between natural wound healing and tumorigenesis, but with the distinction that as opposed to wound healing caused by external injury being a process limited in time, cancer cells are able to initiate and perpetuate the process to support their own continued growth [13].

Infiltration of immune cells to some degree or another is now considered a common feature of human solid tumors [14]. These can be T and B lymphocytes, natural killer (NK) cells, NK-T cells, dendritic cells (DCs), macrophages, neutrophils, eosinophils and mast cells. Infiltrating immune cells produce states of local inflammation, which again affect all the cell types of the tumor microenvironment and their synergistic networks of communication by the local release of bioactive signaling molecules (figure 2)[15, 16]. The concept of tumor-promoting inflammation was therefore adopted as a common enabling characteristic of human cancers by Hanahan and Weinberg in their 2011 revisit of their landmark 'Hallmarks of Cancer' review [15]. In their words, tumor-associated inflammation has the "paradoxical effect of enabling incipient neoplasias to acquire hallmark capabilities". Inflammatory signaling proteins, cytokines, contribute to sustained survival and proliferative signaling, evasion of growth suppression and suppression of apoptosis. Tumor-promoting states of inflammation further involve local release of reactive oxygen species (ROS) and extracellular matrix

(ECM)-remodeling proteases, natural functions especially of innate immune cells, but normally involved in clearance of infectious pathogens and in tissue maintenance. Taking place in a tumor microenvironment, these natural mechanisms instead enhance the genomic instability/mutational rate and invading capability of cancer cells, respectively [15].

Inflammation further enhance the ability of cancer cells to invade neighboring tissue and migrate to and colonize other parts of the body by the release of vascular endothelial growth factor (VEGF) by invading immune cells. VEGF activates vascular endothelial cells and induce angiogenesis; the formation of new blood supply into the tumor, acting as both nutrient and oxygen supply and an escape route into circulation for cancer cells [15, 16]. Figure 2 shows a simplified illustration of the reciprocal heterotypic network of paracrine signaling among cells of the tumor microenvironment, leading to proliferation, inflammation and angiogenesis.

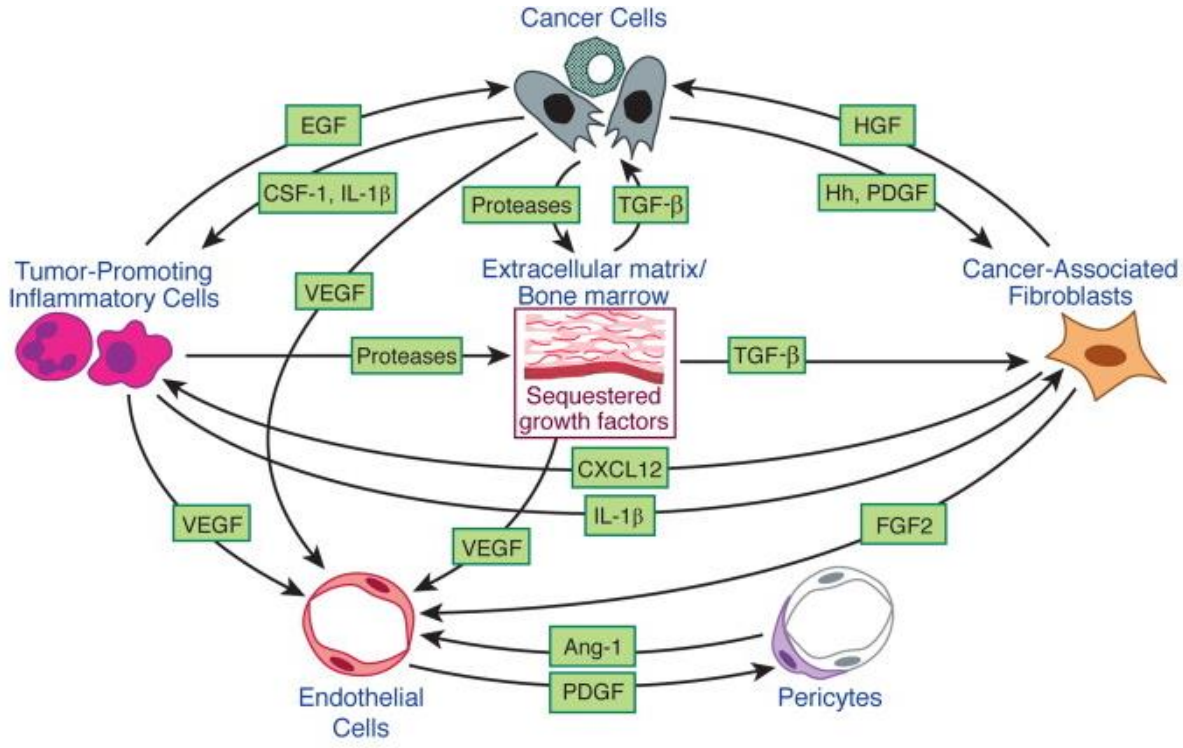

Figure 2: Reciprocal paracrine signaling network between different cell types of the tumor microenvironment. Heterotypic signaling include growth-factor-mediated proliferative and inflammatory signaling and the release of factors enabling angiogenesis and migration. The figure is re-printed from [15] with permission from Dr. Robert Weinberg.

Simultaneously, cell types as myeloid-derived suppressor cells (MDSCs), alternatively activated M2 macrophages and regulatory T cells, can be found associated with tumors and/or

local lymph nodes [14, 15]. Normally involved in wound healing and tissue maintenance and recruited by the release of necrotic cell products, these cells have suppressive functions to avoid overt inflammation in such contexts. Remodeling of the ECM also involves release of the immunosuppressive transforming growth factor beta (TGFβ) [16]. Together with direct immunosuppression by cancer cells as e.g. by novel, cell-surface expression of programmed death ligand 1 (PD-L1), this in sum creates an environment that suppresses the activity of NK- and cytotoxic T cells that might otherwise have antitumoral activity [17].

1.2.1 Interleukin 6 signaling pathway

Interleukin 6 (IL-6) was initially cloned and characterized in 1988 as a 184 amino acid T cell-derived secreted interleukin able to induce the activation of B cells into antibody-secreting plasma cells [18]. It was also soon recognized that IL-6 was identical to previously identified factors able to stimulate proliferation of hepatocytes and differentiation of myeloid blood cell precursors [19]. IL-6 is now considered as one of the canonical inflammatory cytokines, but exerts multiple functions beyond mediating local and systemic, acute phase inflammatory responses. Apart from lymphocyte development and liver regeneration, IL-6 is involved in processes as bone formation, systemic metabolism, endocrine functions, and affect many tissue types as a positive mediator of survival and proliferation [19, 20]. Its principal source is activated macrophages and T-cells, but it can also be released by other cell types as fibroblasts, smooth muscle cells and epithelial cells. As expression of IL-6 is regulated by both other inflammatory mediators and itself, this can create a feed-forward loop of deregulated heterotypic paracrine IL-6 signaling between different cells in the tumor stroma, making IL-6 one of the main mediators of chronic tumor-associated inflammation. IL-6 and its intracellular signaling mediators are further linked to promoting cancer cell survival, proliferation, invasion and cancer stem cell maintenance, while inhibiting induction of apoptosis [21].

IL-6 binds to the extracellular immunoglobulin fold of a specific, 80 kDa transmembrane receptor (IL-6Rα, alternatively glycoprotein (gp) 80) [22]. IL-6Rα has a tissue distribution restricted to CD4+ T cells, monocytes, neutrophils and hepatocytes, but is shed by these cells by proteolytic cleavage and is present in circulation as soluble IL-6Rα (sIL-6Rα) in large amounts, serving as a buffer for IL-6 [19]. IL-6Rα lacks intracellular tyrosine kinase activity. Two heterodimers of IL-6 and IL-6Rα, either transmembrane or soluble receptor, depending

on cell type, instead form a ligand-receptor complex with a homodimer of the more ubiquitously expressed gp130/IL-6Rβ [19, 21]. gp130 only binds (s)IL-6Rα in complex with IL-6. The large intracellular domain of gp130 is on the other hand constitutively associated with Janus kinases (JAK) as JAK1, JAK2 and/or TYK2. Upon formation of the hexameric receptor-ligand complex, conformational changes lead to activation by autophosphorylation of JAKs, which again phosphorylate the intracellular domain of gp130 [19, 21, 23]. This creates recruitment sites for mediators that propagate intracellular signaling cascades, as is summarized in figure 3.

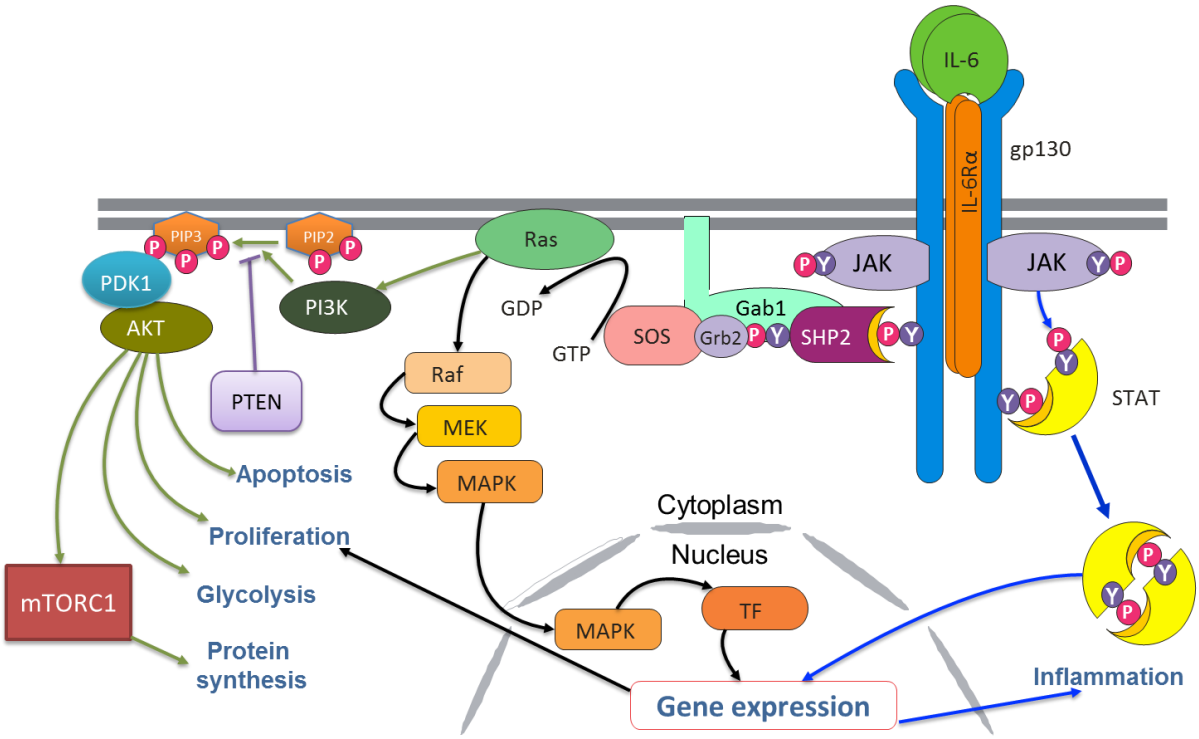

Figure 3: IL-6-mediated intracellular signaling pathways. The figure is reproduced from [23] with permission from Dr. Fred Schaper.

The most direct intracellular pathway starts with the recruitment of signal transducers and activators of transcription (STAT) members STAT3 and to a lesser extent STAT1 via their Src homology 2 (SH2) domains [19]. STATs contain an activation domain, a dimerization domain and a DNA-binding domain. After JAK-mediated phosphorylation of tyrosine residues in their activation domain, they form homo- or heterodimers which translocate to the nucleus where they take part in the regulation of transcription of inflammatory mediators [19].

Furthermore, intracellular gp130 phospho-tyrosine residues recruit SH2-domain containing phosphatase 2 (SHP2), which then becomes activated by JAK phosphorylation [23].

Phosphorylated SHP2 further recruits the adaptor complex of growth factor receptor bound protein 2 (GRB2), GRB2-associated-binding protein 1 (GAB1) and Sons of sevenless (SOS). SOS is a Ras GTPase guanine nucleotide exchange factor, and its proximity to the membrane facilitated by the intracellular receptor complex leads to Ras activation. Downstream of Ras, IL-6-mediated signaling then branches out to activate mitogen activated protein kinase (MAPK) and phosphatidyl-inositol-3 kinase (PI3K) cascades. The MAPK cascade leads to activation of extracellular-signal regulated kinase 1/2 (ERK1/2, also known as p44/p42) through RAF proto-oncogene serine/threonine-protein kinase (RAF) and Dual specificity mitogen-activated protein kinase kinase 1/2 (MEK1/2). Activated ERK1/2 then promote proliferation through its activation of transcription factors as Myc and ELK1, which regulate expression of genes promoting entry into the cell cycle [23].

Activation of PI3K leads increased levels of phosphatidylinositol-3,4,5-triphosphate (PIP3) in the plasma membrane, facilitating the recruitment and interaction of proteins through pleckstrin homology (PH) domains [24]. Among them are 3-phosphoinositide-dependent protein kinase 1 (PDK1) and RAC-alpha serine/threonine-protein (AKT) kinases, and the concurrent interaction leads to PDK1-mediated phosphorylation, activation and release of AKT. AKT kinases goes on to regulate the activity of multiple target proteins by phosphorylation, resulting in inhibition of apoptosis, while inducing proliferation. AKT kinase activity also leads to increased glucose uptake and utilization, while one of its main downstream targets mammalian target of rapamycin complex 1 (mTORC1) stimulates protein synthesis, in sum resulting in increased cell growth [24]. AKT has also been shown to activate the nuclear factor kappaB-pathway (NF-κB) [25], details of which is discussed below.

1.2.2 IL-1β signaling pathway

Similarly to IL-6, Interleukin 1beta (IL-1β) is a macrophage-derived inflammatory cytokine involved in regulation of the hepatic acute phase systemic inflammatory response [26]. IL-1β is the founding member of the interleukin-1 family, now comprising 11 cytokines encoded by distinct genes. Unlike IL-6, bioavailability of IL-1β is regulated by inducible caspase1-dependent proteolytic maturation in the inflammasome protein complex prior to release [27]. As a secreted factor, IL-1β has both paracrine and systemic functions, and is involved both in regulation of immune cell activity and in multiple diseases associated with chronic inflammation, as autoimmune diseases, diabetes and cancer [15, 28].

IL-1β binds to the ubiquitously expressed type 1 IL-1 receptor (IL-1R1) [29]. Upon ligand binding, IL-1R1 undergo conformational changes that allows the association of the co-receptor IL-1 receptor accessory protein (IL-1RAcP), required for initiation of intracellular signaling. Intracellular Toll- and IL-1R-like (TIR) domains of the trimeric ligand-receptor complex then recruit myeloid differentiation primary response gene 88 (MYD88), which again recruits IL-1 receptor activated protein kinase 4 (IRAK4) via death domain (DD) interactions. After IRAK4 autophosphorylation, this pentameric complex becomes a stable, membrane-proximal signaling module that recruits, activates and releases protein complexes consisting of IRAK1, IRAK2 and tumor necrosis factor-associated factor 6 (TRAF6) that propagate intracellular signaling, eventually leading to activation of the NF-κB pathway and MAPK cascades [29], as is shown in figure 4.

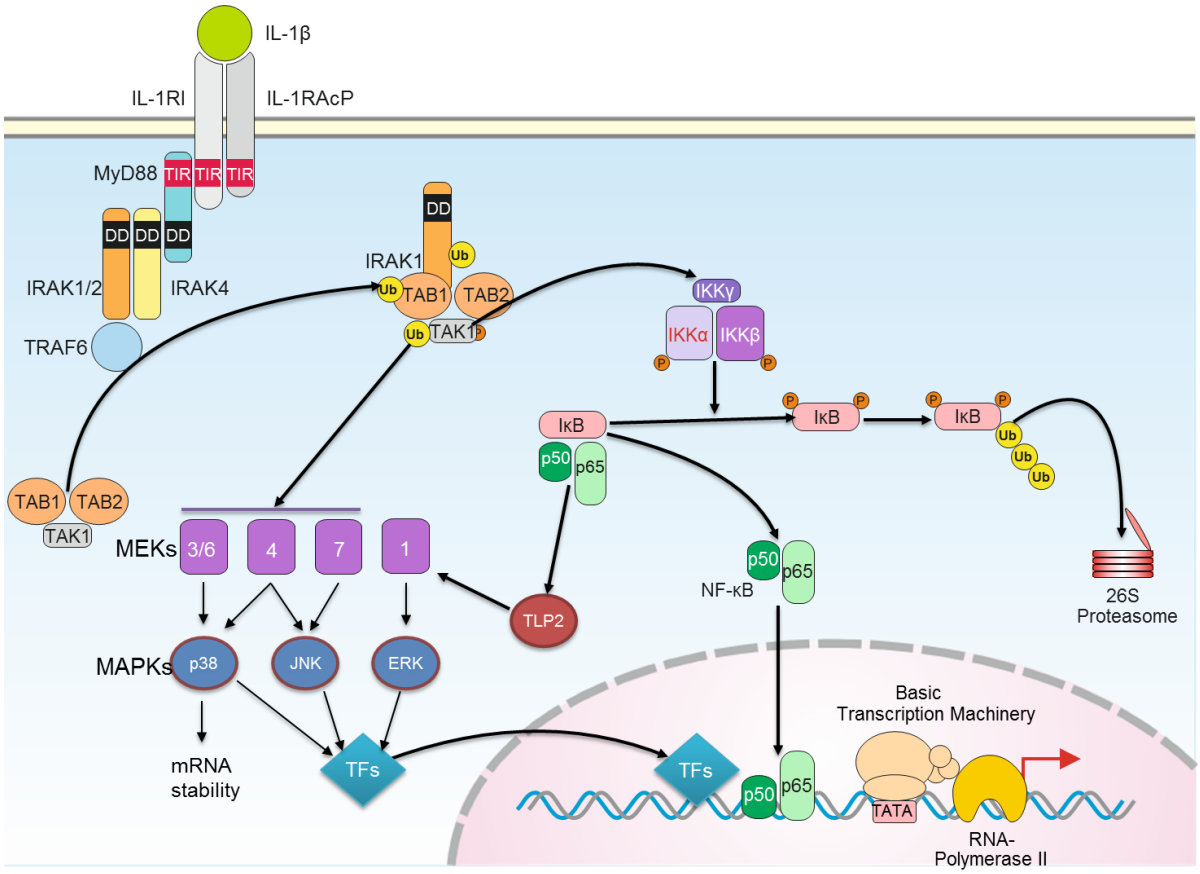

Figure 4: IL-1β-mediated intracellular signaling pathways. Adapted from Löffler/Petrides Biochemie und Pathobiochemie, Springer publishing, with permission from Dr. Fred Schaper.

TRAF6 is a ubiquitin E3 ligase, and activate several other signaling factors by lysine 63-ubiquitinylation. These include IRAK1, transforming growth factorβ-activated kinase (TAK1, a MAP kinase kinase kinase) and TGFβ-activated kinase binding proteins (TAB1-3) [29]. In

complexes with TAB proteins, TAK1 and IRAK1 associates with the NF-κB essential modulator (NEMO, or IKKγ) moiety of the inhibitor of nuclear factor kappa B kinase complex (IKK), leading to activation of IKKα/β. After activation, IKK proceeds to target inhibitor of kappa B (IκB), leading to its proteasomal degradation and the release of bound dimers of NF-κB1/p50 and NF-κB3/p65. After being released from IκB-mediated inhibition, NF-κB translocate to the nucleus and initiates transcription of proinflammatory IL-1β target genes, as cytokines, chemokines and Prostaglandin G/H synthase 2 (COX-2) [16, 29].

TAK1 with TABs further activates MAP kinase kinases (MEKs) 3, 4, 6 and 7 [29, 30]. The MAP kinases mitogen-activated protein kinase 11 (p38) and c-Jun N-terminal kinases (JNK1-3) are subsequently activated by the MEKs. JNK1-3 regulate the activity of several transcription factors, as c-Jun, c-Fos (AP-1) and Cyclic AMP-dependent transcription factor 2 (ATF2), which go on to regulate the expression of pro-growth and survival target genes of IL-1β. p38 also activates ATF2, but in addition target several cytosolic proteins involved in regulating mRNA stability, leading to enhanced stability of IL-1β target gene transcripts [29, 30]. ERK1/2 is also activated by IL-1β, by an usual mechanism downstream of NF-κB [31]. The MAP kinase kinase kinase tumor progression locus 2 (TPL2/MAP3K8) is held inactive in complex with NF-κB1, but is released as the pathway is activated. TPL2 then activates ERK1/2 via MEK1 [30, 31].

1.3 STAMP family of proteins

The history of the six-transmembrane proteins of prostate (STAMP) family begun with screens for genes differentially expressed in prostate cancer (PCa). Two groups independently discovered a previously unknown gene that was predicted to encode a six-pass transmembrane (TM) protein [32, 33]. The protein was named STAMP1. The STAMP1 protein sequence was found to share a high degree of sequence similarity with the previously discovered murine tumor necrosis factor alpha (TNFα)-induced adipose-related protein (TIARP) [34]. The human homolog of TIARP, named STAMP2, was later cloned and characterized as a protein over-expressed in PCa [35]. Sequence alignments also found previously identified, closely related genes in the human six-transmembrane epithelial antigen of prostate (STEAP) [36], pHyde in rats [37] and tumor suppressor activated pathway 6 (Tsap6), found first in mice and later also in humans by the same group [38]. The human homolog of pHyde/Tsap6 was later also independently identified as STEAP3 [39]. This

makes up the current members of the family: STAMP1 (also called STEAP2), STAMP2 (alternatively STEAP4 in humans and TIARP in mice) and STAMP3 (alternatively STEAP3 in humans, Tsap6 in mice or pHyde in rats). The closely related STEAP1/STEAP is also included in the family by others.

1.3.1 Structure and functions of STAMP family proteins

A common feature of the STAMP family and STEAP is a C-terminal domain with a short cytosolic tail and six TM alpha helices. The STAMP TM domain shares distant evolutionary origins with the bacterial YedZ ferric reductase, yeast ferric reductases (FREs) and eukaryotic NADPH oxidases (NOXs) [40]. The STAMP family of proteins are therefore considered members of the heme containing transmembrane ferric reductase domain (FRD) superfamily [40]. The murine STAMPs, but not STEAP, have both ferric and cupric reductase activity when expressed in human HEK-293T cells [39, 41]. In similar experiments with the human STAMP proteins, only STAMP2 demonstrated iron reductase activity [42]. Three dimensional structure studies elucidated that STAMP3 binds one heme group, sandwiched between the six TM helices of the protein in the center of membrane bilayers as they arrange a channel-like structure [43]. Two histidine residues located in TM helices 3 and 5 protruding into the space of the transmembrane "channel" were found to be critical for heme binding. These residues are conserved in all STAMP proteins. Tyrosine residues in TM helices 1 and 3 were similarly found to organize Fe3+ ions adjacent to the heme group, immediately above it on the extracellular/luminal side of the membrane (figure 5) [43].

Unlike STEAP, which has a severely truncated N-terminal domain, STAMP proteins also share a larger, cytosolic N-terminal domain. This domain varies slightly in length among members, but share a high degree of conserved residues, and have similarities with the prokaryotic F420:NADP+ Oxidoreductase (FNO) [35, 41, 44]. X-ray crystallography studies of N-terminal domain fragments of STAMP2 and STAMP3 found remarkable folding similarity between the two. In vitro enzymatic assays with these N-terminal fragments found that they bind and oxidize NADPH in a flavin-dependent manner, although their low measured binding affinities for flavin would require physiologically impossible concentrations of the co-factor [45, 46]. A more recent study found that STAMP3 has a preference for flavin adenine dinucleotide (FAD) over related compounds as flavin mononucleotide (FMN) or riboflavin as co-factor [43]. Furthermore, full-length STAMP3

showed a stronger flavin binding affinity than the N-terminal fragments, as residues located in the cytosolic loops of the TM domain also contributed to the interaction.

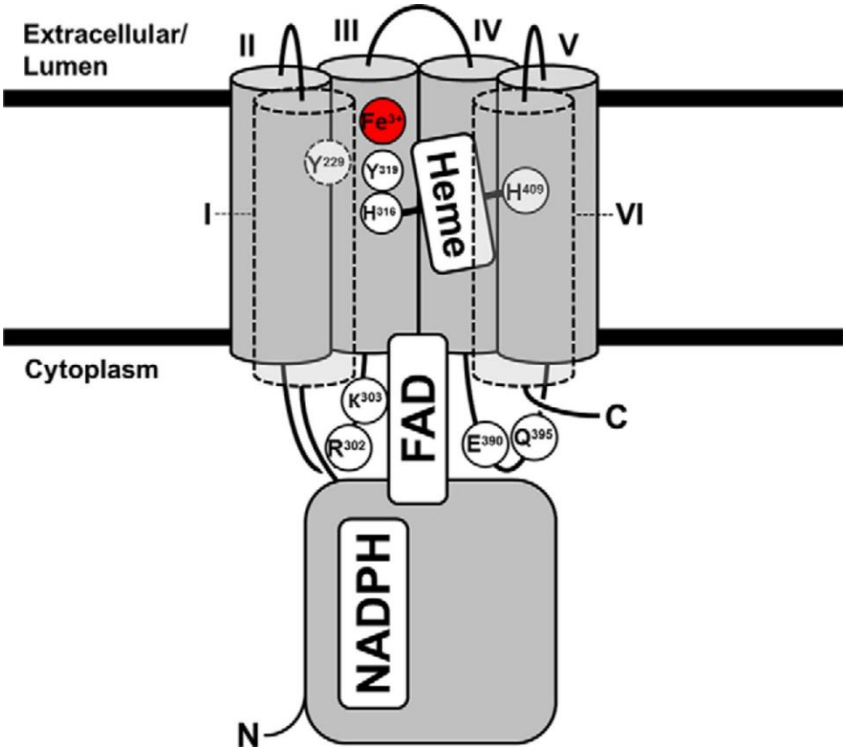

Figure 5: Proposed model of STAMP3 structure. Critical residues involved in organization of FAD and heme co-factors and Fe^{3+} substrate (red) are highlighted. TM helices are numbered with roman numerals from N- to C-terminal, and are displayed open to allow visualization of interior of the transmembrane domain. Re-printed from [43] with permission from Dr. Martin Lawrence.

A model of STAMP3 based on the above mentioned results is shown in figure 5. As the critical residues are conserved among family members, STAMP1 and STAMP2 are predicted to arrange their protein motifs involved in catalytic activity in a similar manner. The model for the family's catalytic activity is as follows: NADPH serves as the initial electron donor. Those are then shuttled via the FAD and heme co-factor intermediaries through the transmembrane domain before they reduce ferric iron to ferrous iron, which in the end allows divalent metal transporters to import Fe2+. It is still unresolved whether STEAP, which is lacking the N-terminal domain with NADPH oxidase activity and part of the FAD-organizing motif, is a functional metal reductase. As it retains the critical residues for heme and iron

binding and part of the interdomain flavin-binding motif, it might have reductase activity in complex with other proteins able to provide an electron source [43].

Green fluorescent protein (GFP)-tagged STAMP1 and STAMP2 ectopically expressed in simian Cos-1 cells have been shown to co-localize with the endosomal marker EEA1, while STAMP2 also co-localized with trans-Golgi markers and was found in cytosolic vesiculotubular structures, implicating both proteins in endo-/exocytic processes [32, 35]. Transplanted fetal liver hematopoietic cells expressing wild-type STAMP3 was able to rescue animals suffering from anemia due to a STAMP3 mutation [39]. The authors argued that the iron-reductase activity of STAMP3 account for this effect, as transferrin (Tf) and transferrin receptor (Tfr1), responsible for ferric iron endocytosis by erythroid precursors, and the divalent metal transporter 1 (Dmt1), all co-localized with STAMP3 in endosomal intracellular compartments. The loop connecting TM helices 2 and 3 oriented into the cytosol has been shown to include an endosomal targeting motif in STAMP3, and its sequence and position is conserved among all the STAMP family members [47]. This indicates that the STAMP family members are involved in endocytic processes and localized in associated cellular compartments.

1.3.2 STAMP proteins and cancer

STAMP1 was also initially identified as a gene with elevated expression both in PCa cell lines and patient samples [32, 33]. STAMP1 shows a prostate-restricted tissue distribution among healthy tissue. It was detected at high levels in AR-positive, but not in AR-negative PCa cell lines, but independently of the presence or absence of androgens. GFP-fused STAMP1 co-localized with cognate markers of trans-Golgi and endosomal compartments, and was detected in the plasma membrane [32, 33]. Over-expression of STAMP1 in STAMP1/AR-negative PCa cell lines increased cell proliferation, while siRNA-mediated knock-down of STAMP1 expression in STAMP1-positive PCa cell lines led to dramatically decreased growth rates [48]. STAMP1 knock-down also reduced PCa cell proliferation, inhibited expression of proliferation marker genes and sensitized the cells to apoptosis-inducing agents. A proposed mechanism by which STAMP1 drives PCa cell proliferation and protects against apoptosis was provided by the observation that activation of the MAPKs ERK1/2 after stimulation with epidermal growth factor (EGF) was positively correlated with the level of STAMP1 [48]. In experiments with moderate (2.2 fold) over-expression of

STAMP1 in the benign prostate cell line PNT2, it was found that increased STAMP1 expression led to both increased migration and invasion, further implicating STAMP1 as a candidate driver of tumorigenesis and a potential PCa biomarker [49].

The STAMP3 rat homolog pHyde was found to make rat PCa cell lines more susceptible to apoptosis [50]. Adenoviral delivery of rat pHyde was later also shown to induce apoptosis by initiating cleavage of caspase-3 in PCa cells both in vitro and in xenografts [51]. Tsap6 has been shown to be induced by tumor suppressor protein 53 (p53) in the murine myeloid M1 cell line. Its human homolog STAMP3, which shares the p53 response element in its regulatory region, was shown to augment p53-mediated cell-cycle arrest and induction of apoptosis in HeLa cells [38]. In line with these previous findings, the growth-limiting properties of STAMP3 was further supported when adenoviral delivery of STAMP3 to the human PCa cell line DU145 significantly limited proliferation, and in addition showed synergistic reduction of proliferation with co-treatment with cytotoxic drugs, both in vitro and in nude mice xenografts [52]. STAMP3 has also been shown to be involved in the transition from pre-cancerous, cirrhotic liver, where expression is higher, to hepatocellular carcinoma, where expression is lower than in healthy liver tissue, respectively [53]. Cirrhosis is liver damage caused by external factors as hepatitis C virus or excessive alcohol intake, and often develops further into cancer of the liver. The expression pattern of STAMP3 in these settings, validated both on mRNA and protein level, could indicate that damaged cells that should undergo apoptosis are associated with a high expression of STAMP3, while cancer cells developing from these pre-neoplastic lesions are able to avoid apoptosis by down-regulating STAMP3 [53]. Taken together, these results indicate that STAMP3, as opposed to STEAP and STAMP1, can play a tumor suppressor role in prostate and lung cancer by acting as a mediator of apoptosis. Contrary to the aforementioned results, STAMP3 has also been shown to aid in iron homeostasis when over-expressed in Raji cells with low innate STAMP3 expression, thereby allowing these cells to grow more rapidly under hypoferric conditions both in vitro and in xenografts. The same group reported higher levels of STAMP3 and higher levels iron storage in colon cancer compared to healthy tissue [54].

1.3.3 Regulation of STAMP2 expression

Both steroid hormones and protein inflammatory cytokines have been found to positively regulate STAMP2 expression in various cell types and experimental settings. For clarity, these results with references are summarized in table 2 before a more in depth discussion of physiological roles and cancer associations of STAMP2 follows below.

Table 2: Summary of positive regulators of STAMP2 expression in various cell types

Stimuli	Cell type	Evidence	Reference
Androgens	LNCaP, VCaP, 22Rv1 PCa cell lines	mRNA	[35, 42]
IL-17 *in vivo*	Mouse keratinocytes	mRNA	[75]
IL-1β	Mouse 3T3-L1 and human MSC adipocytes	mRNA, Protein	[112]
IL-6	Human cultured adipocytes	mRNA, Protein	[100]
IL-6	Mouse 3T3-L1 adipocytes	mRNA	[101, 112]
IL-6	Mouse brown adipose	mRNA	[101]
IL-6 *in vivo*	Mouse liver	mRNA, Protein	[59]
TNFα	Mouse 3T3-L1 adipocytes	mRNA	[55, 112]
TNFα	Human cultured adipocytes	mRNA, Protein	[60, 100]
TNFα, Macrophage-conditioned medium	Human sub-cutaneous adipocytes	mRNA	[56]

1.3.4 Physiological roles of STAMP2

STAMP2 is implicated in several physiological processes. Its expression has been found to be increasing during differentiation of pre-adipocytes and of osteoclast progenitors. It is also a central player in coordinating cellular responses to fluctuating levels of nutrients and inflammatory stimuli. These roles will be summarized in the following sections.

As mentioned, STAMP2 was initially identified due to its sequence similarity with STAMP1. It was identified as an androgen responsive gene, whose expression levels increase in PCa [35]. In the same report, northern blots of tissue mRNA panels identifies significant expression of STAMP2 in several other organs, most notably in heart, placenta, lung and liver where expression levels are higher than those in healthy prostate tissue. STAMP2 was later found to be highly expressed in adipose tissue; specifically, STAMP2 is up-regulated along with the process of pre-adipocyte differentiation into mature adipocytes in both humans and mice [55,56, 57]. STAMP2 was found to be critical for murine 3T3-L1 adipocyte differentiation, as shRNA-mediated knock-down of expression resulted in impaired production of peroxisome proliferator-activated receptor gamma (PPARγ) and CCAAT/enhancer-binding protein alpha (C/EBPα), critical players in the process [57]. STAMP2 has also been shown be involved in osteoclastogenesis; the differentiation of precursor cells of hematopoietic lineage into the multi-nucleated cells responsible for skeletal development and growth [58]. STAMP2 shRNA-mediated knock-down in precursor cells led to markedly decreased osteoclast formation and expression of osteoclast marker genes. It also led to decreased iron uptake and ROS formation, critical for mitochondrial biogenesis and CREB activation, respectively, in this differentiation process. As epitope-tagged STAMP2 was found localized in recycling endosomes, coinciding with the transferrin cycle, the authors conclude that the iron reductase activity of STAMP2 is a critical component of osteoclastogenesis [58].

STAMP2 has been most extensively studied in the context of obesity and the metabolic syndrome (MetS), associated with insulin resistance, diabetes type 2 and cardiovascular disease, among others. In mice, STAMP2 is regulated by nutritional status in visceral white adipose tissue (VAT), regarded as the most important fat depot in regulation of metabolic homeostasis [55]. Feeding induced stamp2 expression in wild-type (wt) murine VAT, but not in a mouse model of leptin-negative, genetically obese mice. Both in vitro siRNA mediated Stamp2 knock-down experiments with murine 3T3-LI adipocytes, and in vivo experiments with Stamp2 knock-out mice, showed that Stamp2 is involved in coordinating VAT nutrient and inflammatory responses; loss of Stamp2 led to decreased insulin-sensitivity and glucose uptake, while it led to an increase in the expression of inflammatory genes and the recruitment of macrophages. Furthermore, Stamp2 knock-out mice accumulated more body fat and developed systemic insulin resistance over time [55]. Stamp2 mRNA expression was also found to fluctuate similarly in murine liver tissue, along with other adipose tissues, by another

group [59]. These fluctuations were not matched on protein level, but kinetics of protein turnover could be outside of their experimental time-frame. This group showed that Stamp2 is a bonafide IL-6 target gene in murine livers, but that Stat3 as an intracellular mediator of IL-6 signaling was not responsible of regulating Stamp2 levels in response to changes in nutritional levels. Instead, this role was convincingly shown to be performed by the transcription factor C/EBPα. Contrary to observations in VAT, murine obesity models showed elevated Stamp2 levels in liver tissue, proposed to be due to heightened hepatic inflammatory signaling in this condition [59].

Similar observations have been made using a collection of 171 samples of human VAT: STAMP2 expression on both mRNA and protein levels were significantly higher in lean individuals compared to obese, while obese individuals with diabetes type 2 had an even lower VAT STAMP2 expression [56]. Furthermore, STAMP2 expression correlated positively with those of genes involved in lipogenesis and that of the inflammatory cytokine IL-6, while it was inversely correlated with parameters of metabolic homeostasis as blood pressure and serum glucose levels. Similar results on differential VAT STAMP2 expression between obese and normal weight control individuals were also published elsewhere [60]. The opposite result - that STAMP2 expression is higher in VAT from obese individuals - was found in another study, but after expression analysis of a lower number of subject samples and without performing cell-type fractionation of the VAT [61]. This study found that obesity was associated with higher expression of inflammation markers in VAT, which increase VAT macrophage infiltration [55] and induce macrophage STAMP2 expression [62]. The higher STAMP2 levels observed in VAT from obese individuals in this study could therefore be contributed by the macrophage fraction, supported by the detection of elevated macrophage cell surface markers [61]. STAMP2 expression was also found to be significantly higher in the stromal vascular fraction (SVF) of VAT, which includes macrophages, compared to the adipocyte fraction [56].

In a study of 97 Chinese volunteers, 48 of whom suffered from MetS, and the remainder served as healthy controls, circulating CD14+ monocyte STAMP2 expression was found to be lower in the MetS group, especially among women [63]. Furthermore, low STAMP2 expression in this cell type correlated with atherosclerosis and other markers of cardiovascular disease. This was corroborated by another study, where STAMP2 knockout further exacerbated atherosclerotic lesion formation in an Apolipoprotein E-negative atherogenic

mouse model background [62]. The same study found STAMP2 up-regulation during human monocyte differentiation and in murine peritoneal macrophages subjected to inflammatory stimuli by lipopolysaccharide (LPS). Furthermore, compared to controls, murine Stamp2-/- macrophages showed significantly elevated expression of IL-6 and inducible nitric oxide synthase (iNOS) after LPS stimulation, indicating that Stamp2 dampens inflammatory responses of macrophages. This modulating effect was showed to depend on the NADPH oxidase activity of Stamp2, both by chemical inhibition and by rescue experiments using N-terminal truncated Stamp2. A mechanism for the effect on inflammatory output was proposed to be through the NADPH sensor protein NMRAL1, which translocate to the nucleus and inhibits NF-κB signaling upon low NADPH levels [62]. Consistently with above mentioned results, in a murine diabetes model, STAMP2 expression was found to be decreased in white adipose tissue (WAT), coupled with a higher number of infiltrating macrophages [64]. Over-expression of STAMP2 in this background led to a decrease in the total numbers of infiltrating macrophages, and importantly also a decrease in the ratio of the more inflammatory M1 macrophage phenotype to alternatively activated M2 phenotype.

Taken together, this body of evidence involving STAMP2 in the regulation of both adipocyte maturation and metabolic and inflammatory homeostasis indicates that STAMP2 is an important mediator in adipose tissue functions in regulating homeostasis on the systemic level. It might similarly play a regulatory role in the liver, another organ equally important for systemic metabolic homeostasis. Likewise, STAMP2 plays an important role in regulating macrophage inflammatory behavior, the proper control of which again is key in multiple processes. Loss of this all important homeostasis, resulting in MetS with all its co-morbidities and/or diseases linked to over-active inflammation, often coincides with deregulation of STAMP2 expression, as has been summarized above. Whether these effects are directly linked to metalloreductase catalytic functions of STAMP2, indirect effects of this activity or other, hitherto unknown function(s) or protein-protein interactions needs to be further established. The direct evidence of STAMP2 NADPH oxidase activity in regulation of macrophage inflammation supports that iron homeostasis and ROS levels regulated by STAMP2 activity are directly involved [62]. Similarly, the implication of STAMP2 in regulation of ROS and overt inflammatory signaling, implicates its catalytic function as a barrier against insulin resistance, hyperglycemia, hepatic steatosis and related disorders with established links to such factors [65, 66].

1.3.5 STAMP2 and cancer

The backdrop of the work presented in this thesis is the association of STAMP2 with prostate cancer (PCa), an association which initially led to its discovery [35]. In this initial study, STAMP2 was detected by northern analysis in the AR-positive, androgen-responsive PCa cell line LNCaP [67], but not in the hormone-unresponsive PCa cell lines PC-3 and DU145 [68, 69]. STAMP2 expression was shown to be induced by androgen in LNCaP, with steadily increasing levels up to 48hrs after induction. Ectopic expression of STAMP2 in the negative cell lines PC3 and DU145, as well as in simian Cos-7 cells, led to increased cell growth compared to controls. Lastly, STAMP2 expression was found to be significantly up-regulated in 26 samples of matched microdissected neoplastic prostate lesions, establishing its association with PCa both in vitro and in vivo [35]

When ectopically expressed in HEK-293T cells, STAMP2 was found to reduce the number of viable cells in suspension culture by 90%, whereas adherent cell growth was unaffected [70]. This was found to coincide with a decrease in the level of activating tyrosine397-phosphorylation of focal adhesion kinase (FAK1), a non-receptor kinase that regulates integrin-mediated, adhesion-dependent survival signaling and whose deregulation is common in human cancers [71]. Both observations were partially reversed by adding STAMP2 mAb to the suspension medium. The inhibitory effect elicited by STAMP2 ectopic introduction on FAK activation, and thereby anchorage-independent growth, was suggested to be by direct regulation, as the two proteins were found to interact by immunoprecipitation assays [70]. The authors further predicted several CpG islands in the STAMP2 promoter and demonstrated by bisulfite genomic sequencing that these are frequently methylated in the STAMP2-negative DU145 PCa cell line, whereas they were not in LNCaP. De-methylating agents were also shown to restore STAMP2 expression in DU145 cells. Although LNCaP also was established from metastatic disease, it was suggested that this might indicate an epigenetic down-regulation of STAMP2 as PCa progress from androgen-responsive cancer to more aggressive, androgen-independent CRPC [70].

That notion was contradicted in the latest report on STAMP2 in PCa [42]. STAMP2 expression in PCa tissue microarrays correlated both with higher Gleason score and with BCR. Increasing STAMP2 expression further correlated with cancer stage in two independent matched primary and CRPC PCa cohorts, clearly showing that it is present at high levels in clinical CRPC. STAMP2 was also shown to be critical for the three PCa cell lines LNCaP,

VCaP [72] and 22Rv1 [73]. Both transient siRNA-mediated and stable shRNA-mediated knock-down of STAMP2, used in multiple in vitro and in vivo xenograft studies, confirmed its importance for PCa cell proliferation. In LNCaP cells, STAMP2 knock-down led to increased sensitivity to apoptosis-inducing drug, while this was reversed by over-expression [42]. Furthermore, a mechanism for PCa cell reliance on STAMP2 for growth was suggested, one depending on the catalytic activity of the protein: First it was established that HEK-293T cells with inducible STAMP2 expression reduce ferric iron in amounts correlated with STAMP2 level. It was then demonstrated that STAMP2 is positively correlated with ROS levels and inversely correlated with NADPH levels in LNCaP cells, products of its catalytic activity. Further, intact STAMP2, but not catalytically inactive mutants, increase LNCaP colony formation and induce the expression of Cyclic AMP-dependent transcription factor 4 (ATF-4). ATF4 is a pro-survival factor involved in adaptation to cell stress [74], and its correlation with STAMP2 expression in PCa was further supported by correlation analyses of three independent PCa microarray datasets. Experimental confirmation of this link was observed by ATF4-mediated rescue of proliferation after knock-down of STAMP2 in LNCaP cells [42].

Recently, Stamp2 was shown to play an integral part in a novel intracellular signaling pathway driving tumorigenesis in a murine model of cutaneous squamous cell carcinoma (SCC) [75]. After following a DMBA (7,12-dimethylbenz(a)anthracene) and TPA (tetradecanoyl phorbol acetate) tumorigenesis protocol for up to 20 weeks of age, the role of the inflammatory cytokine interleukin 17 (IL-17) in early tumorigenesis was studied further. IL-17 had previously been shown to be linked to skin cancer development [76]. That was further supported in the present study, as genetic manipulation of the discovered pathway severely reduced DMBA/TPA-induced tumor burden [75]. Specifically, IL-17 was shown to induce the interaction of Act1 (nuclear factor kappaB activator 1) and TNF receptor associated factor 4 (TRAF4) downstream of the IL-17 receptor (IL-17R). This interaction again led to the activation of the MAP kinase ERK5, a target gene of which proved to be Stamp2. Moreover, Stamp2 was shown to be involved in a positive feedback loop maintaining the TRAF4-ERK5 axis and establishing it as the dominant keratinocyte mitogenic pathway in this setting.

Supporting the significance of these results was the finding that STAMP2 expression was elevated in human SSC samples compared to normal skin. This elevated expression was

correlated with that of TRAF4, which again is over-expressed in multiple human cancers [75]. This observation indicates another possible mechanism for modulation of inflammatory signaling by STAMP2 besides the proposed role of NMRAL1 mentioned above [62]: The TRAF4-ERK5 axis predominates downstream of the IL-17R in keratinocytes as Stamp2 expression maintains TRAF4 at a high level, enabling a stoichiometric advantage over other TRAF members in competition for Act1-dependent activation. Specifically, members as TRAF2/5 and TRAF6 branch out and activate inflammatory output downstream of IL-17R by stabilizing inflammatory cytokine mRNAs and activating the Nuclear Factor kappaB pathway, respectively [77].

Taken together, these data also position STAMP2 as a critical player in cancer, although that might seem contradictory for a protein with demonstrable cell-protective roles in other contexts. Cellular outcomes of elevated STAMP2 expression seem to depend on the biological function, metabolic activity and genetic background of the specific cell type in question. STAMP2 might therefore not be a general cancer biomarker, but could potentially serve as such and a therapeutic target for PCa. As a target, disturbance of its functions would have to be cancer-targeted, to not interfere with its important roles in metabolic and inflammatory homeostasis.

2 Aim of the study

The starting point for the presented work was the role of STAMP2 in the context of PCa. Two parallel projects were followed. These are not directly linked, but both tie STAMP2 to immunology in different ways.

The first project is the identification of short isoform of STAMP2, called STAMP2_v1. The isoform is listed in reference databases after its detection during whole-transcriptome sequencing, but is otherwise not described. As STAMP2 has been shown to be important for PCa cell growth, the aim of the first project was to clarify whether this isoform is in any way linked to PCa. Isoform-pecific primers were designed for this purpose, and RNA from three different PCa cell lines were probed for its presence by quantitative PCR. To investigate whether it is relevant in other contexts besides PCa, multiple tissue cDNA panels were used as template for qPCR. Lastly, online protein domain prediction software was used to investigate its potential structure.

As cancer has established links to chronic inflammation, and regulation of STAMP2 is affected by inflammatory stimuli in other cell types, the aim of the second project was to determine whether inflammatory signaling molecules, cytokines, regulated STAMP2 expression in PCa cells. If so, the second aim of this project was to uncover some of the mechanisms of cytokine-mediated regulation of STAMP2 expression. These questions were investigated using the following strategies:

- *In vitro* cytokine treatments of the commonly used PCa cell line LNCaP followed by STAMP2 expression analysis by qPCR
- Western analysis of changes in protein expression after cytokine signaling
- Use of RNA interference and chemical inhibition to interfere with putative regulators of STAMP2 expression.

3 Materials and Methods

3.1 Materials

AppliChem, Darmstadt, Germany.
- Polyacrylamide (40%)

BI Biological Industries, Kibbutz Beit-Haemek, Israel.
- Fetal bovine serum (FBS)

Bio-Rad Laboratories Inc., Hercules, CA, USA.
- 4 x Laemmli sample buffer
- Protein Assay Dye Reagent Concentrate, cat.# 500-0006
- Clarity™ Western ECL substrate, cat.# 170-5060
- Immunoblot ™ polyvinylidene fluoride (PVDF) membrane
- Precision Plus Dual Color protein standard

Biotool (Selleck chemicals)
- All-in-one cDNA Synthesis SuperMix, cat.#B24408

BioWhittaker-Lonza, Rockland, ME, USA.
- DMEM 1640 media, cat.#BE12-709F
- L-glutamine cat.#BE17-605E
- MycoAlert ® Mycoplasma Detection Kit
- Penicillin/streptomycin, cat.#DE17-603E
- RPMI 1640 media, cat.#BE12-115
- RPMI 1640 media w/o L-Gln Phenol-red, cat.#BE12-918F
- SeaPlaque® Agarose
- Trypsin EDTA, cat.#CC-5012

Calbiochem, Merck Millipore, Darmstadt, Germany
- PD98059 MEK1/2 inhibitor
- SP600125 JNK1-3 inhibitor
- SB203580 p38 inhibitor

Cell Signaling Technology, Boston, MA, USA.
- Erk1/2 rabbit pAb
- Phospho-Erk1/2 rabbit pAb
- JNK rabbit pAb
- Phospho-JNK rabbit pAb
- NF-κB p65 rabbit pAb
- Phospho-NF-κB p65 rabbit pAb
- p38 MAPK11 rabbit pAb
- Phospho- p38 MAPK11 rabbit pAb
- Phospho-STAT3 rabbit mAb
- Phospho-STAT3 rabbit pAb

Clontech Laboratories, Mountain View, CA, USA.
- Human MTC cDNA panels, Cat#636742, #636743

GenScript, Piscataway, NJ, USA.
- Plasmid DNA

Invitrogen, Carlsbad, CA, USA.
- Dithiothreitol (DTT)
- Superscript™ II Reverse Transcriptase kit, cat.#18064

Kemetyl AS, Halden, Norway
- Ethanol 100%

Life technologies, Thermo Fisher Scientific Inc.
- Lipofectamine RNAiMAX
- Recombinant human Interleukin 6, cat.#10395-HNAE
- Recombinant human Tumor necrosis factor alpha, cat.#PHC3015

New England Biolabs ® Inc., Ipswich, MA, USA.
- 2-Log DNA Ladder
- DNA loading buffer
- dNTP (deoxyribonucleotide) mix

Promega, Madison, WI, USA.
- Recombinant RNasin® Ribonuclease Inhibitor

Proteintech, Manchester, U.K.
- HDAC1 rabbit pAb
- STAMP2 rabbit pAb

QIAGEN, Hilden, Germany.
- RNeasy® MiniKit (250)
- siRNA

Roche Diagnostics Corp., IN, USA.
- Lightcycler ® 480 SYBR green I Master
- Magnesium chloride ($MgCl_2$)
- PCR grade H_2O
- 4-(2-Hydroxyethyl)piperazine-1-ethanesulfonic acid (HEPES)
- Acetic acid
- Activated charcoal
- Ammoniumpersulfate (APS)
- Bovine serum albumin (BSA)
- Bromphenol blue
- Chloroform
- Dry skimmed milk
- Ethidium bromide
- Glycine
- Horseradish peroxidase (HRP)-conjugated α-mouse IgG antibody
- Horseradish peroxidase (HRP)-conjugated α-rabbit IgG antibody
- Phenylmethylsulfonyl fluoride (PMSF)
- Protease inhibitor cocktail (PIC)
- Sodium azide (NaN_3)
- Sodium dodecyl sulphate (SDS)
- Tetramethylethylenediamine (TEMED)
- Octyl phenoxy polyoxy ethanol (Triton® X-100)
- Whatman® cellulose chromatography papers

Santa Cruz Biotechnology Inc., Santa Cruz, CA, USA.
- Androgen Receptor mouse mAb
- beta Actin mouse mAb
- c-Jun rabbit pAb
- phosho-c-Jun rabbit pAb
- GAPDH mouse mAb
- IκBα rabbit pAb

Selleck chemicals, Houston, TX, USA.
- AZD1480 JAK2 inhibitor

Sigma-Aldrich, St. Louis, MO, USA.
- 10x PBS
- 2-propanol
- 37% HCl
- Dimethyl sulfoxide (DMSO)
- Oligo-dT reverse transcription primer
- PCR primers
- R1881 synthetic androgen
- Recombinant human Interleukin 1β, cat.#I9401
- TRI reagent, cat.#T9424
- Tween ® 20

Thermo Scientific, Rockford, IL, USA.
- Restore™ western blot stripping buffer

TransGen Biotech, Beijing, China
- *ProteinExt*™ Mammalian Nuclear and Cytoplasmic Protein Extraction kit, cat.#DE201

VWR International, Leuven, Germany.
- Ethylenediaminetetra-acetic acid disodium salt (EDTA)
- Methanol
- Sodium chloride (NaCl)
- Sodium hydroxide (NaOH)
- Tris(hydroxymethyl)aminomethane

3.2 Methods

Cell culture

LNCaP cells (human prostate carcinoma, lymph node metastasis, ATCC# CRL-1740) and 22Rv1 cells (derived from serial xenografts of the parental human prostate carcinoma CWR22R in nude mice, ATCC#CRL-2505) were routinely maintained in RPMI 1640 culture medium (Lonza) supplemented with 10% fetal bovine serum (FBS, BI) and 50 U/mL Penicillin/Streptomycin (Lonza). LNCaP cells used for all experiments were from passages between 20 and 30.

VCaP cells (human prostate carcinoma, vertebral metastasis-derived cell line, ATCC#CRL-2876) were routinely maintained in Dulbecco's Modified Eagle's Medium (DMEM, Lonza) supplemented with 5% FBS, 50 U/mL Penicillin/Streptomycin and 2mM L-Glutamine (L-Gln, Lonza).

For hormone induction experiments with androgen, PCa cell lines were cultured in RPMI1640 medium supplemented with 10% charcoal-stripped FBS (CS-FBS).

For all cell lines, the culture medium was changed every two-three days. Cells were incubated at 37°C in a humidified 5% CO2, 95% air incubator. MycoAlert Mycoplasma Detection Kit (Lonza) was used to ensure that the cells were free of mycoplasma contamination.

Cell culture treatments

Synthetic androgen R1881 (methyltrienolone, Sigma) was dissolved in ethanol and stored dark at -20^{o}C. For hormone induction of PCa cell lines, the cells were hormone starved for 24hrs prior to induction, and induced by adding R1881 to a final concentration of 1nM. Ethanol was used as vehicle control.

Lyophilized recombinant human interleukin 1β (IL-1β, Sigma) was reconstituted in pure water to a concentration of 0,1mg/mL as per the manufacturer's instruction. Aliquots of 10µg/mL were prepared by diluting the stock solution in phosphate-buffered saline (PBS, Sigma) and stored in -20^{o}C. Lyophilized recombinant human interleukin 6 (IL-6, Life Technologies) and recombinant human tumor necrosis factor alpha (TNFα, Life Technologies) was prepared as described for IL-1β.

For cytokine treatment experiments, LNCaP cells were cultured for one to two days in regular growth medium before medium starvation in serum-free RPMI medium for 5 or 13 hrs. The cells were then treated dropwise with IL-1β, IL-6 or TNFα and incubated for the indicated time prior to RNA or protein extraction. Equal volumes of PBS were used as vehicle control.

Small-molecule kinase inhibitors, along with their producers, intended molecular targets, stock- and working concentrations are listed in table 3. The inhibitors were dissolved in dimethyl sulfoxide (DMSO, Sigma) and stored dark in -80^{o}C. For kinase inhibitor experiments, LNCaP cells were cultured for three days in regular growth medium before the cells were treated with serum-free RPMI medium containing the final inhibitor concentration for two hours prior to cytokine induction. Medium containing equal volumes of DMSO was used as vehicle control.

Table 3: List of small-molecule kinase inhibitors

Chemical/ inhibitor	Company/ cat.#	Target kinase	Stock concentration	Final concentration
AZD1480	Selleckchem #S2162	JAK2	0.5 mM	0.5 µM
PD98059	Calbiochem #513000	MEK1, MEK2	50 mM	50 µM
SP600125	Calbiochem #420119	JNK1, JNK2, JNK3	10 mM	10 µM
SB203580	Calbiochem #559389	p38/MAP kinase 11	20 mM	20 µM

RNA interference

Knock-down of gene expression by RNA interference (RNAi) by transfection of short interfering RNAs (siRNA) was performed using the Lipofectamine RNAiMAX Reagent (Invitrogen) according to the manufacturer's protocol for forward transfection with slight modifications. Briefly, LNCaP cells were cultured in in 6-well plates until 70-80% confluence prior to transfection. The transfection mixtures of siRNAs and RNAiMAX were prepared in serum-free RPMI 1640 medium w/o L-Gln and Phenol red (Lonza), and applied to the cells to a final siRNA concentration of 10nM per well. siRNA molecular targets and their suppliers are listed in table 4.

Table 4: siRNA target sequences

Target	Gene ID	Target sequence 5'-> 3'	Company, cat#
NFκB1/p50	4790	AACAGAGAGGATTTCGTTTCC	Qiagen, #SI003009958
STAT3 #7	6774	CAGCCTCTCTGCAGAATTCAA	Qiagen, #SI02662338
STAT3 #8	6774	CAGGCTGGTAATTTATATAAT	Qiagen, #SI02662898

RNA isolation

Total RNA was isolated using the RNeasy mini kit (Quiagen) according to the manufacturer's instructions, or by using the TRI reagent (Sigma) according to the manufacturer's instructions with modifications. Briefly, medium above cells was removed by aspiration followed by a wash with cold PBS. TRI reagent was then added directly to the culture plates to lyse cells for 5 minutes, followed by chloroform extraction and isopropanol precipitation. RNA pellets were then washed twice with 70% ethanol before resolving RNA in DEPC-treated/RNAse free water.

Integrity of isolated RNA was examined using agarose gel electrophoresis. RNA concentration and purity was measured using a NanoDrop 1000 (ThermoFisher) spectrophotometer. Isolated RNA was stored at -80^{o}C or used immediately for cDNA synthesis.

Agarose gel electrophoresis

Agarose gel electrophoresis was used to investigate integrity, size and purity of total RNA, plasmid preparations and PCR products. Briefly, agarose gels are cast by boiling 1 or 1.5% w/v agarose (Lonza) powder in Tris acetate EDTA (TAE) buffer. The gels are submerged and run in the same TAE buffer after applying samples mixed with 6x loading buffer (New England Biolabs).

Reverse transcription

Complementary DNA (cDNA) synthesis was performed using SuperScript II Reverse Transcriptase (Invitrogen) or All-in-one cDNA Synthesis SuperMix (Biotool) according to the manufacturers' recommendations. For SuperScript II Reverse Transcriptase reactions, 1 or 1.5 µg total RNA was diluted to equal volumes in DEPC-treated/RNAse-free water, mixed with 10 mM dNTP mix (New England Biolabs) and 0,5 µM oligo-dT primer and incubated at 65°C for 5 minutes. Then a reaction mixture was added containing 1x first strand buffer, DEPC-

treated/RNAse-free water, 0.01 M DTT, 40 U RNAsin Rnase inhibitor and 200 U SuperScript ™ II Reverse Transcriptase. cDNA synthesis was carried out at 42°C for 50 min, followed by enzyme inactivation at 70°C for 15 min.

For All-in-one cDNA Synthesis SuperMix, 1 or 1.5 µg total RNA was diluted to equal volumes in DEPC-treated/RNAse-free water before adding the SuperMix. cDNA synthesis was carried out with the following consecutive steps: pre-incubation at 25^{o}C for 10 minutes, extension at 42^{o}C for 30 minutes and termination at 85^{o}C for 5 minutes. cDNA was used immediately or stored at -20°C until use.

Plasmid DNA

The SRalpha3HA expression vector containing the open reading frame (ORF) of STAMP2 isoform 1 mRNA (NM_024636.3) was cloned as described previously [42]. The pcDNA3.1(+) expression vector containing the STAMP2 isoform 2 (STAMP2_v1) mRNA (NM_001205316.1) ORF was purchased from GenScript. The vectors were used in qPCR analyses as positive control and in dilution series for standard curve measurements.

Real-time quantitative polymerase chain reaction (qPCR)

qPCR was carried out on the Lightcycler 96 or Lightcycler 480 platforms using the SYBR Green I Master (all from Roche Diagnostics). The master mix was added gene-specific primers to a final concentration of 0.5µM per primer per reaction and mixed beforehand in one Eppendorf tube per gene under investigation. Master mixes with primers were then added to multiwell 96 plates (Roche) before adding 4µL diluted cDNA for final reaction volumes of 10µL per reaction. cDNA synthesized from 1µg total RNA was diluted 1:7.5 or 1:10 before qPCR, while cDNA synthesized from 1.5 µg total RNA was diluted 1:12 or 1:15. qPCR was run with the parameters listed in table 5.

Melting curve analysis was routinely used to ensure specificity of PCR product. A list of all target mRNAs with their corresponding primer sequences are given in table 6, along with primer annealing temperature as provided by the manufacturer (Sigma). Annealing temperatures in individual experiments varied depending on primer sets used.

Table 5: Parameters for qPCR

Step	Temperature	Duration	Cycles
Pre-incubation	95°C	10 minutes	1
Denaturing	95°C	10 seconds	50
Annealing	60-65 °C	10 seconds	
Elongation	72 °C	10 seconds	
Denaturing	95°C	10 seconds	1
Annealing	65°C	60 seconds	1
Melting	Continuous, 65-97 °C	0.2 °C/second	1

Table 6: List of primers used in qPCR analysis

Target	Forward primer, 5'-3'	Tm	Reverse primer, 5'-3'	Tm
A20	GACCATGGCACAACTCATCTCA	67.3	GTTAGCTTCATCCAACTTTGCGGCATTG	74.2
βActin	GGCTACAGCTTCACCACCAC	64.7	GTCAGGCAGCTCGTAGCTCT	63.8
CCL2	TGTCCCAAAGAAGCTGTGATC	64.2	ATTCTTGGGTTGTGGAGTGAG	62.9
GAPDH	GTCAGTGGTGGACCTGACCT	64.2	TCGCTGTTGAAGTCAGAGGA	63.9
IκB	CCGCACCTCCACTCCATCC	70.4	ACATCAGCACCCAAGGACACC	68.5
IL-6	CCCAGGAGAAGATTCCAAAGAT	64.3	GCTGCTTTCACACATGTTACTC	61.4
IL-8	CTGCGCCAACACAGAAATTA	63.7	CATCTGGCAACCCTACAACA	63.6
KLK4	GCTAACGACCTCATGCTCATCAAG	67.8	CTCCTCAGACACCACCGACAC	67.2
NFkB1/ p50	AAGTACAGGTCCAGGGTATAG	56.3	ATGCTTCATCCCAGCATTAG	61.5
PSA	CCCTGAGCACCCCTATCAAC	65.6	TGAGTGTCTGGTGCGTTGTG	66.3
SOCS3	CCCAGAAGAGCCTATTACATCTAC	60.9	AGCTGGGTGACTTTCTCATAG	59.9
STAMP2	CTTGGTAGCTCTGGGATTTG	61.2	GAGAATCCATTTAGCACCTCC	61.4
STAMP2_ v1	AGTCGGCAGGCAATACTCA	63.5	CTGGACAAATCGGAACTCTCTC	64.0
STAT3	CAACCTTGACTCCCTTTCTC	60.3	GGAAGCCAGAATCAGAAGTATC	60.7
TMPRSS2	GGACAGTGTGCACCTCAAAGA	66.0	TCCCACGAGGAAGGTCCC	67.6

10-fold dilution series of template solutions containing the targets under investigation were run with each experiment to produce standard curves for each gene under investigation in a given experiment. Internal reference reactions targeting one or two of the reference genes beta Actin and/or glyceraldehyde-3-phosphate dehydrogenase (GAPDH) were included in each experiment. The crossing point (Cp) values, the maximal value of the second derivative of the fluorescence curves measured in real-time for each reaction, were then used to calculate relative gene expression on mRNA level, normalized by internal reference(s).

To specifically detect and quantify STAMP2_v1, primer sets were designed using the online software PrimerQuest (Integrated DNA technologies) and optimized for qPCR. One sequence of each primer pair was limited to the sequence around the exon 2-4 junction, unique to this isoform. To explore tissue distribution of STAMP2_v1, two multiple tissue cDNA panels (Clontech) were used as template. They each consisted of 8 samples of first-strand cDNA synthesized from tissue-specific RNA, pooled from multiple healthy donors varying across both gender and age. To compare ratios of STAMP2_v1 to the full-length, predominant isoform, standard curves were produced using known concentrations of plasmid DNA containing both ORFs.

Statistical analysis

Two-tailed, two-sample homoscedastic Student's t-tests were performed using Microsoft Excel software for statistical analysis of gene expression data. P-values below 0.05 were considered statistically significant. In figures, * refers to $0.05 > p > .01$, while ** refers to $p < 0.01$.

Bioinformatic analyses

Sequence alignments were performed with Clustal Omega 1.2.1 (EMBL). Protein domain predictions were performed by the online tools InterPro (EMBL), Prosite (expacy.org) and the Conserved Domain Database (NCBI).

Protein extraction

Cultured cells were washed with ice-cold PBS before being harvested in ice-cold PBS using cell scrapers, collected and spun down at 2500rpm in 4^{o}C for three minutes. Cell pellets were either stored in -80^{o}C or immediately re-suspended in ice-cold WCB lysis buffer containing proteinase and phosphatase inhibitors (20mM Hepes pH 7.7, 300mM NaCl, 0.2mM EDTA,

0.1% Triton X100, 1.5mM $MgCl_2$, 1mM DTT, 10mM phenylmethylsulfonyl fluoride (PMSF), 10mM protease inhibitor cocktail (PIC) and 1x PhosSTOP) and incubated on rotation in 4^{o}C for 30-60 minutes. Cell debris was spun down at 12,000rpm at 4^{o}C for 5 minutes and concentrations of supernatant protein lysates were measured using a Bradford protein assay reagent (Bio-Rad) according to the manufacturer's instructions. Absorbance at 595nm was measured using a Wallac 1420 Victor2 plate reader (PerkinElmer). 1µg/µL bovine serum albumin (BSA) solutions were used to produce standard curves.

Nuclear protein fractions were isolated using a subcellular fractionation kit (TransGen) according to the manufacturer's instruction.

Sodium dodecyl sulphate polyacrylamide gel electrophoresis (SDS-PAGE)

SDS-PAGE was performed according to Laemmli [78] with modifications. Equal amounts of protein were diluted to equal volume in WCB buffer before being added 4xLaemmli loading buffer (50mM Tris-HCl, pH 6.8, 2% SDS, 0.1% bromphenol blue, 10% glycerol) and DTT to a final concentration of 5mM. Samples were incubated for a minimum of 10 minutes, including a denaturing step at 98^{o}C for 3 minutes, before samples were applied on 10% or 12% polyacrylamide gels. Precision Plus Dual Color protein standard (Bio-Rad) was included as molecular weight marker.

Western blotting

After separation by SDS-PAGE, proteins were transferred to methanol-activated polyvinylidene fluoride (PVDF) membranes (0.2 µm, Bio-Rad) by semi-dry transfer, performed by applying 0.2A for 30 minutes per blot in semi-dry transfer buffer (20% methanol, 50mM Tris, 40mM glycine, 1.2mM SDS). After transfer, membranes were blocked in 5% w/v skimmed milk dissolved in tris-buffered saline with tween (TBS-T, 0.2M Tris-HCl, 1.4M NaCl, 0.1% Tween 20) for 30-60 minutes. After wash in TBS-T, membranes are incubated with primary antibodies on rotation at 4^{o}C overnight. A list of primary antibodies with their preparation conditions is given in table 7. After wash the next day, membranes were incubated for 45-60 minutes in room-temperature with horseradish peroxidase-conjugated (HRP) secondary/detection antibodies (Roche). Anti-rabbit and anti-mouse secondary antibodies were diluted 1:10,000 and 1:5,000 in TBS-T, respectively. Membranes were then washed four times, incubated briefly in Clarity^{TM} HRP substrate (Bio-Rad) and

developed using a Kodak 4000R Image Station. Membranes were incubated in Restore™ stripping buffer for 10-20 minutes and re-blocked in 5% skimmed milk for 30 minutes to detect other target proteins, as e.g. reference proteins for gel loading controls.

Table 7: List of primary antibody targets, size, species of origin, along with manufacturer's catalogue numbers and individual antibody preparation conditions.

Target protein	Size, kDa	Origin	Provider, cat.#	Preparation (in TBS-T)
βActin	43	Mouse mAb	SantaCruz, #47778	1:1000, 1% BSA w/NaN_3
AR	132	Mouse mAb	SantaCruz, #52309	1:500, 1% BSA w/NaN_3
c-Jun	39	Rabbit	SantaCruz, #42	1:500, 1,5% BSA w/NaN_3
phospho-c-Jun (S63/S73)	39	Rabbit	SantaCruz, #16312	1:500, 1,5% BSA w/NaN_3
ERK1,2 MAPK	42, 44	Rabbit	Cell Signaling, #9102	1 :1000, 5% BSA w/NaN3
phospho-ERK1,2 MAPK (T202, Y204)	42, 44	Rabbit	Cell Signaling, #9101S	1 :1000, 5%BSA w/NaN_3
GAPDH	37	Mouse mAb	SantaCruz, #47724	1:2000, 1% BSA w/NaN_3
HDAC1	55	Rabbit IgG	Proteintech, #10197-1-AP	1:800, 1% BSA w/NaN_3
IkBα	40	Rabbit	SantaCruz, #371	1:333, 1% BSA w/NaN_3
JNK/SAPK1-3	46, 54	Rabbit	Cell Signaling, #9252	1 :1000, 5% BSA w/NaN_3
phospho-JNK/SAPK1-3 (T183/T185)	46, 54	Rabbit	Cell Signaling, #9251	1 :1000, 5% BSA w/NaN_3
NF-κB p65	65 (80)	Rabbit	Cell Signaling, #3034	1 :1000, 5%BSA w/NaN_3
phospho-NF-κB p65 (Ser536)	65 (80)	Rabbit	Cell Signaling, #3031	1 :1000, 5%BSA w/NaN_3

Target protein	Size, kDa	Origin	Provider, cat.#	Preparation (in TBS-T)
p38 MAPK11	43	Rabbit	Cell Signaling, #9212	1 :1000, 5% BSA w/NaN_3
phospho-p38 MAPK11 (T180, Y182)	43	Rabbit	Cell Signaling, #9211	1 :1111, 5% BSA w/NaN_3
STAMP2	54	Rabbit	Proteintech, #11944-1-AP	1:1000, 1%BSA w/NaN_3
phospho-STAT1 (Y701)	86, 91	Rabbit mAb	Cell Signaling, #7649	1:1000, 5% BSA w/NaN_3
phospho-STAT3 (Y705)	α-86 β-79	Rabbit mAb	Cell Signaling, #9145	1:2000, 3,25% BSA w/NaN_3
phospho-STAT3 (S727)	86	Rabbit	Cell Signaling, #9137	1:1000, 3,25% BSA w/NaN_3

4 Results

4.1 STAMP2 transcript variants

The STAMP2 gene (Gene ID 79689) contains five exon and four introns. Three alternative splice variants of STAMP2 have been identified and published in the NCBI database. Variant 1 (NM_024636.3) is listed as the predominant transcript. Variant 2 (NM_001205315.1) differ from the other two in the 5‘ untranslated region (UTR); it contains an extra non-coding 99 base-pair (bp) exon immediately upstream of the start codon. Variant 1 and 2 encode the same protein product. Since the PCR primer-pair used in these experiments to detect STAMP2 mRNA target the ORF, they cannot distinguish transcript variants 1 and 2. The two transcripts are therefore below referred to as “the full-length transcript” or *STAMP2* in the meaning that they encode full-length STAMP2. This is a simplification that does not preclude the possibility that the difference in the 5’ UTR might lead to differences in properties as e.g. stability, localization or regulation of translation between the two variants.

The difference in mRNA sequence between variant 3 (NM_001205316.1) and the other two is in the open reading frame (ORF) of the transcript. Alternative splicing of STAMP2 pre RNA excludes exon 3, as is illustrated in figure 6. Transcript variant 3 therefore encodes a shorter putative protein product. Alignment of primary protein structures is given in figure 7.

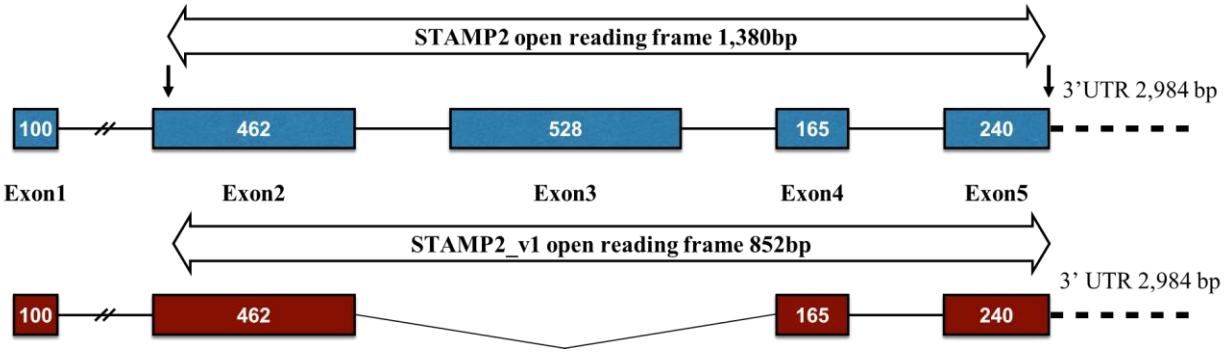

Figure 6: Structures of STAMP2 mRNAs. The five exons of STAMP2 are displayed in relative sizes and numbered with length in base-pairs. Transcription start- and stop sites are indicated by arrows. The figure illustrates how alternative splicing affects the size of the ORF of STAMP2 variants.

The reference sequence of STAMP2 transcript variant 3 (NM_001205316.1) originates from three independent cDNA sequencing consortia; it was found in a cDNA clone synthesized from lung tissue mRNA by the National Institutes of Health Mammalian Gene Collection (MGC) Program [79] and submitted in 2002; in a clone arising from lymph node mRNA and submitted in 2005 by the German cDNA Consortium [80]; and by the NEDO human cDNA project in Japan, which have entered the sequence directly into the database twice in January 2008 outside of any publications, but have previously published their methods [81]. By this group, transcript variant 3 was sequenced from cDNA clones originating from mRNA from hippocampus- and rheumatoid arthritis synovial membrane tissue. Beyond these sequence entries, there is no other reference to transcript variant 3 or its hypothetical protein product in humans.

```
STAMP2          MEKTCIDALPLTMNSSEKQETVCIFGTGDFGRSLGLKMLQCGYSVVFGSRNPQKTTLLPS     60
STAMP2_v1       MEKTCIDALPLTMNSSEKQETVCIFGTGDFGRSLGLKMLQCGYSVVFGSRNPQKTTLLPS     60
                ************************************************************

STAMP2          GAEVLSYSEAAKKSGIIIIAIHREHYDFLTELTEVLNGKILVDISNNLKINQYPESNAEY     120
STAMP2_v1       GAEVLSYSEAAKKSGIIIIAIHREHYDFLTELTEVLNGKILVDISNNLKINQYPESNAEY     120
                ************************************************************

STAMP2          LAHLVPGAHVVKAFNTISAWALQSGALDASRQVFVCGNDSKAKQRVMDIVRNLGLTPMDQ     180
STAMP2_v1       LAHLVPGAHVVKAFNTISAWALQSGALDASRQ---------------------------     152
                ********************************

STAMP2          GSLMAAKEIEKYPLQLFPMWRFPFYLSAVLCVFLFFYCVIRDVIYPYVYEKKDNTFRMAI     240
STAMP2_v1       ------------------------------------------------------------     152


STAMP2          SIPNRIFPITALTLLALVYLPGVIAAILQLYRGTKYRRFPDWLDHWMLCRKQLGLVALGF     300
STAMP2_v1       ------------------------------------------------------------     152


STAMP2          AFLHVLYTLVIPIRYYVRWRLGNLTVTQAILKKENPFSTSSAWLSDSYVALGILGFFLFV     360
STAMP2_v1       ----------------------------AILKKENPFSTSSAWLSDSYVALGILGFFLFV     184
                                            ********************************

STAMP2          LLGITSLPSVSNAVNWREFRFVQSKLGYLTLILCTAHTLVYGGKRFLSPSNLRWYLPAAY     420
STAMP2_v1       LLGITSLPSVSNAVNWREFRFVQSKLGYLTLILCTAHTLVYGGKRFLSPSNLRWYLPAAY     244
                ************************************************************

STAMP2          VLGLIIPCTVLVIKFVLIMPCVDNTLTRIRQGWERNSKH  459
STAMP2_v1       VLGLIIPCTVLVIKFVLIMPCVDNTLTRIRQGWERNSKH  283
                ***************************************
```

Figure 7: Protein sequence alignment of STAMP2 isoforms. Sequence alignment was produced by entering the reference sequences of both isoforms into the Clustal Omega 1.2.1 online software.

4.1.1 Prediction of STAMP2 short isoform protein structure

The putative short STAMP2 isoform (STAMP2_v1) would miss an internal 173 amino acid (aa) long part of the sequence compared to full-length STAMP2. The online protein domain prediction software InterPro (EMBL) was used to predict and compare protein domains in the two STAMP2 primary structures to investigate possible structure-functions of STAMP2_v1. As is shown in figure 8, InterPro predicts the six 21aa transmembrane (TM) helices in the full-length structure, a hallmark of the STAMP family of proteins and part of their names. Orientations of the N- and C-terminals, which both face the cytosolic side of the membrane, along with those of the loops (alternating) connecting TM helices are also shown in the figure. InterPro also predicts the coupled functional or catalytic domains of STAMP2. First, this is the N-terminal NADPH-binding domain with its FAD-dependent catalytic core motif, recognized due to its similarity to Pyrroline-5 carboxylate reductase [82]. Second is the iron reductase domain, which is shown to span the middle four of the six transmembrane domains. The two conserved histidine residues, H304 and H397, shown to be critical for human STAMP2 iron reductase activity by site-directed mutagenesis [42], is found within this domain located in TM helices 3 and 5, respectively.

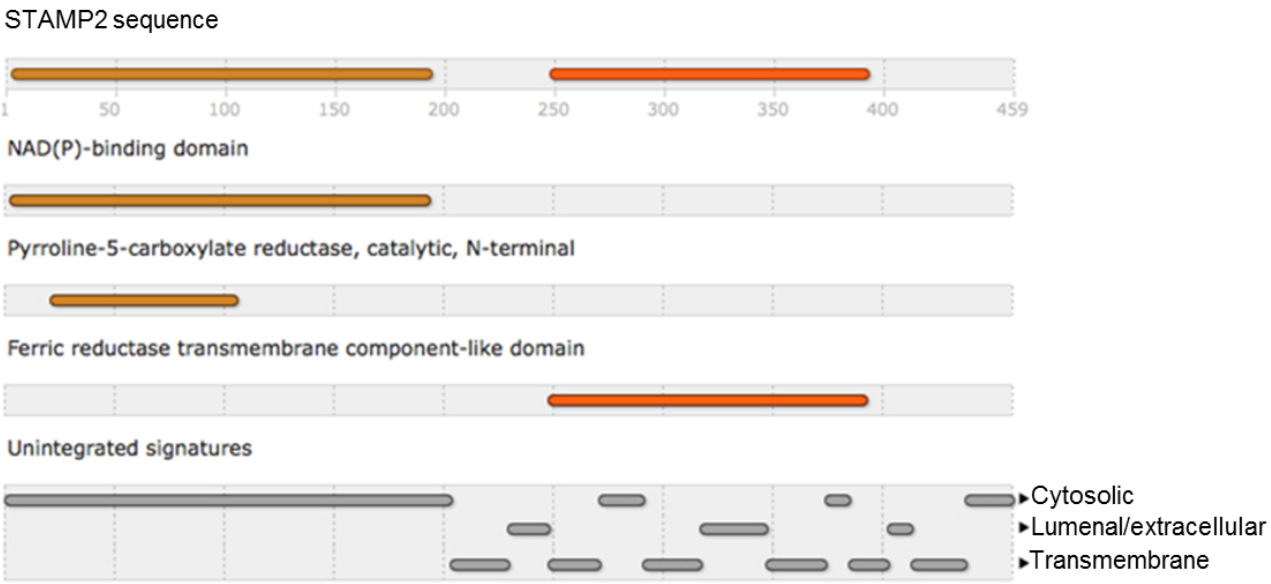

Figure 8: Predicted STAMP2 protein domains. Screen-grab of output after entering STAMP2 protein sequence into the InterPro domain prediction software.

The result of an InterPro search using the predicted STAMP2_v1 primary protein structure as query sequence is shown in figure 9. The missing exon 3 in STAMP2_v1 mRNA encodes three of the six transmembrane helices, resulting in the loss of a predicted iron reductase

domain. When the number of transmembrane domains changes from an even to an odd number it has the surprising structural consequence that the orientation of either the N- or the C-terminus of STAMP2_v1 must be found on the luminal/extracellular side of the membrane. As is shown in figure 9, this is predicted to be the N-terminal with the NADPH-oxidoreductase domain. For full-length STAMP2, domain orientations as shown in figure 9 is predicted with probabilities close to one by the algorithm built into the program [83]. For STAMP2_v1 on the other hand, the calculated probability for the N-terminal domain to be orientated as predicted (luminal/extracellular) is around 0.8 (data not shown) from the beginning of the sequence until a stretch of sequence between 120 and 145 aa, which contains several hydrophobic residues. After this stretch, probabilities that the orientations of remaining loops and C-terminus as given in figure 9 is true, is closer to 1 for the predicted STAMP2_v1 structure as well. The probability that the stretch between amino acids 120-145 is an alternative transmembrane helix was calculated to be around 0.15.

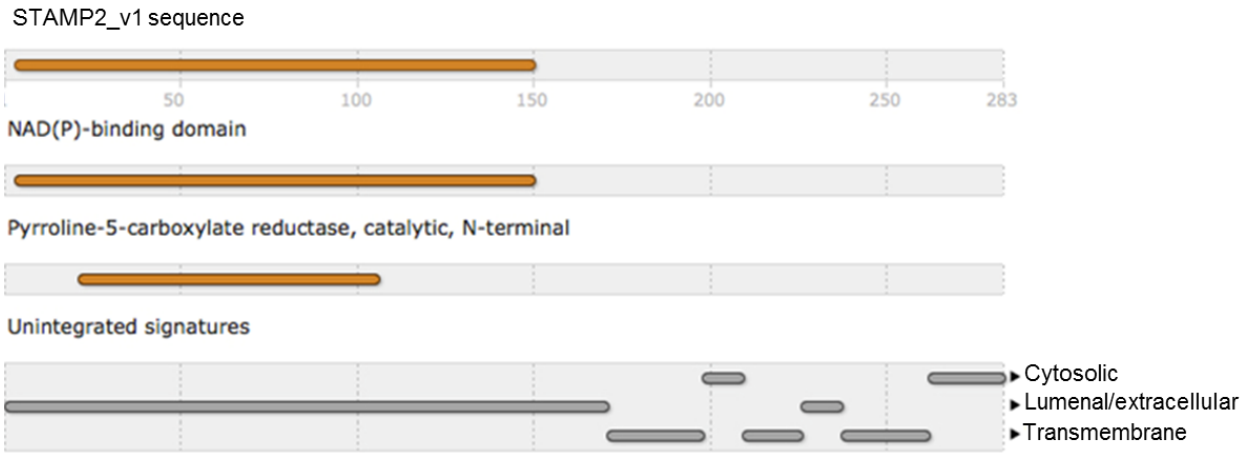

Figure 9: Predicted STAMP2_v1 protein domains. Screen-grab of output after entering STAMP2_v1 protein sequence into the InterPro domain prediction software.

4.1.2 Critical motifs for STAMP2 catalytic activity is absent in STAMP2_v1

The STAMP2_v1 protein sequence is identical to that of STAMP2 until residue 152 (figure 7). The majority of the N-terminal domain would be retained in STAMP2_v1, but the truncation excludes 50 aa of the C-terminal part of the full STAMP2 N-terminal domain. None of the residues directly involved in NADPH binding is lost by this truncation [46]. On the other hand, in vitro NADPH oxidase assays using sequentially truncated N-terminal domains of the rat STAMP2 homolog, in which all the residues involved in catalytic activity

is conserved, have shown that the last eight of these 50 residues are important for full activity. Several residues predicted to be involved in binding of flavin co-factors, crucial for NADPH oxidase activity, are found here [46].

It is also predicted by InterPro that the iron-reductase domain will be absent in STAMP2_v1 (figure 9). Among the conserved residues of the STAMP family missing in the STAMP2_v1 primary structure is the heme-organizing H304 located in TM helix 3, crucial for iron reductase activity [42, 43]. Even though the other heme-binding histidine residue, H397 located in TM helix 5, is retained in STAMP2_v1, both are needed for the structure to be able to coordinate the correct positioning of a heme group. Several of the residues predicted to be directly involved in binding of enzymatic substrate Fe^{3+}, located adjacent to- and on the luminal/extracellular side of the heme binding site [43], are also not present in the predicted STAMP2_v1 structure. The loop connecting TM helices 2 and 3 in STAMP3 has been shown to contain a conserved endosomal targeting motif, and its sequence and position is conserved among all the family members [47]. This targeting motif would be absent in STAMP2_v1.

Complementing the STAMP2_v1 structure prediction by using the Prosite database of protein domains (expasy.org) and the Conserved Domain search engine (NCBI) further supported the predicted lack of STAMP2_v1 iron reductase capability. Prosite recognized a heme-binding domain in STAMP2 similar to that in hemopexin, the main heme scavenger protein in blood. This was not detected in STAMP2_v1. The NCBI search recognized features of ferric reductase transmembrane components common to mammalian cytochrome B-245 heavy chain and the ferric reductase Frp1 in yeasts in both isoforms, but with an E-value for STAMP2 five orders of magnitude lower than that for STAMP2_v1. Prosite also predicted that several other features would be missing in STAMP2_v1, as post-translational modification (PTM) sites. Predicted structural differences between the isoforms are summarized in table 8. Taken together, these structure predictions shows that if STAMP2_v1 is successfully translated into protein in humans, it would encode a severely altered protein compared to STAMP2 likely to affect its biological function: It would retain ability to bind, but possibly not oxidize, NADPH; its NADPH-binding pocked would possibly be located in the opposite topology; it would lack the ability to bind FAD, heme and Fe^{3+}, and thereby lack iron reductase activity; it could have novel localization; and it would have an altered pattern of PTMs, potentially affecting structure, along with regulation of localization, activity and potential interaction partners.

Table 1: Summary of predicted structural differences of STAMP2 isoforms

Feature/Isoform	STAMP2	STAMP2_v1	Prediction Software
Length	459 aa	283 aa	(RefSeq alignment)
Mol. weight	52.0 kDa	31.3 kDa	(RefSeq alignment)
TM helices	6	3	InterPro
NADPH binding	Yes	Yes	InterPro, NCBI
NADPH oxidored.	Yes	?	
FDN binding	Yes	No	InterPro, NCBI
Heme binding	Yes	No	InterPro, Prosite
Fe^{3+} reductase	Yes	No	InterPro, Prosite, (NCBI)
N-linked glycosylation sites	3	1	Prosite
Phsophorylation sites	7	5	Prosite

4.2 STAMP2_v1 expression is androgen-regulated in PCa cell lines

STAMP2 is an androgen-regulated gene in the three PCa cell lines LNCaP, VCaP and 22Rv1 [35, 42]. Therefore, androgen induction was chosen as a starting point in an attempt to detect the variant transcript and thereby establish whether the PCa cell lines express *STAMP2_v1*. The three PCa cell lines were cultured in steroid hormone-free, charcoal-stripped medium with or without 1nM synthetic androgen R1881. Total RNA was harvested 24hrs after androgen-induction and subjected to RT-qPCR analysis. Under androgen starved conditions, *STAMP2_v1* was not detected by qPCR in either cell line, whereas STAMP2 was detected at low levels (figure 10a-c). After androgen induction, both transcript variants were detected at higher levels compared to the level of full-length STAMP2 in androgen-starved conditions (figure 10a-c). Next, the ratios of short isoform-to-full-length isoform mRNAs after androgen induction were calculated for each cell line. As shown in figure 10d, this ratio is below 1:10 for both androgen-responsive cell lines LNCaP and VCaP. Interestingly, the ratio of short isoform is significantly higher in the androgen-independent cell line 22Rv1. Taken together,

these results show that the STAMP2 short variant is androgen-induced and expressed at mRNA level in three different PCa cell lines.

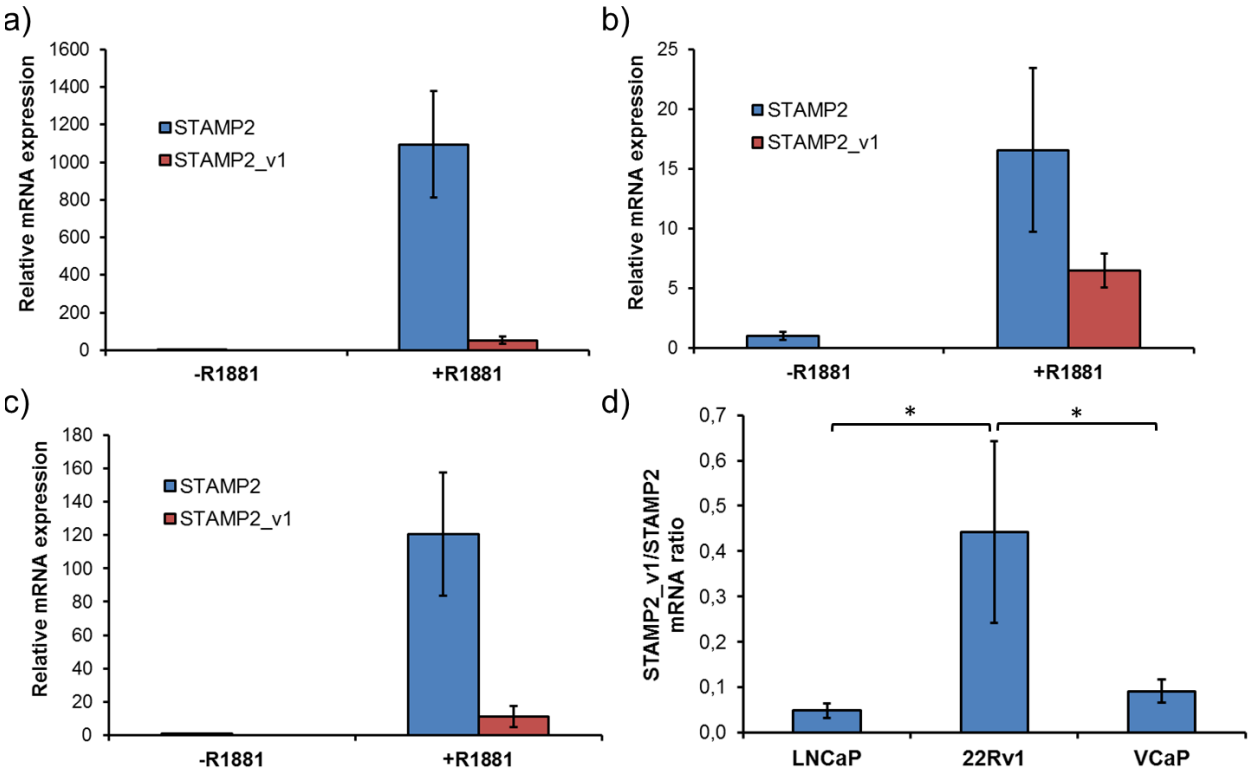

Figure 10: STAMP2 expression in PCa cell lines. LNCaP (a), VCaP (b) and 22Rv1 (c) cell lines were androgen-starved for 24hrs followed by 1nM R1881 induction for 24hrs before total RNA was harvested and subjected to qPCR analysis. GAPDH served as internal reference. d) Ratio of STAMP2_v1/STAMP2 mRNA after in androgen induction in the three cell lines.

4.3 Comparison of androgen-induction of STAMP2 isoforms in over time

In order to investigate whether the relative mRNA levels of the two transcripts as a result of androgen induction differ over time, a time-course analysis was performed with the PCa cell line LNCaP. The cells were cultured in androgen-starved medium with or without 1nM R1881, harvested 1, 2 and 3 days after androgen-induction and STAMP2 isoform expression was analyzed by qPCR. After androgen induction, levels of both isoform mRNAs rise continuously over time (figure 11). Relative to the level of *STAMP2* in androgen-starved conditions 24hrs after induction, levels of full-length *STAMP2* (figure 11a) are comparatively much higher than those of *STAMP2_v1* (figure 11b), but the kinetics of androgen induction is similar for both isoforms.

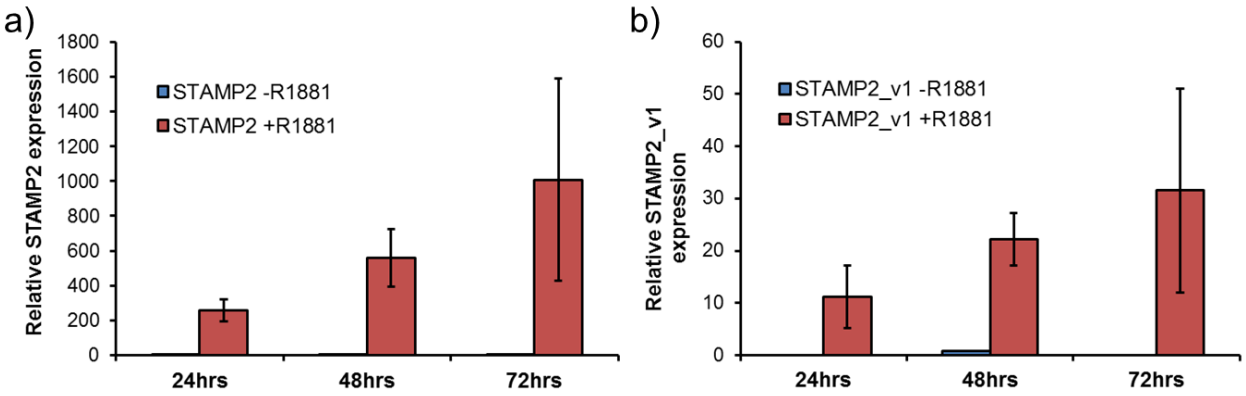

Figure 11: STAMP2 isoform expression in LNCaP over time. LNCaP cells were androgen starved for 24hrs followed by 1nM R1881 induction. Total RNA was harvested 24, 48 and 72hrs post induction before STAMP2 (a) and STAMP2_v1 (b) mRNA levels were measured by qPCR. GAPDH served as internal reference. Levels of both isoforms are given relative to the level of STAMP2 in LNCaP cells after 24hrs of androgen starvation.

4.4 Tissue distribution of STAMP2 isoforms

As STAMP2_v1 mRNA was detected only at low levels in PCa cell lines, it was of interest whether the transcript was differentially expressed in other tissues. To this end, two human multiple tissue cDNA libraries (Clontech), in total comprising 16 different tissues, was used as template for qPCR. Figure 12 shows the tissue distribution of comparable isoform mRNA levels, relative to full-length *STAMP2* in prostate. Consistently with previously published results, STAMP2 is expressed at higher levels in prostate, heart, placenta and lung tissue [35]. *STAMP2_v1* tissue distribution is on the other hand more restricted, with low levels detected in most tissues. Lung tissue and peripheral blood leukocytes show the stand-out results among the samples in these panels, where the level of *STAMP2_v1* was measured to be similar to- and significantly higher than that of *STAMP2*, respectively.

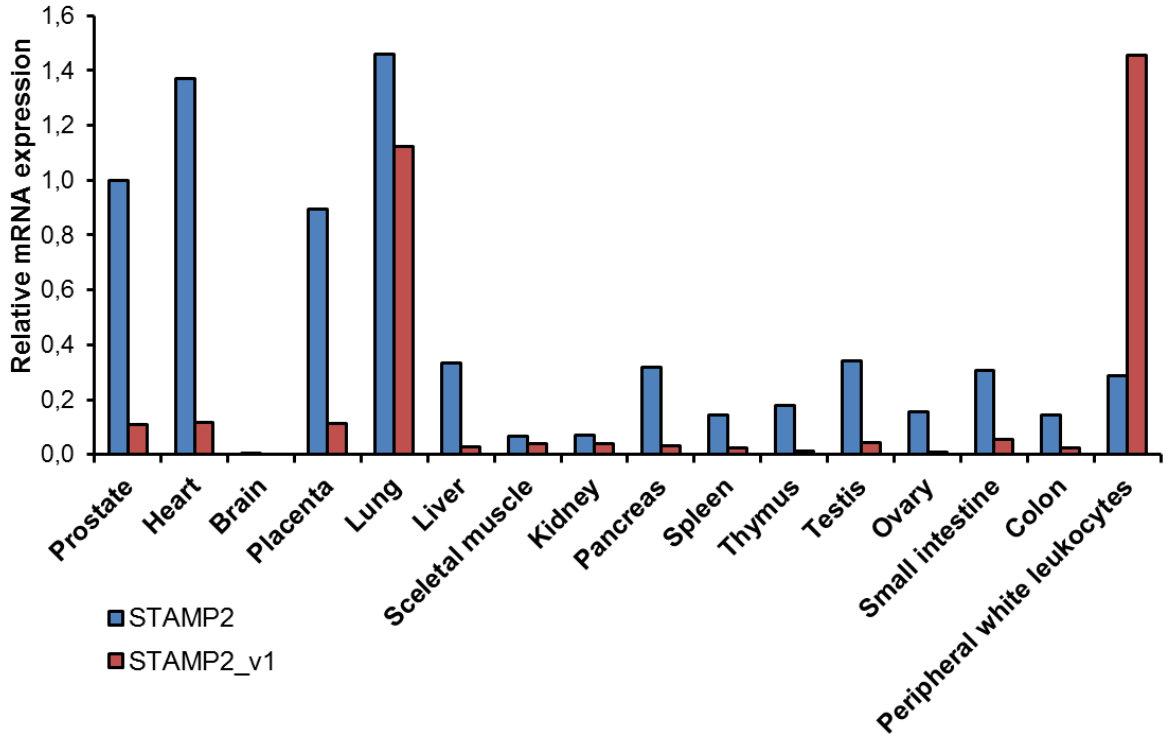

Figure 12: STAMP2 isoform tissue distribution. STAMP2 isoform levels were measure in tissue cDNA panels by qPCR. Levels of each isoform across tissues is given relative to STAMP2 in prostate.

4.5 *STAMP2_v1* is expressed at high levels in monocytes

The ratios of the two transcripts among the 16 tissues are given in figure 13a. The ratio of *STAMP2_v1*/*STAMP2* is 50-60% in skeletal muscle and kidney tissue, but in these two tissues the expression levels of the full-length transcript were also low compared to that in prostate. Strikingly, the ratio was found to be around 1:1 in lung tissue and 5:1 in peripheral white leukocytes. The distinctly different expression profile of *STAMP2* variants in the white blood cell pool sample suggests a role for STAMP2_v1 here, but multiple functionally distinct cell types can be grouped as 'peripheral white leukocytes', as e.g. monocytes, neutrophils, granulocytes, natural killer cells and B and T lymphocytes. To narrow down the distribution of STAMP2_v1 among this group, one pilot experiment was performed. Blood from one healthy donor was separated into 90% pure fractions of monocytes and T-lymphocytes. Total RNA isolated from these two samples was provided by the Blood Bank at Ullevaal Hospital, Oslo and analyzed by RT-qPCR (figure 13b). *STAMP2* was not detected in the lymphocyte sample, while *STAMP2_v1* was detected at low levels. In monocytes the level of

STAMP2_v1 was found to be higher than that of STAMP2, and both isoforms were detected at higher levels in monocytes compared to that of STAMP2_v1 in lymphocytes.

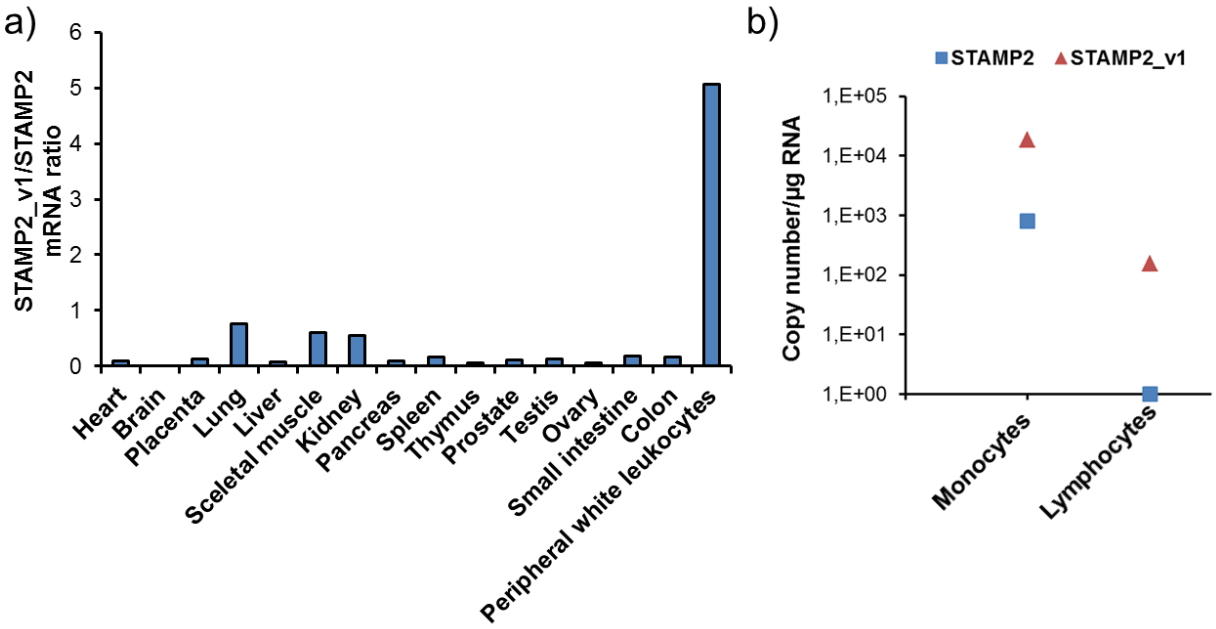

Figure 13: STAMP2_v1 is expressed at high levels in monocytes. a) Calculated ratio of STAMP2_v1/STAMP2 mRNA among tissues. b) Average of two measured STAMP2 isoform levels in total RNA from monocytes and lymphocytes measured by qPCR.

4.6 Inflammatory cytokines induce STAMP2 expression in LNCaP cells

As was discussed previously, tumors are often associated with inflammation. Both tissue damage and chemokines lead to recruitment and infiltration of cells of both the innate and adaptive arms of the immune system [15]. Immune cells then become integrated players in the tumor stroma, contributing to the paracrine network in the tumor microenvironment by their release of inflammatory-, growth- and angiogenesis-inducing factors (figure 2). PCa cells are therefore likely to be exposed to inflammatory stimuli *in vivo*. Expression of STAMP2 has been shown to be positively regulated by inflammatory cytokines in other physiological contexts (table 2), but similar observations has not been reported in PCa cells. Together with the observations that STAMP2 expression increases during PCa development [42], this led to the hypothesis that STAMP2 is also regulated by cytokines in PCa cells.
In order to test this hypothesis, LNCaP cells were treated with increasing concentrations of IL-6, IL-1β and TNFα. Changes in *STAMP2* expression was then measured by qPCR. IL-6 significantly induced *STAMP2* mRNA expression in LNCaP cells in a dose-dependent manner, reaching 70-fold at 40ng/mL (figure 14a). Significant induction of STAMP2 mRNA expression was also observed after IL-1β treatment (figure 14b), peaking at approximately 7-fold at 20ng/mL. TNFα treatment only weakly induced *STAMP2* expression by two fold at 10ng/mL (figure 14c). By comparing IL-6- and TNFα-mediated *STAMP2* induction side-by-side and in combination in the same experiment (figure 14d), it was evident that IL-6 is a much more potent inducer of STAMP2 expression in LNCaP compared to TNFα, where the latter only just significantly up-regulated expression around 2.5-fold over untreated controls. On the other hand, TNFα treatment together with IL-6 led to a significant synergistic induction compared to IL-6 treatment alone (figure 14d).

Taken together, these experiments showed that IL-6 is a strong inducer of *STAMP2* expression in LNCaP cells, whereas IL-1β and TNFα induce moderate and weak expression, respectively. The results therefore support the hypothesis that proinflammatory cytokines increase *STAMP2* expression at mRNA level. As TNFα only had shown weak induction of *STAMP2* expression, no further experiments were performed using this cytokine.

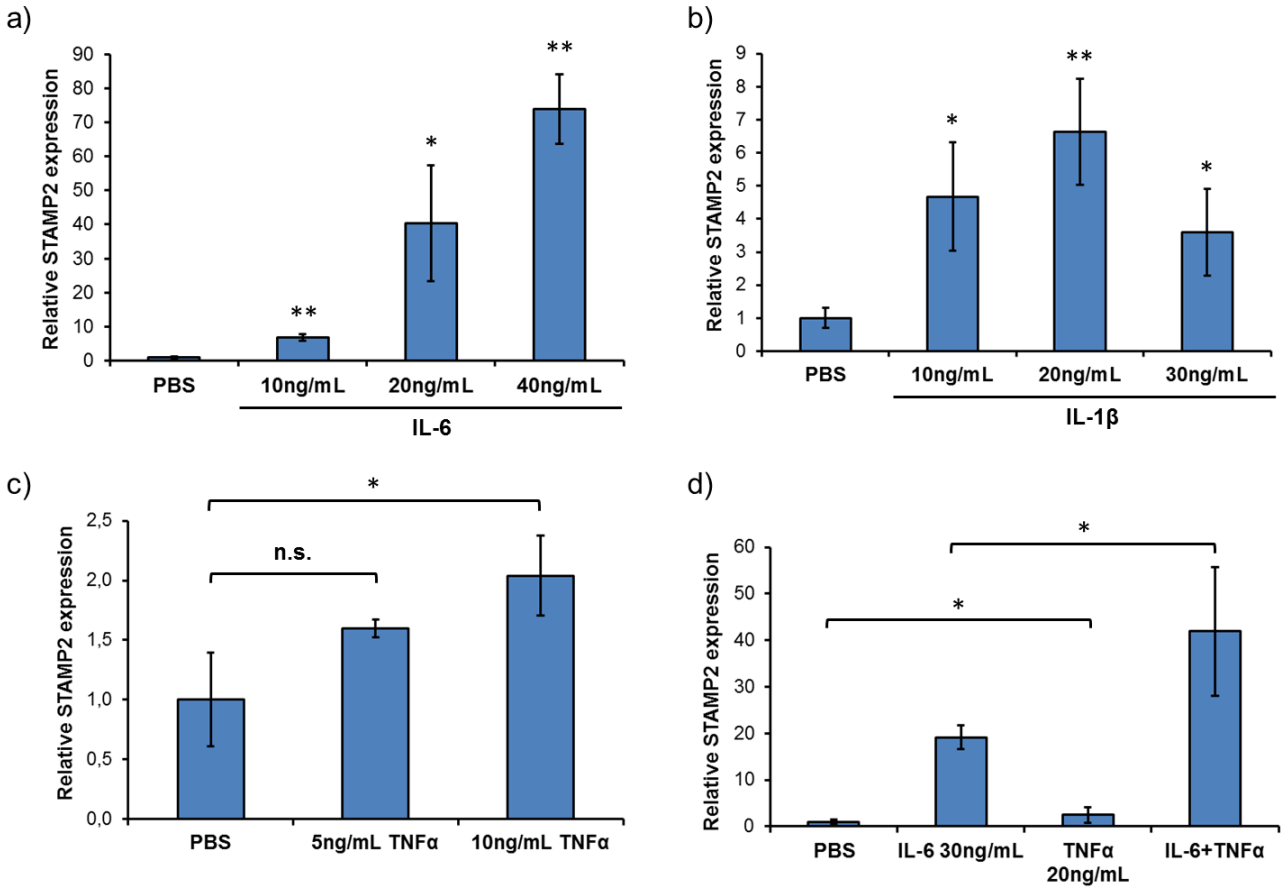

Figure 14: IL-6, IL-1β and TNFα induce STAMP2 expression in LNCaP. a) LNCaP cells were serum-starved for 5hrs and then induced with different concentrations of IL-6 for 16hrs before total RNA was harvested and subjected to RT-qPCR analysis. b) LNCaP cells were serum-starved for 5hrs and then induced then induced with different concentrations of IL-1β for 16hrs before total RNA was harvested and subjected to RT-qPCR analysis. c) LNCaP cells were serum-starved for 13hrs and then induced with different concentrations of TNFα for 9hrs before total RNA was harvested and subjected to RT-qPCR analysis. d) LNCaP cells were serum-starved for 5hrs and then induced with 30ng/mL IL-6 and/or 20ng/mL TNFα for 16hrs before total RNA was harvested and subjected to RT-qPCR analysis.

4.7 IL-6, IL-1β and androgens regulate STAMP2 expression with different kinetics

To investigate the kinetics of *STAMP2* induction mediated by IL-6 and IL-1β, time-course experiments were performed. STAMP2 mRNA induction profiles by both cytokines over time are shown in figure 14. After IL-6 treatment, *STAMP2* levels begin to rise at 1 hour, peaks at 2hrs post induction and then remains at similar levels until 8hrs (figure 15a). Compared to IL-

6 treatment, IL-1β led to a slower induction of *STAMP2* expression, which peaked at 4hrs and then fell back towards base levels by 20hrs (Figure 15b). The induction profile of interleukin-8 (IL-8) mRNA by IL-1β is included (figure 15c) for comparison of induction profile of STAMP2 with that of a canonical target gene of the NF-κB pathway [29]. *IL-8* levels were up-regulated 500-fold already 30 minutes after treatment and peaked after 1hr. Considering experimental variations, the measurements for 2 and 4hrs should be considered similar.

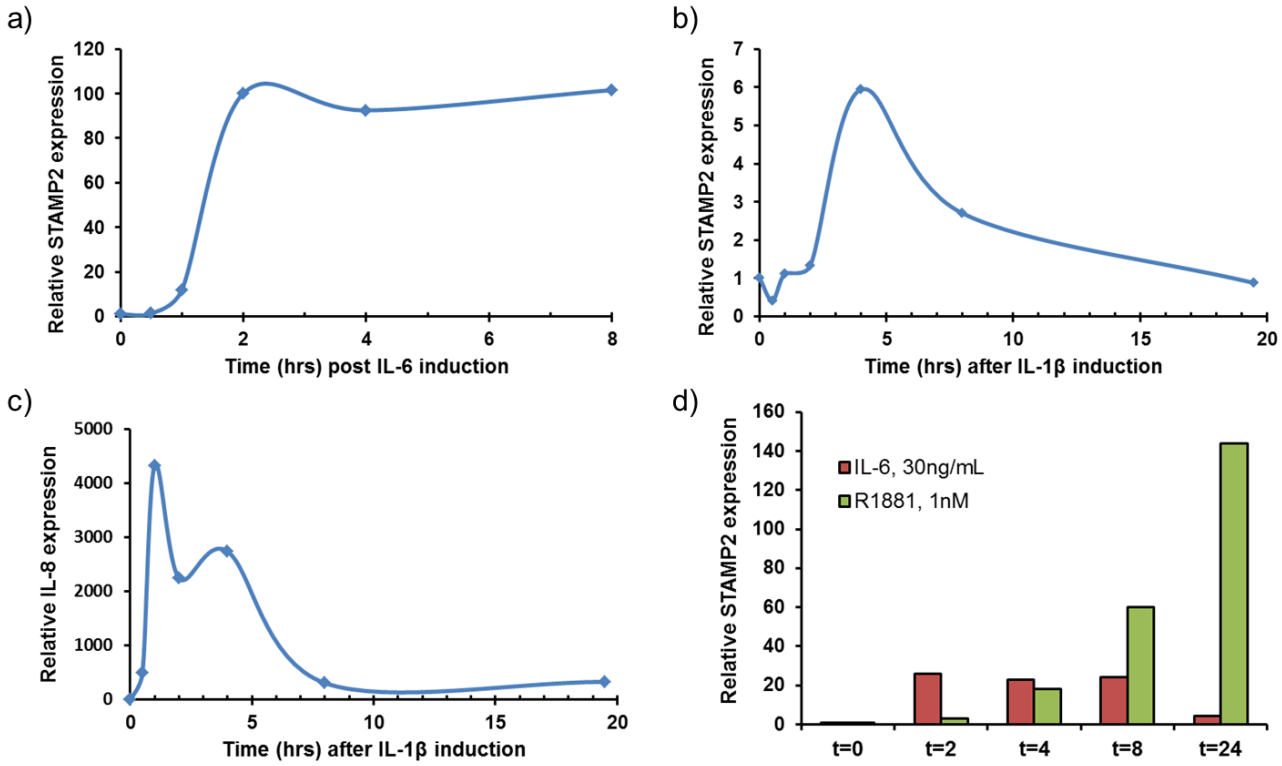

Figure 15: IL-6, IL-1β and androgens regulate STAMP2 expression with different kinetics. a) LNCaP cells were serum-starved for 13hrs before induction with 30ng/mL IL-6, and total RNA was harvested at the indicated time-points and subjected to RT-qPCR analysis. b) LNCaP cells were serum-starved for 13hrs before induction with 20ng/mL IL-1β. Total RNA was harvested at the indicated time-points and subjected to RT-qPCR analysis. c) As for b). d) LNCaP cells were serum-starved for 2,5hrs before induction with either 30ng/mL IL-6 or 1nM R1881. Total RNA was harvested at the indicated times and subjected to RT-PCR analysis.

To compare kinetics of *STAMP2* induction by IL-6 with androgens, changes in relative STAMP2 mRNA levels over time after induction by IL-6 and R1881 were measured side-by-side (figure 15d). IL-6 treatment produced the same induction profile up to 8hrs as measured previously, but which fell dramatically by 24hrs. Induction of *STAMP2* by R1881 was slower, and reached similar levels as in cells treated with IL-6 only after 4hrs. However, *STAMP2*

expression continued to rise even at the last time-point of 24hrs, as was also shown previously (figure 11). These data suggest that regulation of *STAMP2* expression by IL-6 and androgens is likely to be mechanistically different.

After these observations, in later experiments with IL-6 treatment, total RNA was harvested at 2.5hrs post induction, as *STAMP2* levels peaked before this time-point. Similarly, in later experiments using IL-1β treatment, RNA was harvested at 4hrs post induction, as this was shown to be the time point after induction with maximal *STAMP2* mRNA levels. If both cytokines were used side-by-side in the same experiment, RNA was harvested at 4hrs, as IL-6 mediated induction was stable at around peak level until at least 8 hrs.

4.8 IL-6 and IL-1β-mediated STAMP2 expression is independent of the AR

STAT3, downstream effector of IL-6 signaling, is known to transactivate the AR in PCa cells [84, 85]. As *STAMP2* is an androgen-regulated gene in LNCaP cells (figures 9a, 14d),[35, 42], it is possible that the AR was involved in the observed IL-6- and IL-1β-mediated induction of STAMP2. If so, IL-6- and IL-1β would also induce the expression of other AR target genes. To test this possibility, expression of established AR target genes were measured by qPCR after treatment of LNCaP cells with IL-6 (figure 16a) and IL-1β (figure 16b). Expression of neither Kallikrein 4 (KLK4) nor Transmembrane protease serine 2 (TMPRSS2) was induced by IL-6. Interestingly, higher concentrations of IL-6 instead suppressed their expression. Consistently, KLK4 and prostate specific antigen (PSA) mRNA levels decreased over time after treatment with IL-1β.

To further test the hypothesis that AR is involved, the small-molecule- non-steroidal anti-androgen MDV3100 (in clinical use for CRPC patients under the name Enzalutamide) was used at sub-lethal concentrations of 2μM alongside and in combination with IL-6. MDV3100 binds to AR with high affinity and inhibits both nuclear translocation of AR and its binding to both DNA and co-activators in LNCaP cells [86]. Western analysis of nuclear protein extracts from LNCaP cells treated with IL-6 alone and in combination with MDV3100 pre-treatment showed that there was residual nuclear AR in the experimental setting used (figure 16c). IL-6 slightly decreased the level of nuclear AR, while 2 μM MDV3100 completely removed AR from the nucleus. R1881 treatment was used as a positive control for AR detection. Similar

results were obtained after 16hrs of exposure to IL-6, albeit basal levels of nuclear AR were lower at that time-point when compared to the control (data not shown). MDV3100 was then employed with IL-6 treatment in an investigation of *STAMP2* induction by qPCR. Surprisingly, pre-treatment with the inhibitor led to a significant additive effect of IL-6 treatment compared to IL-6 alone (figure 16d). This suggests that AR may be inhibitory for a component of the pathway that is involved in IL-6-mediated *STAMP2* expression.

The effects of IL-6 and IL-1β on *STAMP2* expression were also assessed when LNCaP cells were cultured in charcoal-stripped medium to ensure a more complete androgen starvation. *STAMP2* expression was not detected in untreated controls in this experiment, but was detected at low levels after IL-1β treatment (figure 16e). IL-6 treatment also led to *STAMP2* induction, significantly higher than that seen by IL-1β. Taken together, contrary to the hypothesis, the results presented in figure 16 shows that both IL-6 and IL-1β induce *STAMP2* expression independently of the AR.

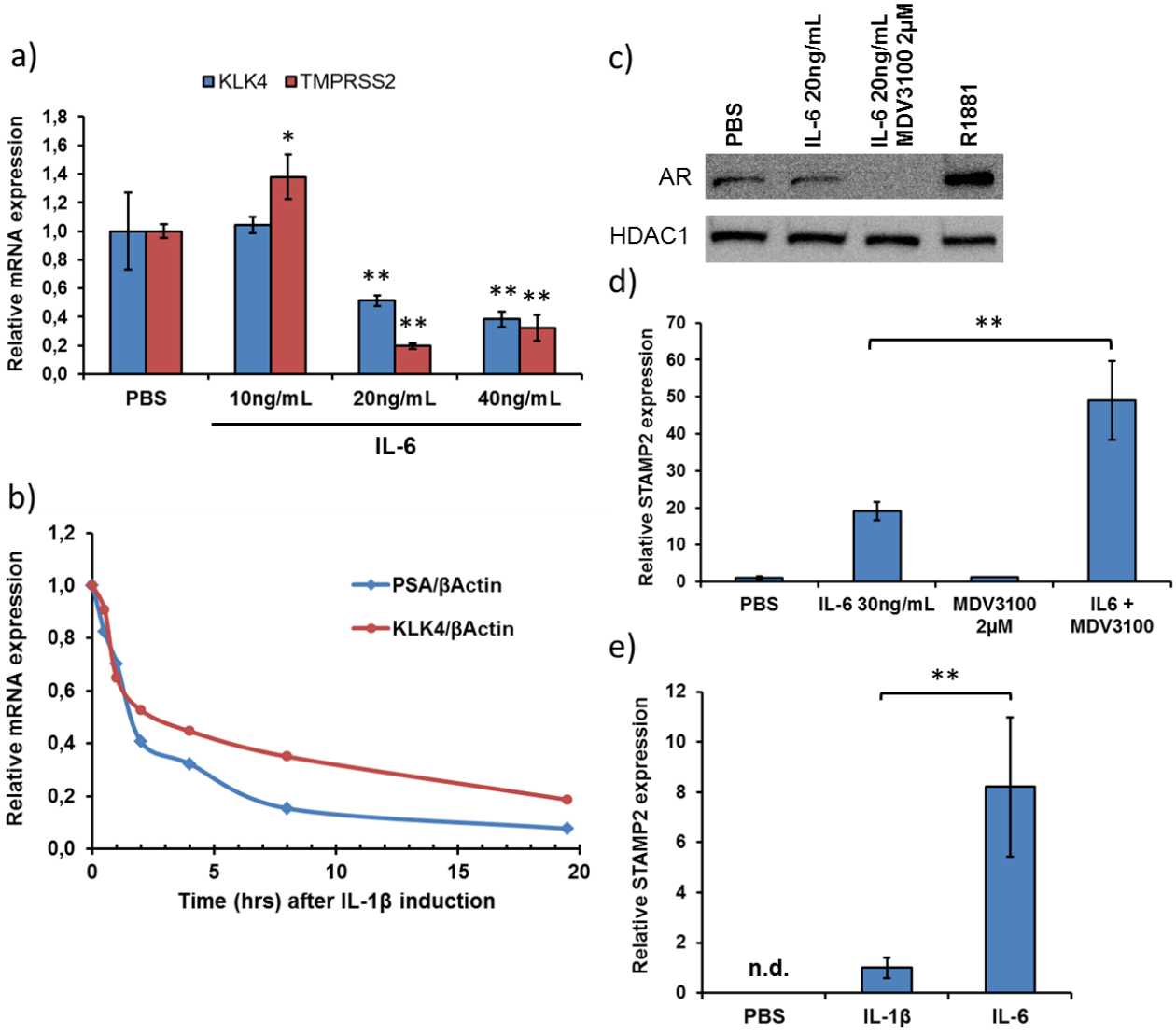

Figure 16: IL-6 and IL-1β-mediated STAMP2 expression is independent of the AR. a) LNCaP cells were serum-starved for 5hrs and then induced with different concentrations of IL-6 for 16 hrs before total RNA was harvested and subjected to RT-qPCR analysis. b) LNCaP cells were serum-starved for 13hrs before induction with 20ng/mL IL-1β. Total RNA was harvested at the indicated time-points and subjected to RT-qPCR analysis. c) LNCaP cells were serum-starved for 3hrs before pre-treatment either with 2μM MDV3100 AR inhibitor or vehicle control for another two hrs. The cells were then treated with either 20ng/mL IL-6 or 1nM R1881 as indicated, before the cells were harvested and subjected to isolation of nuclear protein fraction 2hrs post induction/4hrs post inhibition. d) LNCaP cells were serum-starved for 3hrs before pre-treatment with 2μM MDV3100 or vehicle control for another two hrs. The cells were then induced with 30ng/mL IL-6 for 16hrs before total RNA was harvested and subjected to RT-qPCR analysis. e) LNCaP cells were androgen-starved for 38hrs before induction with 30ng/mL IL-6 or IL-1β and total RNA was harvested 4hrs later and subjected to RT-qPCR analysis.

4.9 Signaling events in LNCaP cells after cytokine induction

JAK-STAT1/3 cascades are the main signaling pathways downstream of IL-6 and its receptor complex (figure 3) [19]. To determine the response of these pathways in LNCaP cells after IL-6 treatment, whole cell protein extracts were harvested at various time-points after induction with IL-6 and subjected to Western analysis. GAPDH was used as loading control. As is shown in figure 17a, LNCaP cells respond to IL-6 with a strong increase in the level of tyrosine 705-phosphorylated STAT3 after 30 min, a residue that is targeted by activated JAKs [19]. STAT3 remains phosphorylated in what looks like a bi-phasic activation pattern that lasts up to 8hrs. Note that the last sample had a loading error, when comparing to GAPDH serving as loading control. The intensity of the band in the other parallel harvested at 8hrs is comparable to those from 1hr post induction. On the other hand, there were no observable changes in STAT3 serine 727-phosphorylation. Similar to that found for STAT3, JAK-mediated STAT1 tyrosine 701 phosphorylation was strongly induced 30 min after treatment and is detectable after 1hr, but contrary to STAT3 phosphotyrosine levels, STAT1 tyrosine phosphorylation does not return at later time-points.

IL-6 can also activate Ras/MAPK cascades [23], and the kinetics of ERK1/2 activation was therefore also determined. IL-6 induction resulted in a strong activation of ERK1/2 after 30 minutes (figure 17b), but phospho-ERK1/2 levels then fell again and is weak within 1hr, resembling the activation pattern observed for STAT1. MAPK11/p38 is not activated downstream of IL-6R/Ras, but was included as it is a stress- and cytokine-regulated MAP kinase [30]. p38 activation was more gradual than that of ERK1/2 and the STATs, and was sustained until 8hrs.

IL-6 also activates the PI3K/AKT pathway [23], which again can activate the NF-κB pathway [25]. Activation of the NF-κB pathway involves release of NF-κB transcription factors from Inhibitor of kappaB alpha (IκBα), which is followed by proteasomal degradation of IκBα [87]. A decrease in IκBα is therefore a marker of pathway activation. No change in the levels of IκBα was observed in this experiment, while phosphorylated NF-κB3/p65 was not detected (data not shown). Together, these data indicate that IL-6 does not activate the NF-κB pathway LNCaP cells.

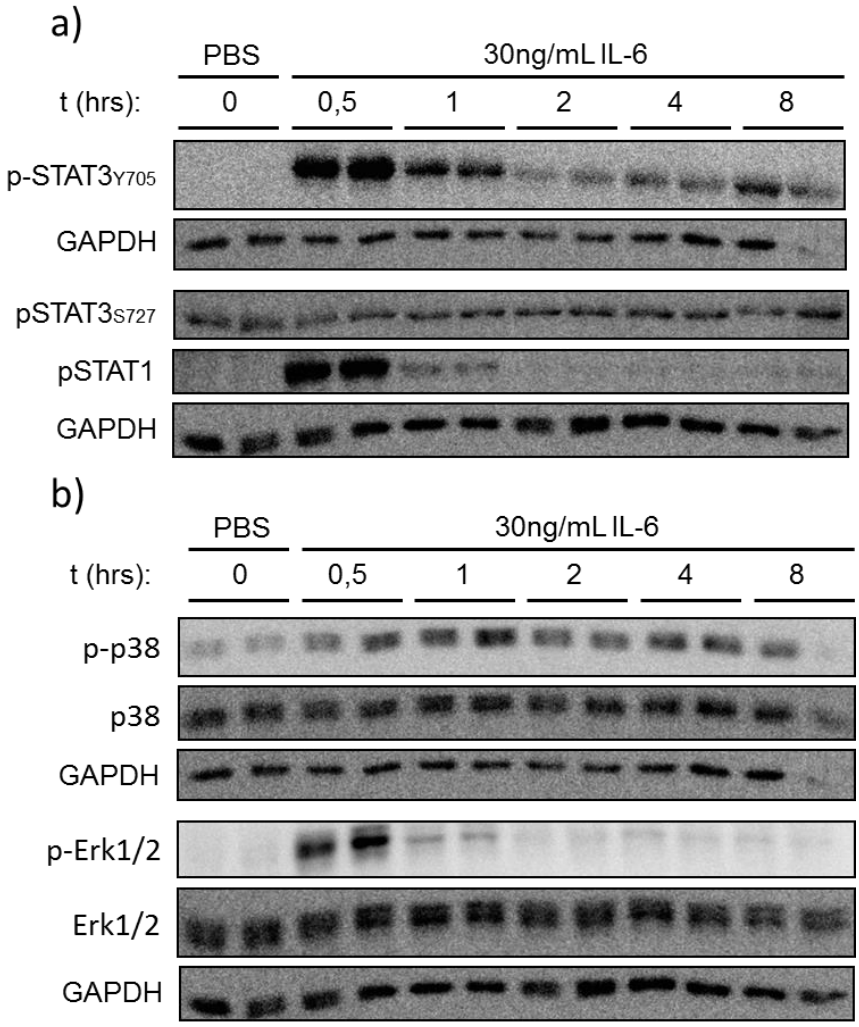

Figure 17: Signaling events in LNCaP cells after IL-6 induction. LNCaP cells serum-starved for 13hrs before induction with 30ng/mL IL-6. Whole-cell lysates were then harvested at the indicated time-points and subjected to Western analysis. a) Changes in phospho-STAT levels over time. b) Changes in ERK and p38 MAPKs over time.

Intracellular signaling downstream of the IL-1R1 is known to activate MAPK cascades and the NF-κB pathway [29]. The behavior of these pathways in LNCaP cells after IL-1β treatment was therefore investigated. Whole cell protein extracts harvested at various time-points after induction with IL-1β was subjected to Western analysis (figure 18a). All three MAP kinase branches were found to behave similarly. Phosphorylation levels of Erk1/2, p38 and JNK1-3 were strongly induced within 30 min after treatment. Their levels of activation were then sharply down-regulated within 1 hr and was sustained at lower levels until 20hrs post induction.

The transcription factor c-Jun is regulated downstream of the MAPKs [30]. Elevated phosphorylation of c-Jun was observed between 0.5-2hrs, and possibly again after 20hrs. The band corresponding to dual serine 63,73 phosphorylated c-Jun in the second parallel of the 0.5hr time-point is missing. This band was possibly disturbed during transfer, as an intensely stained irregular shape was observed immediately above where the band ought to be found. Thus, this experiment requires further investigation.

Figure 18a further shows how the protein levels of IκBα is significantly reduced both at the earliest time-points and 20hrs after IL-1β treatment. IκBα is also a target gene of the NF-κB pathway, involved in negative feedback regulation [87]. The induction profile of IκBα mRNA by IL-1β (figure 18b) shows that a fast re-synthesis also took place after induction. IκBα mRNA levels decreased again after 2hrs, but remained elevated until 20hrs relative to untreated controls.

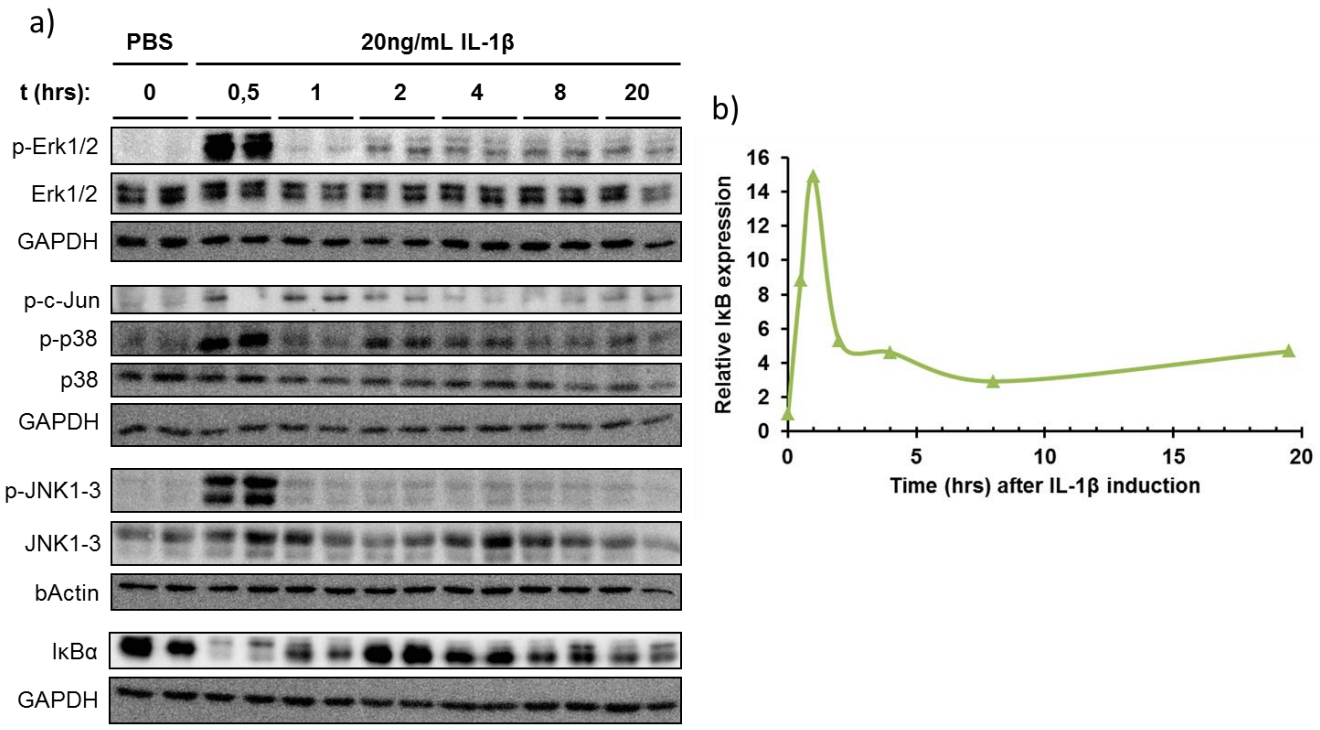

Figure 18: Signaling events in LNCaP cells after IL-1β induction. a) LNCaP cells were serum-starved for 13hrs before induction with 20ng/mL IL-1β. Whole cell lysates were harvested at the indicated time-points and subjected to Western analysis. b) LNCaP cells were serum-starved for 13hrs before induction with 20ng/mL IL-1β. Total RNA was harvested at the indicated time-points and subjected to RT-qPCR analysis.

4.10 Mechanisms of cytokine-mediated STAMP2 expression

As shown above, STAT1/3, along with ERK1/2 and p38 MAPKs, were activated in LNCaP cells after IL-6 induction (figure 17). Therefore, the STATs, along with transcription factors downstream of the MAPKs, were considered as candidate regulators of the IL-6-mediated induction of *STAMP2* expression shown previously (figure 14a, 15a,d, 16d,e). Likewise, as the NF-κB pathway and the ERK1/2, p38 and JNK1-3 branches of the MAPKs were found to be activated after IL-1β treatment of LNCaP cells (figure 18), transcription factors downstream of these pathways were considered as candidate regulators of the IL-1β-mediated induction of *STAMP2* shown above (figure 14b, 15b and 16e). To further investigate the mechanisms of cytokine-mediated *STAMP2* induction, small molecule kinase inhibitors and RNA interference (RNAi) was used to interfere with these pathways. Potential mechanisms of STAMP2 induction is illustrated in figure 19. Targets for chemical or siRNA-mediated inhibition are also highlighted in the figure.

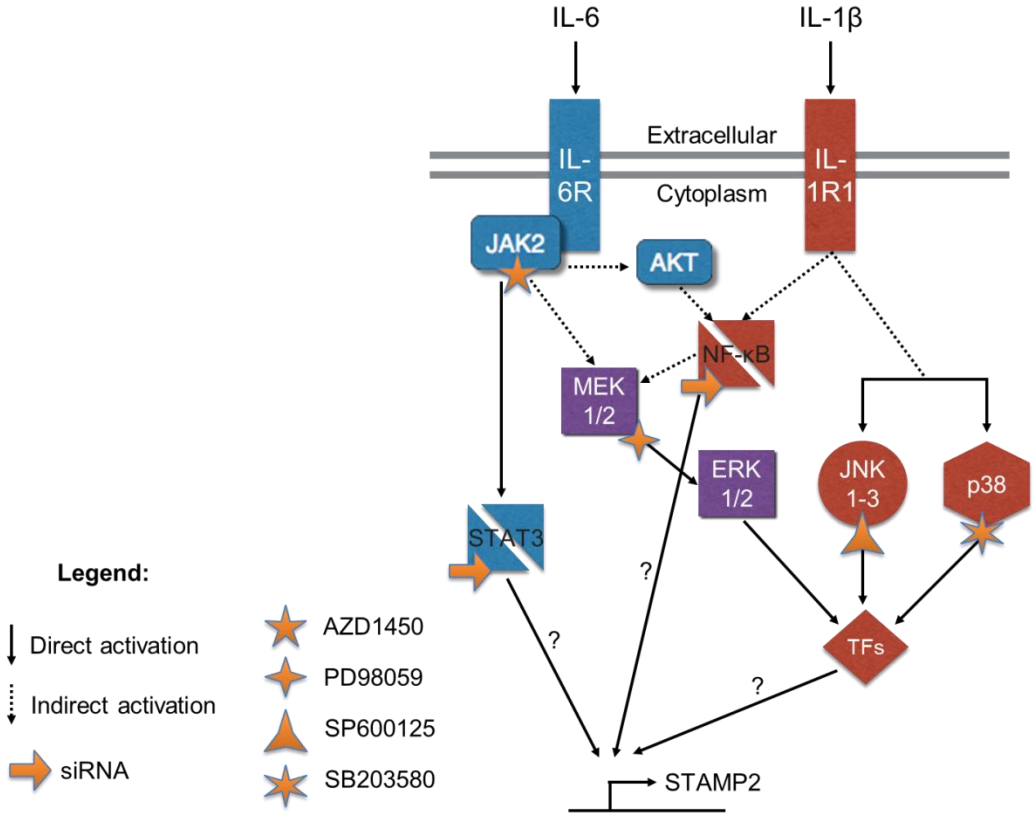

Figure 19: Potential mechanisms of cytokine-mediated STAMP2 expression. The figure shows a summary of the two signaling pathways with the players targeted by RNAi or chemical inhibition highlighted with yellow symbols.

4.10.1 Validation of small-molecule kinase inhibitors

First, effects of four small-molecule inhibitors on downstream kinase targets were validated by Western analysis. LNCaP cells were pre-treated with inhibitor concentrations as recommended by the manufacturers prior to induction with IL-6 or IL-1β. AZD1480 (Selleckchem) is an ATP-competitive inhibitor of JAK2 [121]. Reduction in STAT tyrosine phosphorylation would indicate that AZD1480 is effective. PD98059 (Calbiochem) is a flavonoid compound that binds to the regulatory domain of MEK1/2 and lock the MAP kinase kinases in inactive conformation, thereby inhibiting downstream ERK1/2 activation [118]. SP600125 (Calbiochem) is an ATP-competitive inhibitor of JNK1-3 [119]. Reduced phosphorylation of c-Jun would indicate that the inhibitor is effective. SB203580 (Calbiochem) is an ATP-competitive inhibitor of p38 [120]. Unfortunately, no antibodies against proper downstream targets of p38 were available for this experiment.

The JAK2 inhibitor AZD1250 efficiently inhibited STAT1/3 activation, with a near complete loss of tyrosine-phosphorylated STATs (figure 20). AZD1450 also efficiently inhibited phosphorylation of ERK1/2 after IL-6 treatment, whereas it had no effect on IL-1β-mediated ERK1/2 activation (figure 20). This observation highlights how signaling events upstream of ERK1/2 activation differ between the two cytokines (figure 3, 4).

The MEK1/2 inhibitor PD98059 showed good efficacy of blocking ERK1/2 phosphorylation after treatment with either cytokine (figure 20). PD98059 also had a partially inhibitory effect on c-Jun phosphorylation after IL-1β-treatment, but not as complete as with the JNK1-3 inhibitor SP600125, in line with the notion that these MAPKs are the main activators of c-Jun [88]. Figure 20 further shows that SP600125 affected unexpected protein targets, as both STAT1/3 and ERK1/2 phosphorylation after IL-6 treatment also were down-regulated. Unfortunately, efficacy of the p38 inhibitor SB203580 could not be validated properly. Of the targets tested for the other compounds, SB203580 seems to have a positive effect on ERK1/2 activation when compared to non-inhibited positive control and total ERK1/2 in the same samples. GAPDH served as loading control in this experiment. In summary, the JAK2 and ERK1/2 inhibitors was found to work as intended, but the JNK1-3 inhibitor is effective against downstream target, while simultaneously affecting other protein kinases.

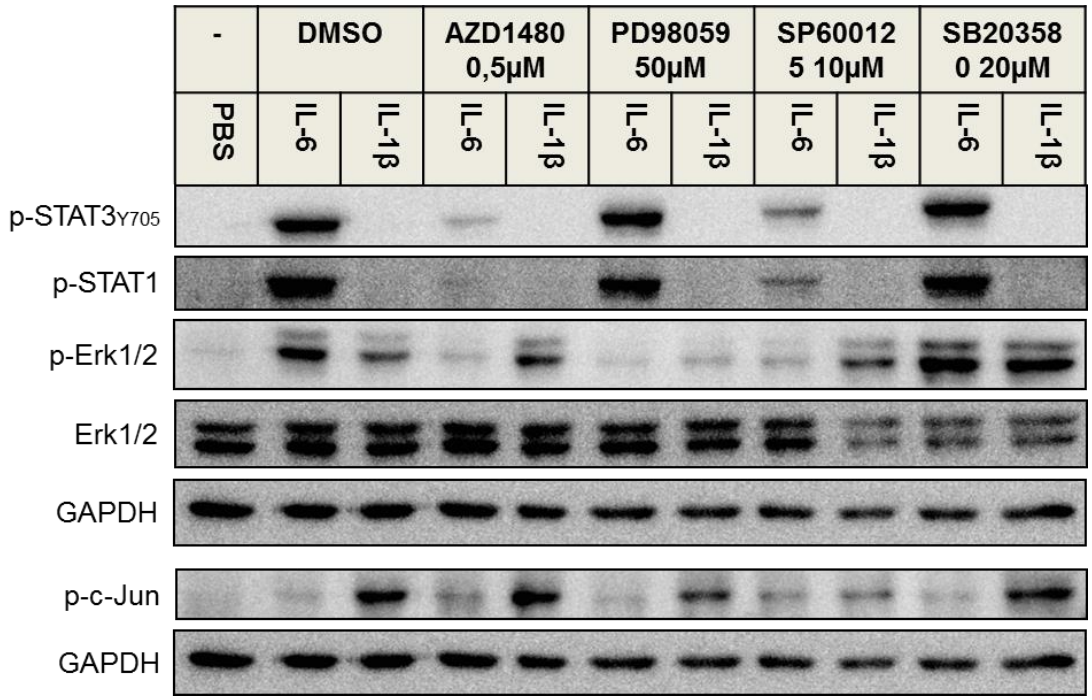

Figure 20: Validation of kinase inhibitors. LNCaP cells were pre-treated with serum-free medium with indicated concentrations of kinase inhibitors. DMSO was used as vehicle control. The cells were then treated with 20ng/mL IL-6 or IL-1β for 30 minutes before whole-cell protein lysates were harvested and subjected to Western analysis.

4.10.2 STAT3 is the main regulator of IL-6-mediated STAMP2 expression

To determine possible effects of the kinase inhibitors on *STAMP2* expression, LNCaP cells were pre-treated with inhibitors prior to IL-6 treatment before *STAMP2* expression was measured by qPCR. As shown in figure 21a, the JAK2 AZD1450 inhibitor completely blocked IL-6 mediated STAMP2 mRNA expression. Similarly, the JNK inhibitor SP600125 almost completely blocked IL-6-mediated *STAMP2* expression. The MEK1/2 inhibitor PD98059 had a modest, but significant effect on *STAMP2* induction by IL-6, whereas the p38 inhibitor SB203580 had no observable effect.

Next, siRNA-mediated knockdown was used to assess the role of STAT3 in this context. LNCaP cells were transfected with 10nM siRNA targeting STAT3 or AllStar non-targeting siRNA control prior to IL-6 treatment, before gene expression was measured by qPCR. A STAT3 knockdown efficiency of around 80% was achieved, as measured at the time of RNA harvest 2.5hrs post induction (figure 21b). STAT3 knock-down reduced IL-6-mediated induction of *STAMP2* to around 25% compared to control cells (figure 21c).

As noted above, the NF-κB pathway can be activated by IL-6 via the PI3K/AKT pathway [25]. The possibility that NF-κB is implicated in regulation of *STAMP2* expression was therefore also investigated, using RNAi targeting NF-κB1/p50. A knock-down efficiency of around 70% was measured (figure 21b). p50 knockdown had no significant effect on IL-6-induced *STAMP2* expression (figure 21c).

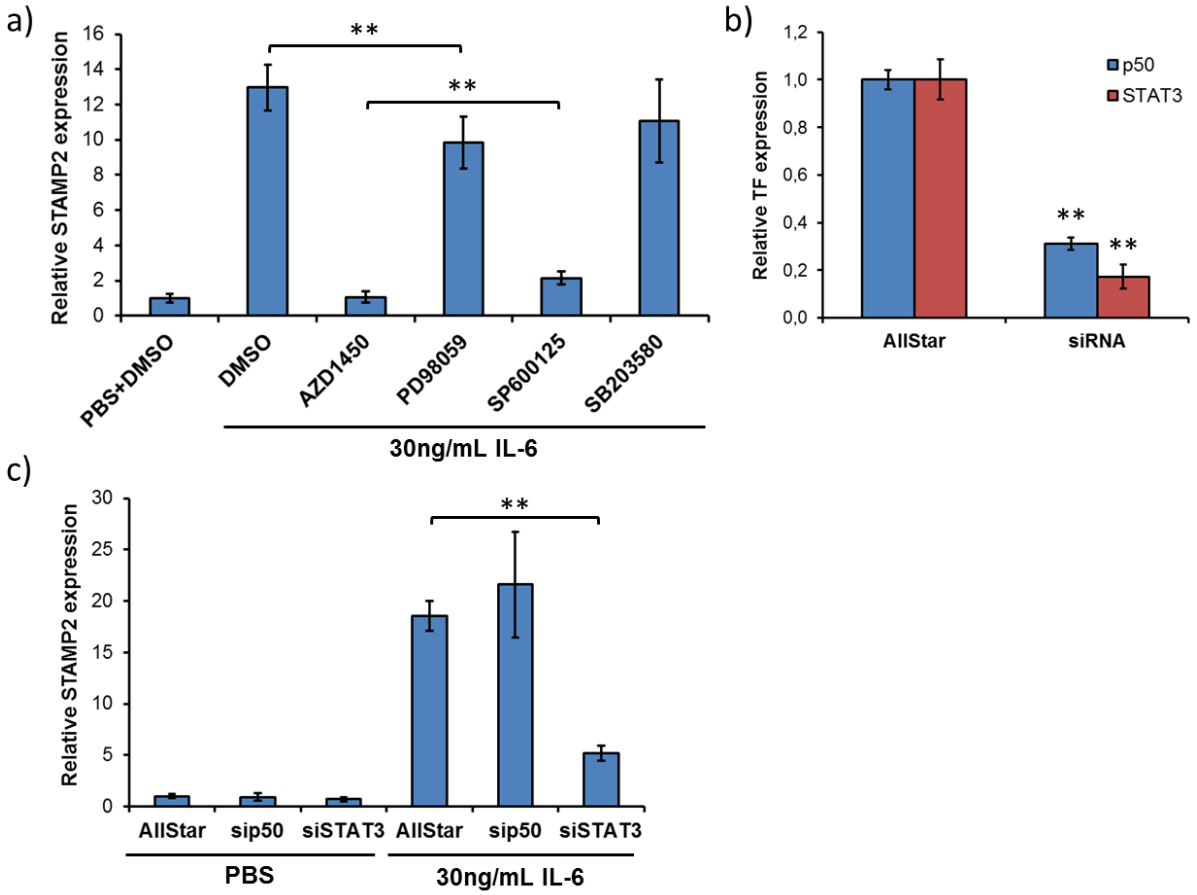

Figure 21: Interleukin 6-mediated induction of STAMP2 mRNA expression is regulated by STAT3. a) LNCaP cells were pre-treated with serum-free medium with kinase inhibitors for 2hrs prior to induction with 30ng/mL IL-6. Inhibitor concentrations as in fig. 20 were used. Total RNA was harvested 2,5hrs post induction and subjected to RT-qPCR analysis. b) LNCaP cells were forward transfected with 10nM of siRNAs targeting STAT3 or p50/NFkB1. 17hrs after transfection, the cells were serum-starved for 5,5hrs before induction with 20ng/mL IL-6. Total RNA was harvested 2,5hrs later and subjected to RT-qPCR analysis. c) As for b).

Taken together, these results show that JAK2-STAT1/3 is the main intracellular signaling axis downstream of the IL-6 receptor complex responsible for *STAMP2* expression in LNCaP cells. They further implicate ERK1/2 in the process, while the NF-κB pathway does not seem to be involved. The potential role of JNK1-3 in the process is discussed later.

4.10.3 NF-κB, ERK1/2 and STAT3 are involved in IL-1β-mediated STAMP2 induction

Both kinase inhibitors and RNAi was used similarly to determine the dominant pathways regulating IL-1β-mediated STAMP2 induction. Pre-treatment with kinase inhibitors was performed as described above, before relative levels of *STAMP2* expression was measured by qPCR. As is shown in figure 22a, only the MEK1/2 inhibitor PD98059 had a significant inhibitory effect on *STAMP2* expression mediated by IL-1β, suggesting that the ERK1/2 takes part in the mechanism of IL-1β-mediated STAMP2 induction, while this is not the case for JAK2, JNK1-3 or p38.

Next, prior to IL-1β induction, LNCaP cells were transfected with 10nM control siRNA or siRNAs targeting p50 or STAT3. Knock-down efficiency as measured at the time of harvest 4hrs after induction, showed that residual levels of p50 and STAT3 mRNA levels were significantly reduced to around 55% and 20%, respectively (figure 22b). Despite the medium efficiency of knockdown, depletion of p50 significantly reduced induction of *STAMP2* expression (figure 22c). Surprisingly, STAT3 knockdown had similar effect.

These data indicate that both STAT3 and NF-κB pathways are required for STAMP2 expression upon IL-1β stimulation of LNCaP cells, while ERK1/2 is implicated as a co-regulator.

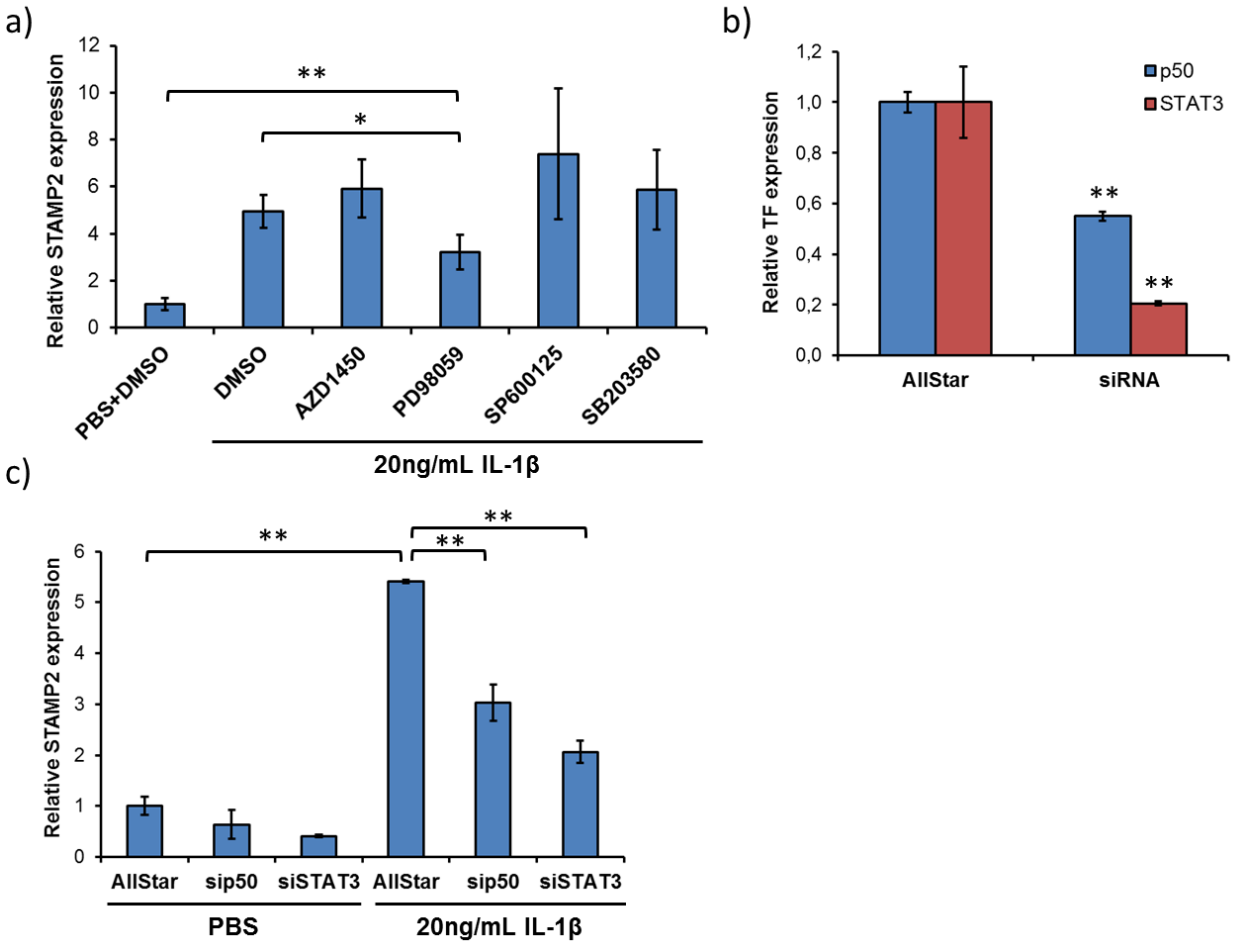

Figure 22: NF-κB, ERK1/2 and STAT3 are involved in IL-1β-mediated STAMP2 induction. a) LNCaP cells were pre-treated with serum-free medium with kinase inhibitors for 2hrs prior to induction with 20ng/mL IL-6. Inhibitor concentrations as in fig.20 were used. Total RNA was harvested 4hrs post induction and subjected to RT-qPCR analysis. b) LNCaP cells were forward transfected with 10nM siRNAs targeting STAT3 or p50/NFkB1. 7hrs after transfection, the cells were serum-starved for 15hrs before induction with 20ng/mL IL-6. Total RNA was harvested 4hrs later and subjected to RT-qPCR analysis. c) As for b).

5 Discussion and future perspectives

5.1 STAMP2_v1

STAMP2_v1 mRNA levels in PCa cell lines followed those of the full-length transcript at a certain fixed, fractional amount. This suggests that it is not a functional transcript, but rather a by-product of androgen-induced transcription that does not encode any functional protein product. Therefore, significantly closer ratios of short-to-full-length transcripts in other tissues or induced by other stimuli in PCa cells would indicate the opposite; If the transcript is differentially regulated and expressed at higher levels in other contexts, it would indicate that it indeed is a functional transcript that might serve a separate biological function, one that is not regulated by androgens in PCa cell lines. This is in fact what was demonstrated in these experiments.

5.1.1 A shorter variant of the STAMP2 homolog has been identified in pigs

Apart from the previously mentioned entries from transcriptome sequencing efforts, the putative short isoform of STAMP2 has not been described in humans. A shorter STAMP2 isoform in meishan pigs (*Sus scrofa*) has been detected on both mRNA and protein level, cloned and partially characterized [89]. Porcine STAMP2 shows a distributed tissue expression, with high levels of mRNA detected in lung, kidney and adipose tissue, and medium levels detected in cerebellum, heart, liver and small intestine. The shorter variant mRNA, on the other hand, was expressed in a more restricted pattern, and was mainly found in lung tissue, with low levels also detected in heart and adipose tissue. As is the case for the human STAMP2_v1, the porcine short isoform mRNA lacks exon 3. Due to different exon sizes between species, the difference in size between the two porcine STAMP2 isoforms is smaller than that between the putative STAMP2_v1 and the full-length isoform in humans. On protein level, the difference in size is 117 aa/13kDa, versus 173 aa/21 kDa in humans. Difference in the size of full-length STAMP2 between the two species is 11 aa, sharing 84,7% overall sequence identity, while size, position and sequences of conserved STAMP2 family functional domains still have a higher degree of similarity [89].

Of note is that the porcine STAMP2 short isoform is predicted to have four transmembrane helices. Some functional analyses were also published: Whereas porcine full-length STAMP2 ectopically expressed in the human hepatocellular carcinoma cell line HepG2 leads to a significant reduction in the mRNA expression of genes involved in fatty acid *de novo* synthesis and gluconeogenesis, and leads to lower levels of accumulated triglycerides after fatty acid treatment, the shorter porcine variant does not show this effect in the same experiments. On the other hand, ectopic expression of *both* porcine STAMP2 variants in murine RAW264.7 macrophages did show a significant reduction in the expression of IL-6 and TNFα mRNA compared to vector control [89].

5.1.2 Differential STAMP2 isoform ratios among tissues suggest functionality

The differentially regulated expression pattern among tissues, along with the detection of a short variant at the protein level of STAMP2s homolog in pigs, is a strong indication that there also exists a short STAMP2 isoform in humans. Interestingly, when comparing tissue distributions of the two isoforms in pigs and humans, the porcine isoforms were also detected at similar levels (equal ratio) in lung tissue, as they were in the humans (figure 13). Unfortunately, levels in immune cells were not investigated in pigs. Similarly, the tissue cDNA panel used here (figure 13) did not include a sample obtained from adipose tissue for comparison. Stand-out interspecies differences is the high levels of porcine (full-length) *STAMP2* detected in brain and kidney tissue compared to corresponding human tissues, but the short isoform levels were also low in these tissues in pigs.

That the mRNA expression of STAMP2_v1 varies so markedly between tissues indicates that the isoform is not simply a by-product of transcription that accompany transcription of *STAMP2* at a certain low percentage. Instead, the high levels of STAMP2_v1 mRNA in especially lung tissues and peripheral blood mononuclear cells, where the ratio of the transcript is similar to- or even higher than that of full-length STAMP2, respectively, indicates that expression of STAMP2_v1 is differentially regulated in certain biological contexts. Separate regulation of an isoform restricted to a small set of circumstances indicates that it might serve a specialized important function(s). Since STAMP2_v1 is predicted to have a severely altered structure (figure 7-9), it is expected to have a biological function that is different than that of full-length STAMP2.

These result therefore warrants further functional studies of the isoform that would inform whether there is a possibility that the isoform also plays a role in prostate cancer. There is also a need to establish whether the low level of STAMP2_v1 mRNA is successfully translated into protein in PCa cells. That STAMP2_v1 mRNA is detected only at both generally low and at comparatively lower levels than STAMP2 in PCa cell lines does not in itself mean that its function is insignificant, assuming the isoform is also expressed at the protein level. Proteins with important regulatory functions, as e.g. protein kinases and transcription factors, are able to dramatically affect cell behavior despite their low abundance [90]. The observation that the ratio of STAMP2_v1/STAMP2 is higher in androgen-independent 22Rv1 PCa cells compared to androgen-responsive LNCaP and VCaP PCa cells is therefore very interesting and require further investigation (figure 10). However, its expression pattern suggest that STAMP2_v1 might be more relevant in the context of immunology and/or the respiratory system, something that requires further exploration

5.1.3 Potential STAMP2_v1 structure-functions

Based on the comparison of the predicted STAMP2_v1 protein sequence with full-length STAMP2, and taking into account what is known about the structure/function of the STAMP family at present, it is clear that STAMP2_v1 would be quite a different protein. It is not expected to have the same catalytic activity as STAMP2, if any. Crucial residues for interaction with iron, heme and FAD substrates and co-factors are not present. Furthermore, it lacks the targeting motif directing other STAMP members to recycling endosomes where iron processing and uptake takes place [47]. STAMP2_v1 is predicted to have fewer TM helices, and therefore cannot form the same channel-like structure composed of six transmembrane helices as present in STAMP2, which underlies its iron reductase catalytic activity (figure 5) [43]. Precisely the iron reductase activity, which is coupled with consumption of NADPH and ROS formation, is considered to be the mechanism behind many of the functions attributed to STAMP2 so far. Mitochondria are the main consumers of cellular ferrous iron, where it together with $NADP^+$ is necessary for the electron transport chain [91]. By providing both of these substrates, STAMP2 is therefore linked to mitochondrial respiration and energy production, crucial for cellular metabolic homeostasis. STAMP2-mediated ROS formation, byproducts of both the same respiration and of ferrous iron-dependent Fenton chemistry, further links STAMP2 to osteoclastogeneis and PCa cell survival [42, 58]. The reported alterations in the expression of genes involved in metabolism and redox balance after

interfering with STAMP2 expression might be secondary responses to altered metabolic and redox homeostasis [55, 62]. By its predicted lack of catalytic activity, STAMP2_v1 cannot be part of these processes in the same way. Although homologous STAMP2 protein sequences, and especially its functional residues, are highly conserved among the species, experiments where porcine proteins are expressed in human or murine cells are artificial [41, 89]. Still, the observed STAMP2-mediated effect on metabolic genes in those experiments add weight to the total picture where STAMP2, but not STAMP2_v1, is involved in the regulation of metabolic homeostasis due to its catalytic activity.

STAMP2_v1 may have functions in immune cells. It was found at its highest level here, where its level of expression is comparable to that of full-length STAMP2 in prostate tissue (figure 12). Of the genes tested, expression of inflammatory cytokines was the only category where ectopic expression of the porcine STAMP2_v1 had an effect. It is therefore interesting to note that two of the sources of the STAMP2_v1 mRNA reference sequence is from lymphatic tissue and rheumatoid arthritis (RA) tissue, known to be infiltrated by inflammatory immune cells. STAMP2 has previously been found to be associated with RA both in an experimental, glucose-6-phosphate isomerase (GPI)-induced mouse model and in human patient samples, where it co-localized with macrophage cellular markers [92]. TNFα is an important driver of the autoimmune disease. By administering TNFα mAb in the mouse RA model, the STAMP2 murine homolog TIARP was found to be the most potently TNFα-regulated gene in splenocytes. Innate immune cell surface marker CD11b-positive splenocytes were the main source of TIARP mRNA. Taken together with the observation of high monocyte STAMP2_v1 expression (figure 13), this links both STAMP2 isoforms with innate immune cells. As the isoforms have severely different structures, and therefore likely perform different functions, and both are present at considerable levels, design of future studies of STAMP2 isoforms in this context must be made with these factors in mind. Primers pairs and antibodies used to measure expression should be able to distinguish the isoforms from each other in order to properly uncover their different functions. The same holds for design of siRNA/shRNA used in RNAi.

5.1.4 Future perspectives for STAMP2_v1 studies

Attempts to detect STAMP2_v1 mRNA were made alongside detection of *STAMP2* in the initial cytokine titration experiments in LNCaP cells. In individual experiments with IL-6-treatment, the transcript variant could be detected at very low levels and with variability between replicates. Any quantification would therefore not be meaningful. In the majority of experiments with cytokine induction, expression of *STAMP2_v1* was not detected. The possible induction of *STAMP2_v1* by these cytokines was therefore not investigated further. The regulation of RNA processing giving rise to STAMP2_v1 might be regulated by other factors in PCa cells.

To further investigate possible roles of STAMP2_v1, use of expression vectors in model systems would be a logical place to start. Confocal microscopy of cells expressing STAMP2_v1 conjugated to fluorescent moieties would reveal which sub-cellular structures the isoform localize to, and could inform future searches for potential direct protein-protein interaction partners. Epitope-tagging followed by immunostaining could further determine the true orientation of the N- and C-terminals of the protein. If microscopy studies would reveal that STAMP2_v1 localize to the plasma membrane, N-linked epitopes would be accessible for immunostaining of whole cells if the switched N-terminal orientation is true. Negative staining would on the other hand indicate the presence of an alternative, fourth TM helix. If the protein is found to localize intracellularly, the same results could possibly be obtained after fractionation of intracellular membranes. Further, the predicted lack of catalytic activity should be validated experimentally in model systems. This would involve NADPH oxidase, iron reductase and ROS formation assays. Potential effects on the expression of metabolic, redox and inflammatory reporter genes should likewise be investigated and compared by ectopic expression of both human STAMP2 isoforms in the same experiments.

Distribution of STAMP2_v1 among immune cell sub-types should be further explored. The role(s) STAMP2_v1 plays in the type(s) of cells where it is expressed could then further be investigated by isoform-specific genetic studies, followed by both functional assays and transcriptomic analyses. Since STAMP2_v1 is detected in monocytes, it would be of special interest to investigate whether it plays a role in the differentiation into macrophages, what sort of stimuli regulates its expression and whether it is differentially expressed between the M1 and M2 macrophage phenotypes. STAMP2 has already established links to differentiation

processes in adipocytes and in regulating macrophage behavior [57, 64]. *In vitro* culturing and activation of purified monocytes would be a simple way to start this line of investigation.

As STAMP2 has established links to cancer, especially of the prostate, it should be further explored whether that also is true for STAMP2_v1. The altered ratio among STAMP2 isoforms observed in 22Rv1, a CRPC model cell line, warrants a further exploration of STAMP2 isoform expression during the different stages of PCa progression. As STAMP2_v1 is expressed at high levels in lung tissue and immune cells, lung cancer, lymphoma and leukemia are other potential candidates. The lack of knowledge of and attention to the isoform is a problem in that regard, as expression data might not be available in published cohorts. That requires junction-specific probes able to distinguish it from STAMP2. On the other hand, higher resolution, genome-wide arrays able to detect differentially expressed isoforms and RNA-seq datasets are available and are increasingly being used.

5.2 Cytokine-mediated induction of STAMP2 expression in LNCaP cells

LNCaP is a commonly used PCa cell line for both *in vitro* and *in vivo* studies [93]. One property of the LNCaP cell line is that it harbors a deletion in the tumor suppressor phosphatase and tensin homolog (PTEN), a negative regulator of the PI3K pathway. [67, 93]. The significant role the PI3K-AKT-mTOR pathway plays for growth of PCa cells is well recognized, and was further underpinned when genomic profiling revealed that it was constitutively activated in all of a cohort of 218 PCa patient samples [10]. In above 40% of cases was this due to loss of PTEN function. Supported by transcriptomic profiling, PCa with PTEN loss has been suggested as a separate genetic sub-type after discovery of mechanisms of reciprocal negative feedback between the AR- and the PI3K-pathway [94, 95]. The following discussion is made considering the limitations of the applicability of *in vitro* studies in LNCaP cells. The results are not suggested to be of general validity for PCa, but rather a proof-of-principle study in this one commonly used model cell line that open the door to future studies.

5.2.1 Interactions of cytokine pathways with the AR

The hypothesis that cytokine treatments would lead to activation of AR-mediated transcription predicts that rise in canonical AR target genes would follow cytokine treatment. The opposite was observed (figures 16a,b). There are several possible explanations for this. First, nuclear translocation of a new set of transcriptional regulators after cytokine-mediated activation of intracellular signaling pathways would alter the balance of active nuclear transcription factors. It is conceivable that the new recruits operate in concert with several general co-factors also utilized by the AR in regulation of gene expression. In other words, down-regulation of AR target gene output was due to a stoichiometric competition for transcriptional machinery. The observation that a small-molecule inhibitor of AR nuclear translocation increased IL-6-mediated induction of *STAMP2* could support this option (figure 16d). Another possibility is that target gene expression activated by the cytokines in this experimental setting and in the genetic background of LNCaP cells would lead to synthesis of proteins that more directly repress AR activity. Inverse correlation of AR and STAT3 has been found previously in a study of PCa stem-like cells [99]. By shRNA-mediated knockdown of either transcription factor in DU145 PCa cells, levels of the other factor increased. A third possibility, as STAT3 has been shown to directly interact with AR [110], is that STAT3 interaction with AR blocks its nuclear translocation. The observation of a slight observable difference in nuclear AR with and without IL-6 treatment support the third option, but the relative intensities of the protein bands was not quantitatively measured in that experiment (figure 16c). Potential cross-talk between AR and cytokine pathways that affects STAMP2 expression should be further investigated.

5.2.2 IL-6 and STAT3 are implicated in prostate cancer progression

There are indications of inflammation caused by infection, trauma or environmental/dietary factors playing a role in the initiation of PCa, but this remains controversial [96]. IL-6 and STAT3 have clear links to PCa progression, as they do with other cancer types. Elevated levels of both IL-6 and its receptor have been found in localized PCa samples compared to adjacent healthy tissue, and correlated with elevated proliferation measured by Ki67 expression [97]. Elevated circulating IL-6 levels is a prognostic factor for poor prognosis in PCa patients [98]. Furthermore, STAT3 has been found to be involved in maintaining a stem-like PCa cell type which survive independently of the AR [99].

In the experiments presented here, STAMP2 expression was positively regulated by the inflammatory cytokines IL-6, IL-1β- and TNFα in LNCaP cells. STAT3 was involved in these processes after IL-6 and IL-1β treatment. As these factors are implicated in PCa progression, while STAMP2 has been shown to be critical for PCa cell growth and survival [42], these results warrants future studies of the potential role of STAMP2 in the intersection of inflammation and PCa progression.

5.2.3 IL-6 mediated induction of STAMP2 expression

The experiments presented here showed that IL-6 treatment induced STAMP2 expression on mRNA level in LNCaP cells *in vitro*. Attempts were made to detect STAMP2 by Western analysis of LNCaP membrane protein fractions harvested 24hrs after treatments with IL-6 and IL-1β, but the results were inconclusive (data not shown). The available polyclonal antibody against STAMP2 is not very dependable. It produces several strong, unspecific bands in the region where STAMP2 is expected to be found, while STAMP2 detection is weak. Results from western blot experiments using this antibody have been published, but with protein extracts from mature adipocytes [57, 100], where STAMP2 mRNA levels are 1-2 orders of magnitude higher than they are in LNCaP cells after cytokine induction (FS lab data, not shown). STAMP2 protein levels after cytokine induction might therefore be below the detection limit of the antibody. Alternatively, the protocol needs to be refined to achieve conclusive detection. Due to these technical difficulties, conclusions derived from these experiments cannot be translated onto protein level at present. This is a weakness of the presented study and something that needs to be established in the future.

There can on the other hand be no doubt that IL-6 up-regulates STAMP2 mRNA synthesis in LNCaP cells. This coincides with activation of STAT1/3 and ERK1/2 (figure 17). Use of a JAK2 kinase inhibitor and STAT3 siRNA-mediated knockdown (figure 21) further showed that the JAK2-STAT3 axis downstream of the IL-6R complex is critical for IL-6-mediated induction of *STAMP2* expression. Apart from a definite demonstration of enrichment of STAT3 on the STAMP2 promoter by chromatin immunoprecipitation (ChIP) analysis, these results showed that STAMP2 is an IL-6-STAT3-regulated gene in LNCaP cells. This was furthermore found to be independent of both the AR and NF-κB. The conclusion is supported by ChIP experiments showing that *Stamp2* is a direct Il-6-Stat3 target gene in murine liver tissue *in vivo* [59]. The murine proximal *Stamp2* promoter contains three Stat3 consensus

binding sites. By mutagenesis studies of reporter constructs containing the murine *Stamp2* promoter, only one of the binding sites was found to be critical for Stat3-mediated *Stamp2* expression. Importantly, the critical Stat3 binding site is the only of the murine sites that is conserved in the human *STAMP2* promoter [59]. IL-6 has also been shown to activate expression of both STAMP2 mRNA and protein in both murine and human adipocytes *in vitro* [100, 101].

The kinase inhibitor experiments showed that chemical inhibition of MEK1/2 upstream of ERK1/2 had a slight, negative effect on IL-6-mediated *STAMP2* expression (figure 21a). A similar result was found for IL-1β. What role ERK1/2 plays in the regulation of *STAMP2* expression remains to be established. IL-1β treatment induced strong c-Jun phosphorylation, whereas IL-6 did not (figure 20). The MEK1/2 inhibitor affected the level of phospho-c-Jun after IL-1β treatment, but the observation that the JNK1-3 inhibitor failed to suppress STAMP2 induction suggests that c-Jun is unlikely to be a co-regulator. The JNK1-3 inhibitor had a strong negative effect on IL-6 mediated STAMP2 expression on the other hand, but this is likely due to an unintended inhibition of JAKs. This assumption is warranted by the effect that the JNK1-3 inhibitor had on STAT1/3 and ERK1/2 activation (figure19), where it produced very similar results as the JAK2 inhibitor. Furthermore as neither phospho-JNK1-3 (data not shown) nor phospho-c-Jun (figure 20) were detected after IL-6 treatment, it is unlikely that AP-1 participates in IL-6-mediated *STAMP2* expression.

5.2.4 STAT1 and serine727-phosphorylation of STAT3

Serine727 phosphorylation is regarded an auxiliary modification that is not necessary for STAT3 dimerization, nuclear translocation and base-line transcriptional activation, but may influence transcriptional activity negatively or positively in different contexts [102]. No change was seen over time in the level of STAT3 ser727 phosphorylation after IL-6 treatment. This was somewhat surprising, as this modification among others is mediated by MSK1 [103], which again is activated by ERK2 and p38 [104], both of which were shown to be active in the same cells (figure 17). It was also unexpected to find that STAT3 was phosphorylated on serine727 in untreated controls. This might indicate that some other factor is active under experimental basal conditions and act as the main regulator of this STAT3 modification in LNCaP cells. One candidate that is often over-expressed and constitutively active in PCa is Protein kinase C epsilon (PKCε), which has been shown to interact with

STAT3 and mediate its phosphorylation at ser727 when over-expressed in LNCaP cells [105]. Another more likely candidate, as LNCaP cells have lost functional PTEN, is mammalian target of rapamycin (mTOR) or a downstream serine kinase, which have been shown to be implicated in serine phosphorylation of STAT3 in HepG2 hepatocellular carcinoma cells [106]. Higher levels of serine-phosphorylated STAT3 also followed those of phospho-AKT in murine prostate tissues from a PTEN prostate-specific, conditional knock-out mouse PCa model compared to wild-type [107]. Further work is required to determine if ser727 is functionally involved in STAMP2 expression.

STAT1 was also activated by IL-6 in LNCaP cells (figure 17). Its role in the regulation of STAMP2 expression, if any, could be clarified e.g. by immunoprecipitation clarifying whether IL-6 induce formation of STAT1/3 heterodimers in LNCaP cells. STAT1 RNAi alone and in combination with STAT3 followed by RT-qPCR would show whether STAT1 participates in the regulation of STAMP2 expression. STAT1 and STAT3 was found to have distinctly different activation profiles over time as measured by Western analysis of tyrosine-phosphorylated STATs (figure 17). While STAT1 activation was brief, STAT3 was activated in a biphasic pattern over time. An indication that STAT3 is the more important of the two in regulating STAMP2 expression can be seen by comparing STAT activation profiles with the induction profile of STAMP2 mRNA (figure 14a,d), which is sustained in a similar manner as STAT3. Suppressor of cytokine signaling 3 (SOCS3) is a downstream target gene of the JAK-STAT pathway, and its protein product binds to the IL-6R-JAK complex and interferes with JAK kinase activity. Prolonged presence of IL-6 has been found to circumvent negative feedback regulation by the association of IL-6R with the epidermal growth factor receptor [108]. This association forms a complex where JAK1/2 remains active out of reach for SOCS3, and is thereby able to re-activate STAT3. As a similar pattern of STAT3 activation was observed in these experiments, a similar mechanism might operate in LNCaP cells, enabling a more prolonged activation of STAMP2 expression. This remains to be established experimentally.

5.2.5 IL-1β and TNFα mediated induction of STAMP2 expression

TNFα failed to induce *STAMP2* expression in LNCaP cells in a previous publication [111]. That report was contradicted in these experiments, as TNFα treatment induced a small, but significant increase in *STAMP2* expression (figure 14c,d). Both of these observations are

surprising, however, as *STAMP2* is known to be robustly regulated by TNFα in several cell types (table 2). In mice, that is how it was discovered and initially got its name (TIARP) [34]. A20 (TNFα-induced protein 3) is a canonical target gene of TNFα involved in negative feedback regulation of the NF-κB pathway [87]. *A20* expression was measured as positive control to ensure that the TNFα treatment was effective (data not shown). In the combination experiment with IL-6 (figure 13d), similar levels of *A20* induction was found after both treatments with TNFα, irrespective of the presence of IL-6. Further experiments in other PCa cell lines should be conducted to determine if the observed weak TNFα-mediated STAMP2 induction is specific to LNCaP cells or whether it also holds in more general for PCa cells. Furthermore, as multiple inflammatory cytokines are likely to be present simultaneously at sites of inflammation *in situ*, the observed additive effect on STAMP2 expression of combined IL-6 and TNFα treatment (figure 13d) should be explored further. Which cytokines and their relative concentrations used in such studies should preferably be based on experimentally measured results from *in vivo* PCa inflammation models or patient samples. The danger of using artificially high concentrations *in vitro* is a concern, both for the validity of the result presented here and for the design of future studies.

Apart from different receptor complexes, many of the same protein players participate in IL-1β- and TNFα-mediated intracellular signaling cascades [30]. Both cytokines end up activating NF-κB, ERK1/2, p38 and JNK1-3. In the present study, they were not used side-by-side in the same experiment, making an absolute conclusion unwarranted, but IL-1β treatment consistently induced relative STAMP2 expression more than TNFα did. Surprisingly, siRNA-mediated knockdown showed that STAT3 alongside NF-κB was involved in IL-1β-mediated *STAMP2* induction (figure 22b,c). Inflammatory signaling networks are expected to be fast and responsive. Transcription of IL-1β target genes take place within 30 minutes and can last for several hours [29]. Together with the implication of STAT3, comparison of *STAMP2* induction profiles by IL-1β and IL-6 (figure 15a,b) could therefore indicate that IL-1β-mediated *STAMP2* induction is more indirect than that by IL-6. Consistent with those presented here, slower induction of *STAMP2* after IL-1β treatment compared to IL-6 was also reported in 3T3-L1 murine adipocytes [101, 112]. Induction of *STAMP2* expression after IL-1β treatment might therefore be indirectly mediated by NF-κB via expression of factors that by cell-autonomous or paracrine mechanisms lead to STAT3 activation. What role STAT3 plays in this process requires further investigation.

5.2.6 Possible indirect pathways involving STAT3

Induction of the chemokines IL-8/CXCL8 and CCL2/MCP-1, both canonical target genes of NF-κB, were measured by qPCR as positive controls for IL-1β and TNFα treatment (data not shown) [29, 113]. Both of these factors are known to activate JAK-STAT signaling; IL-8 downstream of its receptor C-X-C chemokine receptor type 1/2 (CXCR1/2) [113] and CCL2 downstream of C-C chemokine receptor type 2 (CCR2) [114], but expression of the latter receptor is considered to be restricted to monocytes. IL-6 is also a NF-κB target gene [29]. IL-6 has not been found to be expressed in LNCaP cells at baseline, but is expressed on mRNA level after IL-1β treatment [115]. IL-6 mRNA was detected after IL-1β treatment, but at low levels only at the 1hr time-point (data not shown). It has previously been shown that LNCaP cells can be conditioned over time to express IL-6, but that IL-6 is not successfully secreted by IL-6 naïve LNCaP [109]. This makes IL-6 a less likely candidate auto-/paracrine factor in these experiments, but IL-8 is an NF-κB-regulated chemokine that activates STAT3, and as such is a candidate intermediary factor involved in indirect regulation of STAMP2 expression by IL-1β.

Although the downstream signaling cascades activated by IL-1β- and TNFα are similar, they must also have significant differences in LNCaP cells. That was reflected in the different levels of induction of both CCL2 and IL-8 mediated by the two cytokines. Their expression levels were induced to a much greater extent by IL-1β than by TNFα (data not shown). If IL-8 acts as an intermediate factor in the hypothetical indirect pathway, the difference in its expression levels could explain the difference in STAMP2 induction mediated by IL-1β versus TNFα. Strong induction of IL-8 mRNA expression was found within 30 minutes after IL-1β treatment (figure 15), whereas *STAMP2* levels peaked three hours later than *IL-8* did. If IL-8 is translated into protein, is processed and secreted by LNCaP cells within a reasonable time-frame after transcription, IL-8 could act as an auto- or paracrine factor. Paracrine IL-8 signaling between LNCaP cells should therefore in the future be investigated experimentally, e.g. by enzyme-linked immunosorbent assays (ELISA). JAK2 is activated downstream of the IL-8 receptor CXCR1/2 [113], but the JAK2 inhibitor AZD1450 did not have an effect on IL-1β-mediated *STAMP2* expression (figure 22a). The question thus remains as to whether IL-8-mediated intracellular signaling (or that of other IL-1β target genes not so far considered) would be able to activate STAT3 via other mechanisms. The non-receptor proto-oncogene tyrosine kinase Src has been found to be activated by IL-8 treatment of LNCaP cells [116],

while its activation of STAT3 has been demonstrated in other cell types [102]. A potential role of Src in IL-1β-mediated STAMP2 induction could be investigated by RNAi.

A simpler mechanism of IL-1β-mediated STAMP2 induction involving STAT3 comes from the observation that STAT3 has a certain low level, constitutive activity in LNCaP cells [117]. In this scenario, IL-1β-mediated signaling cascades provide the repertoire of accessory transcription factors necessary to cooperate with residual STAT3 to induce STAMP2 expression. Based on the results from the experiments with siRNA-mediated and chemical inhibition, this would then be NF-κB (figure 21c) and possibly transcription factors downstream of ERK1/2 (figure 22a). Alternatively, ERK1/2 plays an accessory role by other mechanisms. As this still would be STAT3-mediated expression, it might account for the relatively lower levels of induction, but does not account for the difference in kinetics observed between IL-1β- and IL-6-mediated induction of *STAMP2*.

In conclusion, future experiments are needed to uncover the exact mechanism of IL-1β-mediated induction of STAMP2 in LNCaP cells. The role of STAT3 should be more firmly established in this regard. ELISA of conditioned media would reveal whether auto- or paracrine mechanisms could be involved. ChIP experiments performed at various time-points after treatment could reveal whether a delayed recruitment of STAT3 takes place, and whether STAT3 cooperates with NF-κB in any way. Interfering with Src function would indicate whether it is involved in JAK2-independent activation of STAT3. Extending these experiments to other PCa cell lines would also collectively give a clearer picture of how IL-1β regulates STAMP2 expression in PCa.

5.2.7 Duration of cytokine-mediated STAMP2 expression

The STAMP2 induction profiles suggested that up-regulation is a transient response to cytokines in LNCaP cells (figure 15). This raises the question of what happens over longer periods of time. The physiological role of STAMP2 is of a transient nature in other contexts, as in regulating cellular responses to fluctuations in nutrients and inflammation in adipocytes [55]. Here STAMP2 is needed to level off cellular responses during brief peaks of external stimuli. This regulation of STAMP2 is lost in obesity, a condition associated with constant elevated levels of both inflammatory stimuli and nutrients, manifested as insulin resistance, hyperglycemia and elevated serum triglycerides and cholesterol. Prolonged presence of IL-6 in LNCaP culture media has been found to significantly alter the behavior of LNCaP cells

[109]. PSA expression as a marker of AR activity decreased after IL-6 conditioning. Also, whereas IL-6 treatment inhibits proliferation of IL-6 naïve LNCaP cells, conditioned LNCaP cells were unaffected. This indicates that long term treatment abolishes growth limiting mechanisms in LNCaP.

Related to this was the finding that STAT3 performed a tumor suppressor-role both in LNCaP xenografts and in prostate-specific PTEN knock-out mouse models of PCa [107]. Loss of either *IL-6* or *STAT3* in this background led to higher proliferation and more metastases. STAT3 expression was on the other hand down-regulated both in the mouse model over time, and in human patient-matched metastases versus primary PCa. It was shown that STAT3 directly activated the expression of *CDKN2A*, whose protein product $p14^{ARF}$ stabilizes the tumor suppressor p53, which again induce senescence in a PTEN loss background. These results were corroborated by the finding that $p14^{ARF}$ and STAT3 expression correlates with both patient biochemical recurrence (BCR)-free survival and Gleason score; patient samples with high expression of both factors had a lower Gleason score and were from patients with a significantly longer BCR-free survival after treatment compared to those with low expression of both factors [107]. This shows that STAT3 can play different roles in different contexts. It leaves the question of how STAMP2 expression is affected by long term inflammatory stimuli an intriguing open question. The observation that TNFα and IL-6 synergistically induce STAMP2 expression (figure 14d) is also interesting in this regard and requires future investigation. It highlights the potential of different inflammatory pathways to converge and reinforce each other, something that could potentially affect regulation of STAMP2 over time and is likely more similar to an *in vivo* situation.

References

1. Ferlay, J., I. Soerjomataram, R. Dikshit, S. Eser, C. Mathers, M. Rebelo, . . . F. Bray, *Cancer incidence and mortality worldwide: sources, methods and major patterns in GLOBOCAN 2012.* Int J Cancer, 2015. **136**(5): p. E359-86.

2. Prensner, J.R., M.A. Rubin, J.T. Wei, and A.M. Chinnaiyan, *Beyond PSA: the next generation of prostate cancer biomarkers.* Sci Transl Med, 2012. **4**(127): p. 127rv3.

3. Report, *National Prostate Cancer Quality Register Yearly Report*, E. Skaaheim Haug, Editor 2015, National Program for Prostate Cancer: Norwegian National Cancer Registry.

4. Heidenreich, A., P.J. Bastian, J. Bellmunt, M. Bolla, S. Joniau, T. van der Kwast, . . . U. European Association of, *EAU guidelines on prostate cancer. part 1: screening, diagnosis, and local treatment with curative intent-update 2013.* Eur Urol, 2014. **65**(1): p. 124-37.

5. Ohori, M., T.M. Wheeler, and P.T. Scardino, *The New American Joint Committee on Cancer and International Union Against Cancer TNM classification of prostate cancer. Clinicopathologic correlations.* Cancer, 1994. **74**(1): p. 104-14.

6. Humphrey, P.A., *Gleason grading and prognostic factors in carcinoma of the prostate.* Mod Pathol, 2004. **17**(3): p. 292-306.

7. Bostwick, D.G., H.B. Burke, D. Djakiew, S. Euling, S.M. Ho, J. Landolph, . . . B. Timms, *Human prostate cancer risk factors.* Cancer, 2004. **101**(10 Suppl): p. 2371-490.

8. Shappell, S.B., G.V. Thomas, R.L. Roberts, R. Herbert, M.M. Ittmann, M.A. Rubin, . . . R.D. Cardiff, *Prostate pathology of genetically engineered mice: definitions and classification. The consensus report from the Bar Harbor meeting of the Mouse Models of Human Cancer Consortium Prostate Pathology Committee.* Cancer Res, 2004. **64**(6): p. 2270-305.

9. Shen, M.M. and C. Abate-Shen, *Molecular genetics of prostate cancer: new prospects for old challenges.* Genes Dev, 2010. **24**(18): p. 1967-2000.

10. Taylor, B.S., N. Schultz, H. Hieronymus, A. Gopalan, Y. Xiao, B.S. Carver, . . . W.L. Gerald, *Integrative genomic profiling of human prostate cancer.* Cancer Cell, 2010. **18**(1): p. 11-22.

11. Lonergan, P.E. and D.J. Tindall, *Androgen receptor signaling in prostate cancer development and progression.* J Carcinog, 2011. **10**: p. 20.

12. Bluemn, E.G. and P.S. Nelson, *The androgen/androgen receptor axis in prostate cancer.* Curr Opin Oncol, 2012. **24**(3): p. 251-7.

13. Dvorak, H.F., *Tumors: wounds that do not heal. Similarities between tumor stroma generation and wound healing.* N Engl J Med, 1986. **315**(26): p. 1650-9.

14. Pages, F., J. Galon, M.C. Dieu-Nosjean, E. Tartour, C. Sautes-Fridman, and W.H. Fridman, *Immune infiltration in human tumors: a prognostic factor that should not be ignored.* Oncogene, 2010. **29**(8): p. 1093-102.

15. Hanahan, D. and R.A. Weinberg, *Hallmarks of cancer: the next generation.* Cell, 2011. **144**(5): p. 646-74.

16. Guven Maiorov, E., O. Keskin, A. Gursoy, and R. Nussinov, *The structural network of inflammation and cancer: merits and challenges.* Semin Cancer Biol, 2013. **23**(4): p. 243-51.

17. Ostrand-Rosenberg, S., L.A. Horn, and S.T. Haile, *The programmed death-1 immune-suppressive pathway: barrier to antitumor immunity.* J Immunol, 2014. **193**(8): p. 3835-41.

18. Hirano, T., K. Yasukawa, H. Harada, T. Taga, Y. Watanabe, T. Matsuda, . . . et al., *Complementary DNA for a novel human interleukin (BSF-2) that induces B lymphocytes to produce immunoglobulin.* Nature, 1986. **324**(6092): p. 73-6.

19. Schaper, F. and S. Rose-John, *Interleukin-6: Biology, signaling and strategies of blockade.* Cytokine Growth Factor Rev, 2015. **26**(5): p. 475-87.

20. Hodge, D.R., E.M. Hurt, and W.L. Farrar, *The role of IL-6 and STAT3 in inflammation and cancer.* Eur J Cancer, 2005. **41**(16): p. 2502-12.

21. Yu, H., H. Lee, A. Herrmann, R. Buettner, and R. Jove, *Revisiting STAT3 signalling in cancer: new and unexpected biological functions.* Nat Rev Cancer, 2014. **14**(11): p. 736-46.

22. Yamasaki, K., T. Taga, Y. Hirata, H. Yawata, Y. Kawanishi, B. Seed, . . . T. Kishimoto, *Cloning and expression of the human interleukin-6 (BSF-2/IFN beta 2) receptor.* Science, 1988. **241**(4867): p. 825-8.

23. Eulenfeld, R., A. Dittrich, C. Khouri, P.J. Muller, B. Mutze, A. Wolf, and F. Schaper, *Interleukin-6 signalling: more than Jaks and STATs.* Eur J Cell Biol, 2012. **91**(6-7): p. 486-95.

24. Manning, B.D. and L.C. Cantley, *AKT/PKB signaling: navigating downstream.* Cell, 2007. **129**(7): p. 1261-74.

25. Agarwal, A., K. Das, N. Lerner, S. Sathe, M. Cicek, G. Casey, and N. Sizemore, *The AKT/I kappa B kinase pathway promotes angiogenic/metastatic gene expression in colorectal cancer by activating nuclear factor-kappa B and beta-catenin.* Oncogene, 2005. **24**(6): p. 1021-31.

26. Bode, J.G., U. Albrecht, D. Haussinger, P.C. Heinrich, and F. Schaper, *Hepatic acute phase proteins--regulation by IL-6- and IL-1-type cytokines involving STAT3 and its crosstalk with NF-kappaB-dependent signaling.* Eur J Cell Biol, 2012. **91**(6-7): p. 496-505.

27. Pizarro, T.T. and F. Cominelli, *Cloning IL-1 and the birth of a new era in cytokine biology.* J Immunol, 2007. **178**(9): p. 5411-2.

28. Dinarello, C.A. and J.W. van der Meer, *Treating inflammation by blocking interleukin-1 in humans.* Semin Immunol, 2013. **25**(6): p. 469-84.

29. Weber, A., P. Wasiliew, and M. Kracht, *Interleukin-1 (IL-1) pathway.* Sci Signal, 2010. **3**(105): p. cm1.

30. Sabio, G. and R.J. Davis, *TNF and MAP kinase signalling pathways.* Semin Immunol, 2014. **26**(3): p. 237-45.

31. Waterfield, M.R., M. Zhang, L.P. Norman, and S.C. Sun, *NF-kappaB1/p105 regulates lipopolysaccharide-stimulated MAP kinase signaling by governing the stability and function of the Tpl2 kinase.* Mol Cell, 2003. **11**(3): p. 685-94.

32. Korkmaz, K.S., C. Elbi, C.G. Korkmaz, M. Loda, G.L. Hager, and F. Saatcioglu, *Molecular cloning and characterization of STAMP1, a highly prostate-specific six transmembrane protein that is overexpressed in prostate cancer.* J Biol Chem, 2002. **277**(39): p. 36689-96.

33. Porkka, K.P., M.A. Helenius, and T. Visakorpi, *Cloning and characterization of a novel six-transmembrane protein STEAP2, expressed in normal and malignant prostate.* Lab Invest, 2002. **82**(11): p. 1573-82.

34. Moldes, M., F. Lasnier, X. Gauthereau, C. Klein, J. Pairault, B. Feve, and A.M. Chambaut-Guerin, *Tumor necrosis factor-alpha-induced adipose-related protein (TIARP), a cell-surface protein that is highly induced by tumor necrosis factor-alpha and adipose conversion.* J Biol Chem, 2001. **276**(36): p. 33938-46.

35. Korkmaz, C.G., K.S. Korkmaz, P. Kurys, C. Elbi, L. Wang, T.I. Klokk, . . . F. Saatcioglu, *Molecular cloning and characterization of STAMP2, an androgen-regulated six transmembrane protein that is overexpressed in prostate cancer.* Oncogene, 2005. **24**(31): p. 4934-4945.

36. Hubert, R.S., I. Vivanco, E. Chen, S. Rastegar, K. Leong, S.C. Mitchell, . . . D.E. Afar, *STEAP: a prostate-specific cell-surface antigen highly expressed in human prostate tumors.* Proc Natl Acad Sci U S A, 1999. **96**(25): p. 14523-8.

37. Steiner, M.S., X. Zhang, Y. Wang, and Y. Lu, *Growth inhibition of prostate cancer by an adenovirus expressing a novel tumor suppressor gene, pHyde.* Cancer Res, 2000. **60**(16): p. 4419-25.

38. Passer, B.J., V. Nancy-Portebois, N. Amzallag, S. Prieur, C. Cans, A. Roborel de Climens, . . . A. Telerman, *The p53-inducible TSAP6 gene product regulates apoptosis and the cell cycle and interacts with Nix and the Myt1 kinase.* Proc Natl Acad Sci U S A, 2003. **100**(5): p. 2284-9.

39. Ohgami, R.S., D.R. Campagna, E.L. Greer, B. Antiochos, A. McDonald, J. Chen, . . . M.D. Fleming, *Identification of a ferrireductase required for efficient transferrin-dependent iron uptake in erythroid cells.* Nat Genet, 2005. **37**(11): p. 1264-9.

40. Zhang, X., K.H. Krause, I. Xenarios, T. Soldati, and B. Boeckmann, *Evolution of the ferric reductase domain (FRD) superfamily: modularity, functional diversification, and signature motifs.* PLoS One, 2013. **8**(3): p. e58126.

41. Ohgami, R.S., D.R. Campagna, A. McDonald, and M.D. Fleming, *The Steap proteins are metalloreductases.* Blood, 2006. **108**(4): p. 1388-94.

42. Jin, Y., L. Wang, S. Qu, X. Sheng, A. Kristian, G.M. Maelandsmo, . . . F. Saatcioglu, *STAMP2 increases oxidative stress and is critical for prostate cancer.* EMBO Mol Med, 2015. **7**(3): p. 315-31.

43. Kleven, M.D., M. Dlakic, and C.M. Lawrence, *Characterization of a single b-type heme, FAD, and metal binding sites in the transmembrane domain of six-transmembrane epithelial antigen of the prostate (STEAP) family proteins.* J Biol Chem, 2015. **290**(37): p. 22558-69.

44. Warkentin, E., B. Mamat, M. Sordel-Klippert, M. Wicke, R.K. Thauer, M. Iwata, . . . S. Shima, *Structures of F420H2:NADP+ oxidoreductase with and without its substrates bound.* EMBO J, 2001. **20**(23): p. 6561-9.

45. Sendamarai, A.K., R.S. Ohgami, M.D. Fleming, and C.M. Lawrence, *Structure of the membrane proximal oxidoreductase domain of human Steap3, the dominant ferrireductase of the erythroid transferrin cycle.* Proc Natl Acad Sci U S A, 2008. **105**(21): p. 7410-5.

46. Gauss, G.H., M.D. Kleven, A.K. Sendamarai, M.D. Fleming, and C.M. Lawrence, *The crystal structure of six-transmembrane epithelial antigen of the prostate 4 (Steap4), a ferri/cuprireductase, suggests a novel interdomain flavin-binding site.* J Biol Chem, 2013. **288**(28): p. 20668-82.

47. Lambe, T., R.J. Simpson, S. Dawson, T. Bouriez-Jones, T.L. Crockford, M. Lepherd, . . . R.J. Cornall, *Identification of a Steap3 endosomal targeting motif essential for normal iron metabolism.* Blood, 2009. **113**(8): p. 1805-8.

48. Wang, L., Y. Jin, Y.J. Arnoldussen, I. Jonson, S. Qu, G.M. Maelandsmo, . . . F. Saatcioglu, *STAMP1 is both a proliferative and an antiapoptotic factor in prostate cancer.* Cancer Res, 2010. **70**(14): p. 5818-28.

49. Whiteland, H., S. Spencer-Harty, C. Morgan, H. Kynaston, D.H. Thomas, P. Bose, . . . S.H. Doak, *A role for STEAP2 in prostate cancer progression.* Clin Exp Metastasis, 2014. **31**(8): p. 909-20.

50. Rinaldy, A.R., R.P. Menon, J.L. Lerner, and M.S. Steiner, *Role of pHyde novel gene product as an intrinsic factor for apoptotic pathway in prostate cancer.* Gan To Kagaku Ryoho, 2000. **27 Suppl 2**: p. 215-22.

51. Zhang, X., M.S. Steiner, A. Rinaldy, and Y. Lu, *Apoptosis induction in prostate cancer cells by a novel gene product, pHyde, involves caspase-3.* Oncogene, 2001. **20**(42): p. 5982-90.

52. Lu, Y., X. Zhang, B. Beheshti, and J. Zhang, *Adenoviral-mediated pHyde gene transfer and cisplatin additively inhibit human prostate cancer growth by enhancing apoptosis.* Prostate, 2009. **69**(3): p. 234-48.

53. Caillot, F., R. Daveau, M. Daveau, J. Lubrano, G. Saint-Auret, M. Hiron, . . . J.P. Salier, *Down-regulated expression of the TSAP6 protein in liver is associated with a transition from cirrhosis to hepatocellular carcinoma.* Histopathology, 2009. **54**(3): p. 319-27.

54. Isobe, T., E. Baba, S. Arita, M. Komoda, S. Tamura, T. Shirakawa, . . . K. Akashi, *Human STEAP3 maintains tumor growth under hypoferric condition.* Exp Cell Res, 2011. **317**(18): p. 2582-91.

55. Wellen, K.E., R. Fucho, M.F. Gregor, M. Furuhashi, C. Morgan, T. Lindstad, . . . G.S. Hotamisligil, *Coordinated Regulation of Nutrient and Inflammatory Responses by STAMP2 Is Essential for Metabolic Homeostasis.* Cell, 2007. **129**(3): p. 537-548.

56. Moreno-Navarrete, J.M., F. Ortega, M. Serrano, R. Perez-Perez, M. Sabater, W. Ricart, . . . J.M. Fernandez-Real, *Decreased STAMP2 expression in association with visceral adipose tissue dysfunction.* J Clin Endocrinol Metab, 2011. **96**(11): p. E1816-25.

57. Sikkeland, J. and F. Saatcioglu, *Differential expression and function of stamp family proteins in adipocyte differentiation.* PLoS One, 2013. **8**(7): p. e68249.

58. Zhou, J., S. Ye, T. Fujiwara, S.C. Manolagas, and H. Zhao, *Steap4 plays a critical role in osteoclastogenesis in vitro by regulating cellular iron/reactive oxygen species (ROS) levels and cAMP response element-binding protein (CREB) activation.* J Biol Chem, 2013. **288**(42): p. 30064-74.

59. Ramadoss, P., F. Chiappini, M. Bilban, and A.N. Hollenberg, *Regulation of hepatic six transmembrane epithelial antigen of prostate 4 (STEAP4) expression by STAT3 and CCAAT/enhancer-binding protein alpha.* J Biol Chem, 2010. **285**(22): p. 16453-66.

60. Zhang, C.M., X. Chi, B. Wang, M. Zhang, Y.H. Ni, R.H. Chen, . . . X.R. Guo, *Downregulation of STEAP4, a highly-expressed TNF-alpha-inducible gene in adipose tissue, is associated with obesity in humans.* Acta Pharmacol Sin, 2008. **29**(5): p. 587-92.

61. Catalan, V., J. Gomez-Ambrosi, A. Rodriguez, B. Ramirez, F. Rotellar, V. Valenti, . . . G. Fruhbeck, *Six-transmembrane epithelial antigen of prostate 4 and neutrophil gelatinase-associated lipocalin expression in visceral adipose tissue is related to iron status and inflammation in human obesity.* Eur J Nutr, 2013. **52**(6): p. 1587-95.

62. ten Freyhaus, H., E.S. Calay, A. Yalcin, S.N. Vallerie, L. Yang, Z.Z. Calay, . . . G.S. Hotamisligil, *Stamp2 controls macrophage inflammation through nicotinamide adenine dinucleotide phosphate homeostasis and protects against atherosclerosis.* Cell Metab, 2012. **16**(1): p. 81-9.

63. Wang, Z.H., W. Zhang, H.P. Gong, Z.X. Guo, J. Zhao, Y.Y. Shang, . . . M. Zhong, *Expression of STAMP2 in monocytes associates with cardiovascular alterations.* Eur J Clin Invest, 2010. **40**(6): p. 490-6.

64. Han, L., M.X. Tang, Y. Ti, Z.H. Wang, J. Wang, W.Y. Ding, . . . M. Zhong, *Overexpressing STAMP2 improves insulin resistance in diabetic ApoE(-)/(-)/LDLR(-)/(-) mice via macrophage polarization shift in adipose tissues.* PLoS One, 2013. **8**(11): p. e78903.

65. Furukawa, S., T. Fujita, M. Shimabukuro, M. Iwaki, Y. Yamada, Y. Nakajima, . . . I. Shimomura, *Increased oxidative stress in obesity and its impact on metabolic syndrome.* J Clin Invest, 2004. **114**(12): p. 1752-61.

66. Houstis, N., E.D. Rosen, and E.S. Lander, *Reactive oxygen species have a causal role in multiple forms of insulin resistance.* Nature, 2006. **440**(7086): p. 944-8.

67. Horoszewicz, J.S., S.S. Leong, E. Kawinski, J.P. Karr, H. Rosenthal, T.M. Chu, . . . G.P. Murphy, *LNCaP model of human prostatic carcinoma.* Cancer Res, 1983. **43**(4): p. 1809-18.

68. Kaighn, M.E., K.S. Narayan, Y. Ohnuki, J.F. Lechner, and L.W. Jones, *Establishment and characterization of a human prostatic carcinoma cell line (PC-3).* Invest Urol, 1979. **17**(1): p. 16-23.

69. Stone, K.R., D.D. Mickey, H. Wunderli, G.H. Mickey, and D.F. Paulson, *Isolation of a human prostate carcinoma cell line (DU 145).* Int J Cancer, 1978. **21**(3): p. 274-81.

70. Tamura, T. and J. Chiba, *STEAP4 regulates focal adhesion kinase activation and CpG motifs within STEAP4 promoter region are frequently methylated in DU145, human androgen-independent prostate cancer cells.* Int J Mol Med, 2009. **24**(5): p. 599-604.

71. Zhao, J. and J.L. Guan, *Signal transduction by focal adhesion kinase in cancer.* Cancer Metastasis Rev, 2009. **28**(1-2): p. 35-49.

72. Korenchuk, S., J.E. Lehr, M.C. L, Y.G. Lee, S. Whitney, R. Vessella, . . . K.J. Pienta, *VCaP, a cell-based model system of human prostate cancer.* In Vivo, 2001. **15**(2): p. 163-8.

73. Sramkoski, R.M., T.G. Pretlow, 2nd, J.M. Giaconia, T.P. Pretlow, S. Schwartz, M.S. Sy, . . . J.W. Jacobberger, *A new human prostate carcinoma cell line, 22Rv1.* In Vitro Cell Dev Biol Anim, 1999. **35**(7): p. 403-9.

74. Cullinan, S.B. and J.A. Diehl, *Coordination of ER and oxidative stress signaling: the PERK/Nrf2 signaling pathway.* Int J Biochem Cell Biol, 2006. **38**(3): p. 317-32.

75. Wu, L., X. Chen, J. Zhao, B. Martin, J.A. Zepp, J.S. Ko, . . . X. Li, *A novel IL-17 signaling pathway controlling keratinocyte proliferation and tumorigenesis via the TRAF4-ERK5 axis.* J Exp Med, 2015. **212**(10): p. 1571-87.

76. He, D., H. Li, N. Yusuf, C.A. Elmets, M. Athar, S.K. Katiyar, and H. Xu, *IL-17 mediated inflammation promotes tumor growth and progression in the skin.* PLoS One, 2012. **7**(2): p. e32126.

77. Zepp, J.A., C. Liu, W. Qian, L. Wu, M.F. Gulen, Z. Kang, and X. Li, *Cutting edge: TNF receptor-associated factor 4 restricts IL-17-mediated pathology and signaling processes.* J Immunol, 2012. **189**(1): p. 33-7.

78. Laemmli, U.K., *Cleavage of structural proteins during the assembly of the head of bacteriophage T4.* Nature, 1970. **227**(5259): p. 680-5.

79. Strausberg, R.L., E.A. Feingold, L.H. Grouse, J.G. Derge, R.D. Klausner, F.S. Collins, . . . T. Mammalian Gene Collection Program, *Generation and initial analysis of more than 15,000 full-length human and mouse cDNA sequences.* Proc Natl Acad Sci U S A, 2002. **99**(26): p. 16899-903.

80. Wiemann, S., S. Bechtel, D. Bannasch, R. Pepperkok, A. Poustka, and D.N.A.N. German c, *The German cDNA network: cDNAs, functional genomics and proteomics.* J Struct Funct Genomics, 2003. **4**(2-3): p. 87-96.

81. Yudate, H.T., M. Suwa, R. Irie, H. Matsui, T. Nishikawa, Y. Nakamura, . . . Y. Masuho, *HUNT: launch of a full-length cDNA database from the Helix Research Institute.* Nucleic Acids Res, 2001. **29**(1): p. 185-8.

82. Phang, J.M., *The regulatory functions of proline and pyrroline-5-carboxylic acid.* Curr Top Cell Regul, 1985. **25**: p. 91-132.

83. Sonnhammer, E.L., G. von Heijne, and A. Krogh, *A hidden Markov model for predicting transmembrane helices in protein sequences.* Proc Int Conf Intell Syst Mol Biol, 1998. **6**: p. 175-82.

84. Ueda, T., N. Bruchovsky, and M.D. Sadar, *Activation of the androgen receptor N-terminal domain by interleukin-6 via MAPK and STAT3 signal transduction pathways.* J Biol Chem, 2002. **277**(9): p. 7076-85.

85. Malinowska, K., H. Neuwirt, I.T. Cavarretta, J. Bektic, H. Steiner, H. Dietrich, . . . Z. Culig, *Interleukin-6 stimulation of growth of prostate cancer in vitro and in vivo through activation of the androgen receptor.* Endocr Relat Cancer, 2009. **16**(1): p. 155-69.

86. Tran, C., S. Ouk, N.J. Clegg, Y. Chen, P.A. Watson, V. Arora, . . . C.L. Sawyers, *Development of a second-generation antiandrogen for treatment of advanced prostate cancer.* Science, 2009. **324**(5928): p. 787-90.

87. Hayden, M.S. and S. Ghosh, *Regulation of NF-kappaB by TNF family cytokines.* Semin Immunol, 2014. **26**(3): p. 253-66.

88. Minden, A., A. Lin, T. Smeal, B. Derijard, M. Cobb, R. Davis, and M. Karin, *c-Jun N-terminal phosphorylation correlates with activation of the JNK subgroup but not the ERK subgroup of mitogen-activated protein kinases.* Mol Cell Biol, 1994. **14**(10): p. 6683-8.

89. Wang, S.B., T. Lei, L.L. Zhou, H.L. Zheng, C.P. Zeng, N. Liu, . . . X.D. Chen, *Functional analysis and transcriptional regulation of porcine six transmembrane epithelial antigen of prostate 4 (STEAP4) gene and its novel variant in hepatocytes.* Int J Biochem Cell Biol, 2013. **45**(3): p. 612-20.

90. Hucho, F. and K. Buchner, *Signal transduction and protein kinases: the long way from the plasma membrane into the nucleus.* Naturwissenschaften, 1997. **84**(7): p. 281-90.

91. Yoo, S.K., J. Cheong, and H.Y. Kim, *STAMPing into Mitochondria.* Int J Biol Sci, 2014. **10**(3): p. 321-6.

92. Inoue, A., I. Matsumoto, Y. Tanaka, K. Iwanami, A. Kanamori, N. Ochiai, . . . T. Sumida, *Tumor necrosis factor alpha-induced adipose-related protein expression in experimental arthritis and in rheumatoid arthritis.* Arthritis Res Ther, 2009. **11**(4): p. R118.

93. Wu, X., S. Gong, P. Roy-Burman, P. Lee, and Z. Culig, *Current mouse and cell models in prostate cancer research.* Endocr Relat Cancer, 2013. **20**(4): p. R155-70.

94. Mulholland, D.J., L.M. Tran, Y. Li, H. Cai, A. Morim, S. Wang, . . . H. Wu, *Cell autonomous role of PTEN in regulating castration-resistant prostate cancer growth.* Cancer Cell, 2011. **19**(6): p. 792-804.

95. Carver, B.S., C. Chapinski, J. Wongvipat, H. Hieronymus, Y. Chen, S. Chandarlapaty, . . . C.L. Sawyers, *Reciprocal feedback regulation of PI3K and androgen receptor signaling in PTEN-deficient prostate cancer.* Cancer Cell, 2011. **19**(5): p. 575-86.

96. De Marzo, A.M., E.A. Platz, S. Sutcliffe, J. Xu, H. Gronberg, C.G. Drake, . . . W.G. Nelson, *Inflammation in prostate carcinogenesis.* Nat Rev Cancer, 2007. **7**(4): p. 256-69.

97. Giri, D., M. Ozen, and M. Ittmann, *Interleukin-6 is an autocrine growth factor in human prostate cancer.* Am J Pathol, 2001. **159**(6): p. 2159-65.

98. Nakashima, J., M. Tachibana, Y. Horiguchi, M. Oya, T. Ohigashi, H. Asakura, and M. Murai, *Serum interleukin 6 as a prognostic factor in patients with prostate cancer.* Clin Cancer Res, 2000. **6**(7): p. 2702-6.

99. Schroeder, A., A. Herrmann, G. Cherryholmes, C. Kowolik, R. Buettner, S. Pal, . . . R. Jove, *Loss of androgen receptor expression promotes a stem-like cell phenotype in prostate cancer through STAT3 signaling.* Cancer Res, 2014. **74**(4): p. 1227-37.

100. Chen, X., C. Zhu, C. Ji, Y. Zhao, C. Zhang, F. Chen, . . . X. Guo, *STEAP4, a gene associated with insulin sensitivity, is regulated by several adipokines in human adipocytes.* Int J Mol Med, 2010. **25**(3): p. 361-7.

101. Fasshauer, M., S. Kralisch, M. Klier, U. Lossner, M. Bluher, A.M. Chambaut-Guerin, . . . R. Paschke, *Interleukin-6 is a positive regulator of tumor necrosis factor alpha-induced adipose-related protein in 3T3-L1 adipocytes.* FEBS Lett, 2004. **560**(1-3): p. 153-7.

102. Aggarwal, B.B., A.B. Kunnumakkara, K.B. Harikumar, S.R. Gupta, S.T. Tharakan, C. Koca, . . . B. Sung, *Signal transducer and activator of transcription-3, inflammation, and cancer: how intimate is the relationship?* Ann N Y Acad Sci, 2009. **1171**: p. 59-76.

103. Wierenga, A.T., I. Vogelzang, B.J. Eggen, and E. Vellenga, *Erythropoietin-induced serine 727 phosphorylation of STAT3 in erythroid cells is mediated by a MEK-, ERK-, and MSK1-dependent pathway.* Exp Hematol, 2003. **31**(5): p. 398-405.

104. Deak, M., A.D. Clifton, L.M. Lucocq, and D.R. Alessi, *Mitogen- and stress-activated protein kinase-1 (MSK1) is directly activated by MAPK and SAPK2/p38, and may mediate activation of CREB.* EMBO J, 1998. **17**(15): p. 4426-41.

105. Aziz, M.H., H.T. Manoharan, D.R. Church, N.E. Dreckschmidt, W. Zhong, T.D. Oberley, . . . A.K. Verma, *Protein kinase Cepsilon interacts with signal transducers and activators of transcription 3 (Stat3), phosphorylates Stat3Ser727, and regulates its constitutive activation in prostate cancer.* Cancer Res, 2007. **67**(18): p. 8828-38.

106. Kim, J.H., J.E. Kim, H.Y. Liu, W. Cao, and J. Chen, *Regulation of interleukin-6-induced hepatic insulin resistance by mammalian target of rapamycin through the STAT3-SOCS3 pathway.* J Biol Chem, 2008. **283**(2): p. 708-15.

107. Pencik, J., M. Schlederer, W. Gruber, C. Unger, S.M. Walker, A. Chalaris, . . . L. Kenner, *STAT3 regulated ARF expression suppresses prostate cancer metastasis.* Nat Commun, 2015. **6**: p. 7736.

108. Wang, Y., A.H. van Boxel-Dezaire, H. Cheon, J. Yang, and G.R. Stark, *STAT3 activation in response to IL-6 is prolonged by the binding of IL-6 receptor to EGF receptor.* Proc Natl Acad Sci U S A, 2013. **110**(42): p. 16975-80.

109. Hobisch, A., R. Ramoner, D. Fuchs, S. Godoy-Tundidor, G. Bartsch, H. Klocker, and Z. Culig, *Prostate cancer cells (LNCaP) generated after long-term interleukin 6 (IL-6) treatment express IL-6 and acquire an IL-6 partially resistant phenotype.* Clin Cancer Res, 2001. **7**(9): p. 2941-8.

110. Chen, T., L.H. Wang, and W.L. Farrar, *Interleukin 6 activates androgen receptor-mediated gene expression through a signal transducer and activator of transcription 3-dependent pathway in LNCaP prostate cancer cells.* Cancer Res, 2000. **60**(8): p. 2132-5.

111. Gonen-Korkmaz, C., G. Sevin, G. Gokce, M.Z. Arun, G. Yildirim, B. Reel, . . . D. Ogut, *Analysis of tumor necrosis factor alpha-induced and nuclear factor kappaB-silenced LNCaP prostate cancer cells by RT-qPCR.* Exp Ther Med, 2014. **8**(6): p. 1695-1700.

112. Kralisch, S., G. Sommer, S. Weise, J. Lipfert, U. Lossner, M. Kamprad, . . . M. Fasshauer, *Interleukin-1beta is a positive regulator of TIARP/STAMP2 gene and protein expression in adipocytes in vitro.* FEBS Lett, 2009. **583**(7): p. 1196-200.

113. Waugh, D.J. and C. Wilson, *The interleukin-8 pathway in cancer.* Clin Cancer Res, 2008. **14**(21): p. 6735-41.

114. Mellado, M., J.M. Rodriguez-Frade, A. Aragay, G. del Real, A.M. Martin, A.J. Vila-Coro, . . . A.C. Martinez, *The chemokine monocyte chemotactic protein 1 triggers Janus kinase 2 activation and tyrosine phosphorylation of the CCR2B receptor.* J Immunol, 1998. **161**(2): p. 805-13.

115. Stratton, M.S., B. Greenstein, T.S. Udayakumar, R.B. Nagle, and G.T. Bowden, *Androgens block interleukin-1 beta-induced promatrilysin expression in prostate carcinoma cells.* Prostate, 2002. **53**(1): p. 1-8.

116. Lee, L.F., M.C. Louie, S.J. Desai, J. Yang, H.W. Chen, C.P. Evans, and H.J. Kung, *Interleukin-8 confers androgen-independent growth and migration of LNCaP: differential effects of tyrosine kinases Src and FAK.* Oncogene, 2004. **23**(12): p. 2197-205.

117. Mora, L.B., R. Buettner, J. Seigne, J. Diaz, N. Ahmad, R. Garcia, . . . R. Jove, *Constitutive activation of Stat3 in human prostate tumors and cell lines: direct inhibition of Stat3 signaling induces apoptosis of prostate cancer cells.* Cancer Res, 2002. **62**(22): p. 6659-66.

118. Pang, L., T. Sawada, S.J. Decker, and A.R. Saltiel, *Inhibition of MAP kinase kinase blocks the differentiation of PC-12 cells induced by nerve growth factor.* J Biol Chem, 1995. **270**(23): p. 13585-8.

119. Han, Z., D.L. Boyle, L. Chang, B. Bennett, M. Karin, L. Yang, . . . G.S. Firestein, *c-Jun N-terminal kinase is required for metalloproteinase expression and joint destruction in inflammatory arthritis.* J Clin Invest, 2001. **108**(1): p. 73-81.

120. Cuenda, A., J. Rouse, Y.N. Doza, R. Meier, P. Cohen, T.F. Gallagher, . . . J.C. Lee, *SB 203580 is a specific inhibitor of a MAP kinase homologue which is stimulated by cellular stresses and interleukin-1*. FEBS Lett, 1995. **364**(2): p. 229-33.

121. Scuto, A., P. Krejci, L. Popplewell, J. Wu, Y. Wang, M. Kujawski, . . . R. Jove, *The novel JAK inhibitor AZD1480 blocks STAT3 and FGFR3 signaling, resulting in suppression of human myeloma cell growth and survival.* Leukemia, 2011. **25**(3): p. 538-50.